UNIVERSITÀ
DEGLI STUDI
DI PADOVA

Università degli Studi di Padova

Dipartimento di Biomedicina Comparata e Alimentazione

DOTTORATO DI RICERCA IN SCIENZE VETERINARIE

XXVI° CICLO

Tyrosine hydroxylase and HSPB8 interact with the prion protein

Coordinatore: Ch.mo Prof. Gianfranco Gabai

Supervisore: Ch.mo Prof. Alessandro Negro

Dottorando: Mattia Vicario

ANNO ACCADEMICO 2013-2014

TABLE OF CONTENTS

SUMMARY

The prion protein (PrP) is currently one of the most studied molecules in the neurosciences as it causes a group of neurological diseases collectively named transmissible spongiform encephalophaties (TSEs). The TSEs are characterized by a variety of motor and/or cognitive symptoms distinct from those of Parkinson and Alzheimer diseases and severely affect both humans and a variety of mammals. A great effort has thus been made to understand the molecular basis of PrP activity, both in physiological and pathological terms. In this context, the identification of neuronally-relevant interactors of PrP, capable of governing or interfering with its activity, cellular localization and/or expression, plays a crucial role. Through the expression of the proteins of interest in recombinant form in *E.coli* cells and the analysis of their interaction by Western blot and dot-blot, we identified two specific and neurologically relevant interactions involving the prion protein and on the one hand tyrosine hydroxylase, the enzyme that catalyzes the initial and rate-limiting reaction of the biosynthesis of catecholamines dopamine, norepinephrine and epinephrine; on the other hand the heat shock protein B8, member of the small heat shock protein family that appears to play an important role in those diseases that, like transmissible spongiform encephalopathies, are characterized by the accumulation of misfolded proteins. The association/dissociation constants of the complexes have been calculated using surface plasmon resonance and interactions were confirmed by immunohistochemistry. The data obtained show a specific and high affinity interaction (KD in the nano molar range) between the TH N-terminal regulatory domain (1-152) and the C-terminal structured domain (90-230) of PrP. The co-expression of the two proteins causes a shift in prion protein expression from a prevalent membrane-associated expression to a greater cytoplasmic localization, and also a down-regulation of the levels of expression of the prion protein without, however, affecting the topology and expression of tyrosine hydroxylase. The link between PrP and HSPB8 involves the C-terminal domain of the prion protein and the co-expression of the two proteins leads to a down-regulation of both prion protein and HSPB8. The latter, moreover, protects the prion protein from degradation by Proteinase K, while it seems to accelerate the thermal denaturation. The mutants K141E and K141N of the heat shock protein, associated with the development of neuropathy, show minor binding affinity with respect to the wild type protein and they are less effective in regulating the levels of expression, localization and degradation of the prion protein. Our results, in particular if confirmed in pathological patterns, can help to understand the physiological and pathological mechanisms of action of the prion protein and suggest tyrosine hydroxylase and heat shock protein B8 as prion protein modulators, thus as potential targets for therapeutic applications.

SOMMARIO

La proteina prionica è, ad oggi, una delle molecole più studiate nelle neuroscienze poiché essa rappresenta l'agente eziologico di un gruppo di patologie neurologiche chiamate collettivamente encefalopatie spongiformi trasmissibili (TSE). Queste patologie sono caratterizzate da una serie di sintomi motori e cognitivi distinti da quelli delle patologie di Parkinson e Alzheimer e colpiscono l'uomo e una grande varietà di mammiferi. Per tale ragione un grande sforzo è stato fatto per capire le basi molecolari dell'attività di PrP in condizioni fisiologiche e patologiche, le quali, tutt'ora, non sono del tutto comprese. In questo contesto è di cruciale importanza l'identificazione di nuovi partner di legame che regolino o interferiscano con l'attività, la localizzazione cellulare e/o l'espressione della proteina prionica. Tramite l'espressione delle proteine di interesse in forma ricombinante in cellule di *E.coli* e l'analisi delle loro interazioni mediante Western blot e dot-blot, abbiamo identificato due interazioni specifiche e neurologicamente rilevanti della proteina prionica coinvolgenti da un lato la tirosina idrossilasi, enzima che catalizza la reazione iniziale e limitante della biosintesi delle catecolamine dopamina, norepinefrina ed epinefrina; dall'altro l'heat shock protein B8, membro della famiglia delle small heat shock protein, che sembra ricoprire un ruolo particolarmente importante in quelle patologie che, come le encefalopatie spongiformi trasmissibili, sono caratterizzate dall'accumulo di proteine mal ripiegate. Le costanti di associazione/dissociazione dei complessi sono state calcolate mediante surface plasmon resonance e le interazioni sono state confermate tramite immunoistochimica. I dati ottenuti evidenziano un'interazione specifica e ad alta affinità (KD nel range nM) tra il dominio regolatorio N-terminale (1-152) di TH e il dominio strutturato C-terminale (90-230) di PrP. La co-espressione delle due proteine causa sia uno spostamento da un'espressione prevalentemente di membrana della proteina prionica ad una localizzazione maggiormente citoplasmatica, sia una down-regolazione dei livelli di espressione di proteina prionica senza, tuttavia, influenzare topologia ed espressione della tirosina idrossilasi. Il legame tra PrP e HSPB8 coinvolge il dominio C-terminale della proteina prionica e la co-espressione delle due proteine porta ad una down-regolazione sia di proteina prionica che di HSPB8. Quest'ultima, inoltre, protegge la proteina prionica dalla degradazione da parte di proteinasi K, mentre sembra favorirne la denaturazione termica. I mutanti K141E e K141N dell'heat shock protein, associati allo sviluppo di neuropatie, mostrano affinità di binding minori rispetto alla proteina wild type così come sono meno efficaci nel regolare i livelli di espressione, localizzazione e degradazione della proteina prionica. I nostri risultati, in particolare se confermati in modelli di patologia, possono aiutare a comprendere i meccanismi d'azione fisiologici e patologici della proteina prionica e indicano tirosina idrossilasi e heat shock protein B8 come

modulatori della proteina prionica stessa e quindi come potenziali target per applicazioni terapeutiche.

INTRODUCTION

The prion protein

The prion protein is a glycoprotein that is expressed most abundantly in the brain, but has also been detected in other non-neuronal tissues as diverse as lymphoid cells, lung, heart, kidney, gastrointestinal tract, muscle, and mammary glands (Horiuchi et al. 1995). The prion protein is, to date, one of the most studied proteins due to its role in several neurological diseases collectively named TSE (transmissible spongiform encephalopathies).

The term "prion" was first used by Stanley B. Prusiner in 1982 to denote the infectious pathogen causing scrapie of sheep and goats. This new small proteinaceous infectious particle was different from viruses, plasmids and viroids and was extremely resistant to inactivation by most procedures that modify nucleic acid (Prusiner 1982).

PrP may exist in two isoforms: a normal cellular prion protein designated as PrP^{C} and a pathogenic misfolded conformer called PrP^{SC}. The superscript (SC) has been used to refer to scrapie, the first and the most ancient animal transmissible spongiform encephalopathy (TSE). Many authors also use superscripts other than (SC) to distinguish normal and pathogenic (disease-causing) isoforms. These include (Res) for resistant and (Dis) for disease. An abbreviated name of a prion disease can also be used as superscript to point out the origin of the pathogenic isoform (PrP^{SC} or PrP^{CJD}). The pathogenic conformers are simply called prions (Prusiner 1998).

The PrP gene

Both PrP^{C} and PrP^{SC} are encoded from the same sequence of a 16 Kb single copy PRNP gene, which is a member of the PRN gene family that also includes PRND, encoding the doppel protein (Moore et al. 1999), and SPRN, encoding shadoo (Watts and Westaway 2007). The PRN gene is positioned at the short (p) arm of human chromosome 20 (20p13) from base pair 4,666,796 to 4,682,233. The entire ORF of PrP is contained in a single exon in all species although the gene itself comprises two to three exons ruling out the possibility that PrP^{C} and PrP^{SC} differ by alternative mRNA splicing (Stahl and Prusiner 1991). The other exons contain untranslated sequences including the promoter and termination sites. The PrP promoter contains multiple copies of GC rich repeats that may function as a canonical binding site for the transcription factor Sp1 (McKnight and Tjian 1986). The alignment of the translated sequences from more than 40 PrP genes shows a striking degree of conservation between the mammalian sequences, suggesting the retention of some important function for PrP through evolution. However, variations in PrP

sequences exist both between species and between individuals within species (Colby and Prusiner 2011).

The PrP structure

The abnormal PrP^{SC} differs from the normal PrP^{C} isoform in secondary and tertiary structure but not in primary amino acids sequence. The primary sequence of PrP is 253 amino acids long before post translational modification. The protein is synthesized with a NH_2-terminal signal sequence that targets it to the endoplasmic reticulum where the peptide is removed, leaving Lys23 as the amino-terminal residue (Turk et al. 1988). The last 23 COOH-terminal amino acids are cleaved off after the addiction of a glycosylphosphatidylinositol (GPI) anchor which helps the protein to attach to the outer surface of cells membrane. The mature primary sequence of the prion protein is so composed of 208 amino acids. For human and Syrian hamster PrP, two glycosylated sites exist on helices 2 and 3 at Asn181 and Asn197. Murine PrP has glycosylation sites as Asn180 and Asn196. No post-translational modifications to the primary structure differentiate PrP^{C} from PrP^{SC} (Stahl et al. 1993).

The nuclear magnetic resonance (NMR) structures for normal PrP of some species, such as mice, humans, Syrian hamsters and cattle, have been successfully illustrated, sharing common features. The mature PrP^{C} consists of a long flexible amino-terminal tail of about 100 amino acids (residues 23-128) and a C-terminal domain, also of around 100 amino acids.

The C-terminal domain is composed largely of α-helical structure with three α-helices and a short anti-parallel β-sheet. The second β-sheet and the third α-helix are connected by a large loop with interesting structural properties. The carboxyl terminus of PrP^{C} is stabilized by a disulfide bond that links helices two and three and exhibits a globular structure. A crystal structure of PrP has been obtained, largely in agreement with the NMR structures (Antonyuk et al. 2009).

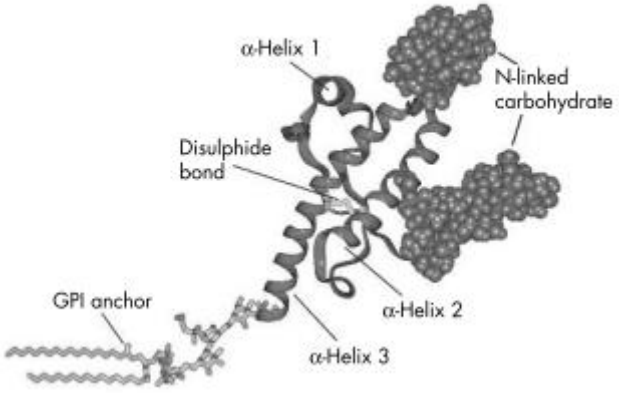

Fig:1. Model of the C-terminal domain of human prion protein indicating positions of N-linked glycans, the single disulphide bond joining helices 2 and 3, and the GPI anchor which attaches the protein to the outer surface of the cell membrane (Collinge 2005).

The N-terminal unstructured domain contains two defined and conserved region (Zahn et al. 2000). The first consists of a segment of five repeats of eight amino acids sequence, called the octapeptide repeat region. Mutations in this region, resulting in addition of integral numbers of additional repeats, lead to forms of inherited prion disease. This region is very highly conserved in evolution and contains two tight binding sites for Cu^{2+} ions. It is proposed that the unstructured N-terminal region may acquire structure following copper binding and a role for PrP in copper metabolism or transport is possible. Disturbance of this function by the conformational transitions between isoforms of PrP could be involved in prion related neurotoxicity (Jackson et al. 2001). The second region contains a highly hydrophobic and conserved profile, which is proposed to be the transmembrane region of the PrP molecule. In addition, the region around histidine-96 in PrP is believed to be the binding site for manganese and zinc, which may also contribute to the pathogenesis of prion diseases (Tian and Dong 2013).

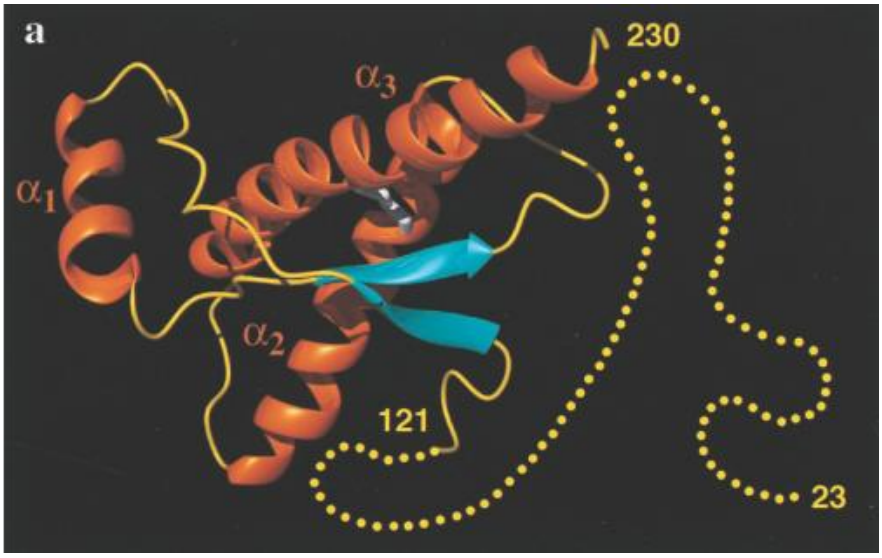

Fig: 2. Cartoon of the three-dimensional structure of the intact human prion protein, hPrP(23±230). The helices are orange, the β-strands cyan, the segments with non-regular secondary structure within the C-terminal domain yellow, and the flexibly disordered "tail" of residues 23±121 is represented by yellow dots (Zahn et al. 2000).

PrP isoforms

A post-translation chemical modification that distinguishes PrP^{C} and PrP^{SC} was considered but no one was found. To date, the most validate hypothesis is that they differed only in their conformation. Fourier-transform infrared (FTIR) spectroscopy and circular dichroism measurements demonstrate that PrP^{C} has a high α-helix content (42%) and no β-sheet (3%). In contrast, the β-sheet content of PrP^{SC} is 43% and the α-helix is 30% (Pan et al. 1993). This conformational discrepancy renders the PrP^{SC} isoform extremely resistant to proteolysis. This

enhanced resistance of PrP^{SC} to protease digestion is a cardinal feature that distinguishes it from PrP^{C}. Whereas PrP^{C} is completely degraded upon incubation with proteinase K, PrP^{SC} loses an NH_2-terminal domain containing the octarepeats. The cleavage site of protease usually locates around the residue 90 and produces a 90-231 core which has an apparent molecular mass of 27-30 KDa, therefore referred as PrP 27-30 (Prusiner et al. 1984). The PrP 27-30 has an even higher β-sheet content (54%) and a lower α-helix content (21%) (Pan et al. 1993).

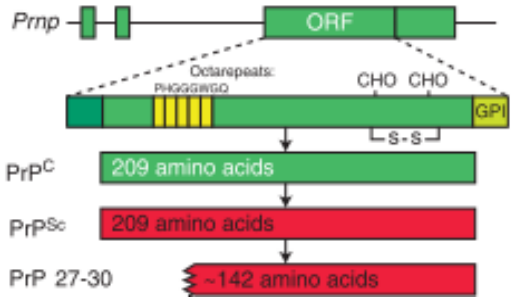

Fig: 3. Scheme of the PRNP gene and PrP isoforms (Colby and Prusiner 2011).

Furthermore, Prp^{C} is soluble in the presence of various detergents whereas PrP^{SC} forms insoluble aggregates, polymerizing into amyloid (Meyer et al. 1986).

The prion topology

During normal expression, PrP^{C} is translocated into the endoplasmic reticulum (ER) lumen, where it undergoes several post-translational modifications, including the addition of the GPI anchor, disulfide bond formation, and core glycosylation at two asparagines, before it passes to the Golgi apparatus for further sugar modification and subsequently been attached to the outer leaflet of the plasma membrane (Norstrom et al. 2007). However, additional forms of PrP have been identified, including two transmembrane forms.

Two distinct forms of PrP can be made at the ER: one that is fully translocated (^{sec}PrP) and one that is transmembrane. Digestion of the transmembrane form with proteases added to the outside of the membrane yielded two fragments: one is COOH-terminal derived and glycosylated, and the other is NH_2-terminal derived and unglycosylated. These data have been interpreted to indicate that transmembrane PrP chains span the membrane twice, with the NH_2- and COOH-termini of the molecule in the ER lumen, protected from proteases added to the cytosolic side. However, the findings suggest that the NH_2- and COOH-terminal fragments reflect the existence of two different transmembrane forms of PrP. One form, termed C-trans transmembrane (^{Ctm}PrP), has the COOH-terminus in the ER lumen with the NH_2-terminus accessible to proteases in the cytosol. The other form, termed N-trans transmembrane (^{Ntm}PrP), has the NH_2-terminus in the ER lumen with the COOH-terminus accessible to proteases in the cytosol. Both transmembrane forms appear to span

the membrane at the same hydrophobic stretch in PrP (roughly residues 110 to 135, termed TM1). For this reason, the proteolytic fragments derived from each transmembrane form share a common domain of PrP approximately from residues 105 to 140 (the residues immediately adjacent to the membrane-spanning domain are not digested by protease, perhaps because of steric hindrance by the membrane itself) (Hegde et al. 1998).

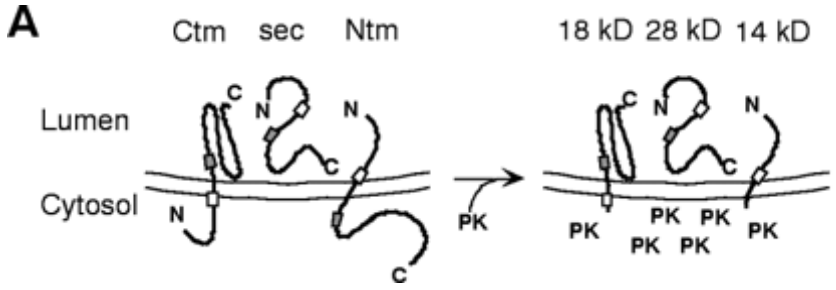

Fig: 4. The three topologic forms of PrP are shown before (left) and after (right) digestion with cytosolically disposed PK (Hegde et al. 1998).

Moreover, cytosolic PrP form has been identified in subpopulations of neurons in the hippocampus, neocortex, and thalamus (Mironov et al. 2003, Fioriti et al. 2005, Ma et al. 2002) in a variety of condition including stress (Orsi et al. 2006). The role of cytosolic PrP is not clear but has been postulated to have an anti-apoptotic function (Roucou et al. 2003).

Trafficking of PrP^{C} seems to be a complex cellular event and may involve more than one internalization mechanism. PrP^{C} is enriched in caveolae-like (raft) both at the transgolgi network and plasma membrane and in interconnecting chains of endocytic caveolae-like domains. It is delivered via caveolae-like domains to the pericentricolar region and via non-classical, caveolae containing early endocytic structures to late endosomes/lysosomes (Zomosa-Signoret et al. 2008).

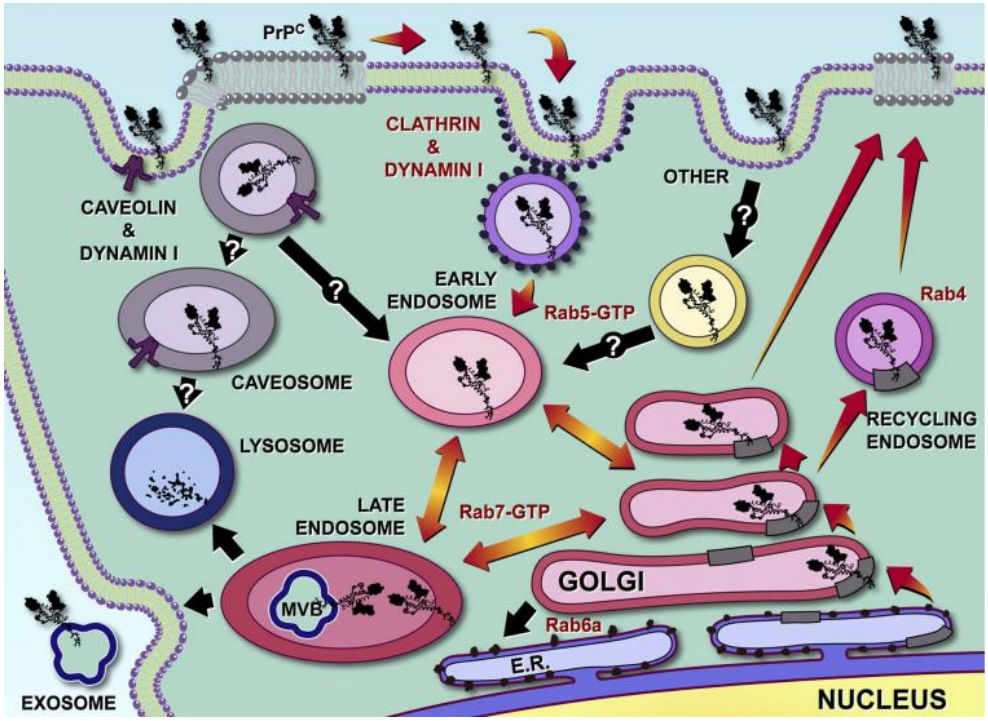

Fig: 5. Subcellular trafficking of PrP^C (Linden et al. 2008).

Prion protein physiological roles

Although PrP is one of the most studied proteins, it is expressed in most tissue and it's highly conserved among species, its cellular role is not completely understood. However, in the last few years, some possible biological functions for the cellular prion protein have been described.

It is well known that PrP binds copper through its N-terminal domain containing octapeptide repeats. There is increasing evidence to support a functional role for PrP^C in copper metabolism and several groups have investigated the physiological meaning of this association. PrP^C may be a principal copper-binding protein in brain membrane fractions and controls the activity of other membrane-associated copper-binding proteins. Prion protein expression alters copper uptake into cells and enhances copper incorporation into superoxide dismutase (SOD) (Zomosa-Signoret et al. 2008). This copper-binding activity may be linked with a role in oxidative stress homeostasis. PrP, in fact, can act as a SOD (Brown et al. 1999) and PrP null cells are more susceptible to oxidative damage and toxicity caused by agents such as copper and hydrogen peroxide (Brown et al. 1998). It also seems that the copper binding on the N-terminal domain of the prion protein can enable the recruitment of Phosphatidylinositol 3-kinase (PI 3-kinase) by PrP^C. PI 3-kinase is a protein kinase that plays a pivotal role in many cellular processes including cell survival and apoptosis. Both mouse neuroblastoma N2a cells and immortalized murine hippocampal neuronal cell lines expressing wild-type PrP^C had a significantly higher PI 3-kinase activity levels than their respective controls (Vassallo et al. 2005). Many other signal transduction pathways have been

associated with PrP, mainly due to its localization in lipid rafts. A few studies provided evidence that PrP^C may lead to activation of Protein Kinase C (PKC) (Botto et al. 2004); treatment of developing retinal tissue with PrP^C binding peptides led to activation of Erk (Chiarini et al. 2002); a caveolin-dependent coupling of PrP^C to the tyrosine kinase fyn was shown (Mouillet-Richard et al 2000) and direct evidence that PrP^C mediates activation of the cAMP/protein kinase A (PKA) pathway was obtained with a peptide that binds PrP^C (Martins et al. 1997). Moreover cells transfected with PRNP presented an increased agonist-induced calcium influx through the plasma membrane, while reducing the release of Ca^{2+} from the ER and Ca^{2+} uptake by mitochondria (Brini et al 2005).

An anti-apoptotic role for the cellular prion protein has also been described. PrP^C protects against Bax-mediated neuronal apoptosis and potently inhibits Bax-induced cell death in human primary neurons, probably acting as a member of the Bcl-2 family. Deletion of four octapeptide repeats of PrP as well as familial D178N and T183A PrP mutations completely or partially suppress the neuroprotective effect of PrP (Bounhar et al. 2001).

Lots of data show that PrP^C may play important roles in the development and maintenance of the immune system, as well as in specific cellular immunological responses. A possible involvement of PrP^C in T cell activation leading to Th1 response has been proposed (Martínez del Hoyo et al. 2006); PrP^C seems to support self-renewal of hematopoietic stem cells (HSC) (Zhang et al. 2006); PrP^C is down-regulated upon differentiation along the granulocyte lineage while maturation of monocyte and dendritic cells leads to PrP^C up-regulation (Zomosa-Signoret et al. 2008).

The fact that the protein is expressed in neurons at higher levels than in any other cell type suggests that PrP^C has special importance in neurons. PrP^C is both pre-sinaptic (Herms et al. 1999) and post-sinaptic. Several experimental observations suggest that PrP^C could play a role in synaptic structure, function or maintenance. $PrP^{-/-}$ mice have been reported to display several neurobiological abnormalities that may also relate to the participation of PrP^C in synapse formation and function. These include alterations in nerve fiber organization, circadian rhythm and spatial learning (Zomosa-Signoret et al. 2008).

Prion propagation and toxicity

According to the "protein only hypothesis", prion propagation requires the conversion of PrP^C to PrP^{SC}, the anomalous conformer resulting from the shift from a predominantly α-helical structure into a predominantly β-sheet structure. This hypothesis was strongly supported by the fact that $PRNP^{0/0}$ mice, not expressing the cellular prion protein, remain free of scrapie symptoms (Büeler et al. 1993). The β-sheet conformer is prone to form compact protein aggregates that accumulate

within the brain. It has been proposed that the conversion of PrP^{C} to PrP^{SC} may also require the assistance of one or more as-yet-unidentified cofactors provisionally designated protein X. Presumably, protein X binds to PrP^{C} and enables it to interact with PrP^{SC} for conversion. Over expression of protein X would thus shorten incubation times for disease, whereas ablation of protein X would prolong or abolish prion disease. Many putative protein X genes have been identified, but transgenic knockouts for these genes have failed to alter incubation times (Prusiner et al. 2011). The precise sub cellular localization of the conversion from PrP^{C} isoform to PrP^{SC} is not well understood but it seems possible that it may in the late-endosome like organelles or lysosomes. The environments of these organelles facilitate protein unfolding at low pH and it is possible that the conversion from the physiological to the pathological isoform is caused by reduction and mild acidification (Collinge 2005).

There are two models to explain the conformational conversion of PrP^{C} into PrP^{SC}. The "template-directed refolding" hypothesis predicates an instructionist role for PrP^{SC} on PrP^{C}. Alternatively, the seeded nucleation hypothesis suggests that PrP^{SC} exists in equilibrium with PrP^{C}. In a non-disease state, such an equilibrium would be heavily shifted toward the PrP^{C} conformation, such that only minute amounts of PrP^{SC} would coexist with PrP^{C}. If this were the case, PrP^{SC} could not possibly represent the infectious agent, since it would be ubiquitous. According to this "seeded nucleation" hypothesis, the infectious agent would consist of a highly ordered aggregate of PrP^{SC} molecules. The aggregated state would be an intrinsic property of infectivity. Monomeric PrP^{SC} would be harmless, but it might be prone to incorporation into nascent PrP Sc aggregates (Aguzzi and Calella 2009).

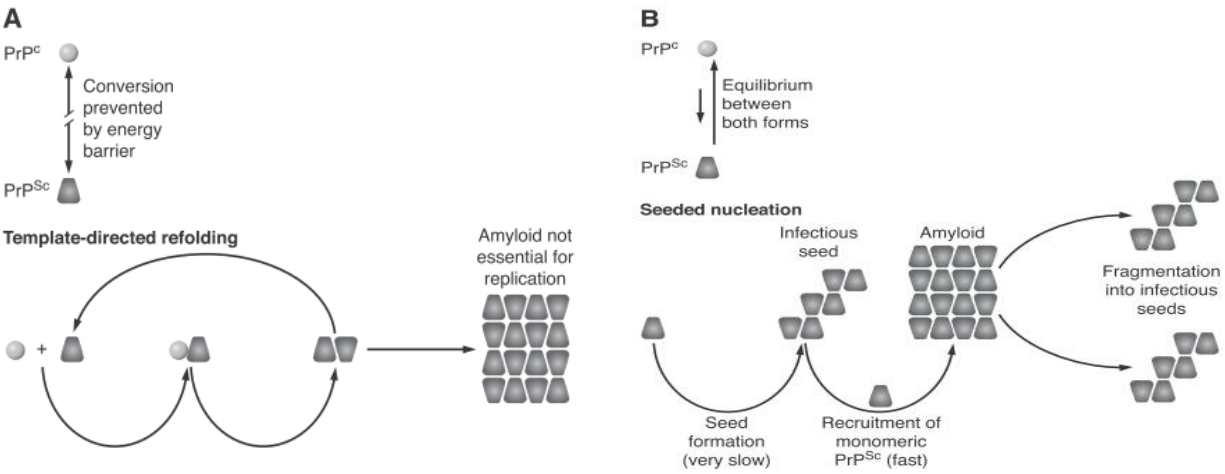

Fig: 6. Models for conformational conversion from PrP^{C} into PrP^{SC}. A) template-directed refolding hypothesis; B) seeded nucleation hypothesis (Aguzzi and Calella 2009).

The molecular mechanisms leading to cerebral damage are mostly unknown. Recent data suggest two major ways for PrP to cause toxicity in the brain: a gain of function hypothesis and a loss of

function hypothesis. According to the gain of function hypothesis PrP^{SC} aggregation sensitizes neurons to programmed cell death and leads to prion disease. The loss of function hypothesis is based on the idea that the toxicity of PrP^{SC} depends on the loss of cellular PrP or the alteration of some PrP^{C} dependent process culminating in neuronal dysfunction and death.

It has also been suggested that the formation of amyloid fibrils, as with other diseases characterized by protein aggregation, might be a protective process that sequesters the more dangerous subfibrillars oligomers or protein into relatively innocuous deposits (Aguzzi and Calella 2009).

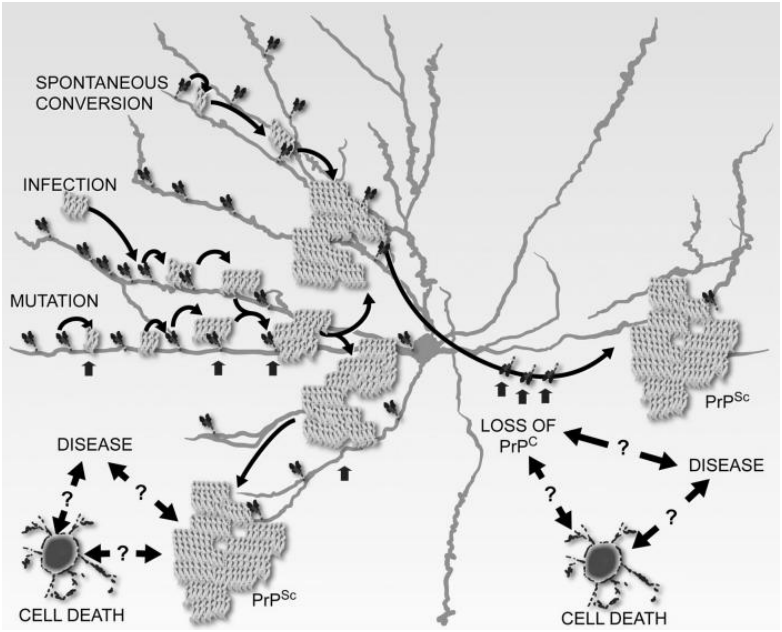

Fig: 7. Schematic representation of the gain of function and loss of function hypothesis of prion diseases (Linden et al. 2008).

Transmissible spongiform encephalopathies

The key features of nearly all prion diseases are transmissibility and a foamy pattern (spongiosis) of brain tissue that is visible on histological sections. Spongiosis is due primarily to intraneuronal vacuoles containing membrane fragments and, sometimes, degenerating organelles, but the etiology of this highly characteristic pathology is unclear.

Prion diseases occur as sporadic, genetic, and transmissible diseases in humans.

Kuru, Creutzfeldt-Jakob disease (CJD), and Gerstmann-Straussler- Scheinker syndrome (GSS), are all human neurodegenerative diseases that are caused by prions and are frequently transmissible to laboratory animals. Individuals at risk can often be identified decades in advance of central nervous system (CNS) dysfunction, yet no effective therapy exists to prevent these lethal disorders (Prusiner 1991). In humans, sporadic and heritable forms of the disease occur much more frequently

than the infectious forms (Colby and Prusiner 2011). To date, over 40 different mutations of the PrP gene have been shown to segregate with the heritable human prion diseases. Familial CJD (or FFI for fatal familial insomnia according to the clinical symptoms) and GSS are genetic disorders.

The first description of GSS was in a large Austrian family with affected members manifesting slowly progressive cerebellar ataxia admixed with cognitive decline at some time in the course of their illness. A variety of mutations in PRNP gene have been associated with this disorder. Some of these are a missense mutation at codon 198 (Dlouhy et al. 1992), a tyrosine to stop mutation at codon 145 (Kitamoto et al. 1993), a proline to leucine mutation at codon 105 (Kitamoto et al 1993b) and a 144 base pair insertion (Poulter et al. 1992). However, the most common mutation is a proline to leucine mutation at codon 102 (Hsiao et al. 1989). Symptoms usually begin in the fifth or sixth decade, but the onset may be as young as 25 years and they include combinations of cerebellar and pyramidal dysfunction, behavioural difficulties, and cognitive decline (Brown et al. 1991).

The sleep disruption, characterized by prominent nocturnal insomnia, constitutes the salient clinical hallmark of FFI. The term was first used in 1986 to depict an illness afflicting five members of a large Italian family but it was not until 1992 that the disorder was proposed as a novel, genetically determined prion disease (Medori et al. 1992). As in the case of GSS, several different mutations has been discovered to cause FFI. Two of these are a PrP gene point mutation at codon 200, resulting in a glutamic acid to lysine substitution (Hsiao et al. 1991), and a GAC to AAC mutation at codon 178 of the gene, causing substitution of asparagine for aspartic acid (D178N) (Goldfarb et al. 1991).

Sporadic Cruetzfeldt-Jacob disease accounts for 85% of all CJD cases with annual worldwide incidence of 1-2 cases/million population. Clinical symptoms include rapidly progressive dementia, cerebellar dysfunction including muscle incoordination, and visual, speech and gait abnormalities. Dementia is the major symptom followed by spontaneous or induced myoclonia. During the disease course, symptoms of pyramidal and extrapyramidal dysfunction with reflexes, tremors, spasticity and rigidity, and behavioral changes with agitation, confusion and depression may also be observed. At the end of the disease course, most of patients go into a state of akinetic mutism (they become unresponsive to exterior stimuli) (Belay 1999). The clinic-pathological and molecular phenotypes of sCJD are greatly influenced by variations in PRNP. PRNP polymorphisms, like M129V or E219K (Palmer et al. 1991, Shibuya et al. 1998) as well as coding sequences have been associated with predisposition to the disease development.

Infectious forms of human prion diseases account for only 5% of cases of human prion diseases (Muhammad et al. 2011). They include kuru, iatrogenic CJD and a new variant form of CJD.

Kuru has occurred exclusively in the Fore linguistic group of Papua New Guinea Eastern Highlands and the neighboring peoples with whom they intermarried. There was a practice among these groups to consume the dead bodies of their relatives as a mark of respect and mourning (ritualistic cannibalism). Women and young children of both sexes were more exposed to the risk material such as brain and viscera than adult men who usually had preferentially to consume muscles. The kuru epidemic killed 1-2% of the population at its peak. With a ban on ritualistic cannibalism in the mid 1950s imposed by Australian authorities, the incidence of the disease started to decline steadily (Glasse 1967). Cerebellar ataxia, tremors and choreiform and athetoid movements are distinctive and prominent clinical signs.

Iatrogenic CJD (iCJD) was first described in 1974 in a person who received cadaveric corneal transplant from a patient of CJD (Duffy et al. 1974). Several cases of human prion disease, since then, have been associated with iatrogenic transmission of CJD due to intramuscular injections of contaminated cadaveric pituitary-derived human growth hormone (hGH) and gonadotrophin hormone or transplants of corneas obtained from people who died of CJD.

vCJD results from prions being transmitted from cattle with bovine spongiform encephalopathy (BSE, or "mad cow" disease) to humans through consumption of contaminated beef products.

In addition to the three prion diseases of humans, four disorders of animals are included in the ensemble of prion diseases: scrapie of sheeps and goats (the most studied of the prion diseases), bovine spongiform encephalopathy (BSE), transmissible mink encephalopathy and chronic wasting disease. Unlike in humans, prion diseases in animals mainly occur as infectious disorders. As in humans, prion disease in animals is characterized by neuropathologic changes, including vacuolation, astrocytic gliosis, and PrP deposition. Bovine spongiform encephalopathy, transmissible mink encephalopathy and chronic wasting disease are all thought to result from the ingestion of scrapie-infected animal products.

The prion protein and its interaction partners (aim of the thesis)

The identification of binding partners of the prion protein has always captured the attention of many research groups. The interest in finding PrP ligands is on one way due to the identification of the protein X, believed to be a necessary component of the pathogenic conformational conversion; on the other way it relies to the fact that PrP might not have an intrinsic physiological activity, but can

modifies the function of other proteins interacting with them. As a GPI-anchored protein, PrP was found to interact with some extracellular or plasma membrane proteins such as apolipoprotein, laminin, GAGs, caveolin-1, tyrosine kinase fyn (Vana et al. 2007 for review). It has also been proved that PrP can bind nucleic acid (Nandi 1997). Finally, PrP can interact with numerous intracellular proteins, most of them located in the cytosol. Among them we can find synapsin-1b, neuroglobin, 14-3-3 protein, tubulin and mahogunin (Nieznanski 2010 for review).
Even if the topological localization of PrP on the plasma membrane suggests that most of its binding partners are extracellular or membrane-associated, there are increasing evidences that the identification of new intracellular interaction partners of the prion protein may be useful to understand both the physiological role of the protein and the mechanism involved in neurodegeneration.

PrP is located in the cytosol in subpopulations of neurons in the hippocampus, neocortex, and thalamus. Cytosolic PrP may have altered susceptibility to aggregation, suggesting that these neurons might play a significant role in the pathogenesis of prion diseases (Mironov et al. 2003). Other studies have suggest that in TSE PrP^{SC} inhibits the proteasome leading to the accumulation of cytosolic PrP (Kristiansen et al. 2007) and that accumulation of even small amounts of cytosolic PrP are strongly neurotoxic in cultured cells and transgenic mice (Ma et al. 2002). Hence, particularly at pathologic conditions, intracellular proteins may be exposed to interactions with PrP. It is also plausible that at its normal, low concentration in the cytoplasm PrP may modulate the physiological functions of the interacting proteins whereas at elevated, pathological levels it may dysregulate them leading to neurodegeneration (Nieznanski 2010). Moreover, some physiological interactions with intracellular proteins may be related to biogenesis/modifications of PrP and trafficking of PrP within the cell and therefore they may control PrP expression, localization and activity.

In this contest, we tried to find out neurologically relevant PrP binding partner conscious that the identification of PrP interactors or inhibitors of interaction can help us to better understand the role of the prion protein in physiological and pathological condition, but also that they may be considered as potential target for drugs.

Tyrosine hydroxylase

Tyrosine hydroxylase (also known as tyrosine 3-monooxygenase) is an enzyme that catalyses the conversion of L-tyrosine to L-dopa, which is the first, rate-limiting step in the biosynthesis of catecholamines dopamine, noradrenaline and adrenaline, important as hormones and neurotransmitters in both the central and peripheral nervous systems, where they are synthesized in the adrenal medulla. Catecholamine neurotransmitters in the brain regulate a wide range of brain function, such as movement, cognition, learning, emotion, memory, biorhythm, reproduction and endocrine function by acting across synapses through dopamine receptors and α- and β- adrenaline receptors of the neuronal network. In peripheral tissue, noradrenergic sympathetic neurons secrete noradrenaline as a neurotransmitter from their nerve endings. The adrenomedullary cells secrete adrenaline as hormones which regulate various functions such as stress reactions, blood pressure, blood glucose level and blood circulation, by acting on cells with α- and β- adrenaline receptors. Deficits and surfeits in the levels of catecholamines have many repercussions and are involved in many diseases including neuropsychiatric diseases (Parkinson's disease and schizophrenia), cardiovascular diseases (hypertension and cardiac diseases) and metabolic diseases (diabetes mellitus). All these functions and involvements into several diseases make tyrosine hydroxylase an enzyme of great interest in many fields of biomedical research (Nagatsu 1995, Daubner et al. 2011).

The TH reaction

Together with phenylalanine hydroxylase and tryptophan hydroxylase, tyrosine hydroxylase belongs to the family of aromatic amino acids hydroxylases (AAAHs), a group of iron-containing, biopterin-dependent amino acid hydroxylases. All three hydroxylases are rate-limiting catalysts that use tetrahydrobiopterin (BH_4) and O_2 to hydroxylate their respective aromatic amino acid substrates (Fitzpatrick 1999). The hydroxylation in the META position of L-tyrosine to DOPA is catalyzed by TH together with BH_4, O_2 and Fe^{2+}. In the reaction, the cofactor 5,6,7,8-tetrahydrobiopterin (BH_4) is converted into tetrahydrobiopterin-4a-carbinolamine (4a-BH_4). Under physiological conditions, 4a-BH_4 is dehydrated to quinonoid-dihydrobiopterin (q-BH_2) by the enzyme pterin-4a-carbinolamine dehydratase (PCD) and a water molecule is released in this reaction. Then, the NAD(P)H dependent enzyme dihydropteridine reductase (DHPR) converts q-BH_2 back to BH_4 (Teigen et al. 2007). The Fe^{2+} is bound to TH and is able to be oxidized to Fe^{3+} by O_2 and when this reaction occurs, the enzyme is inactivated (Ramsey et al. 1996).

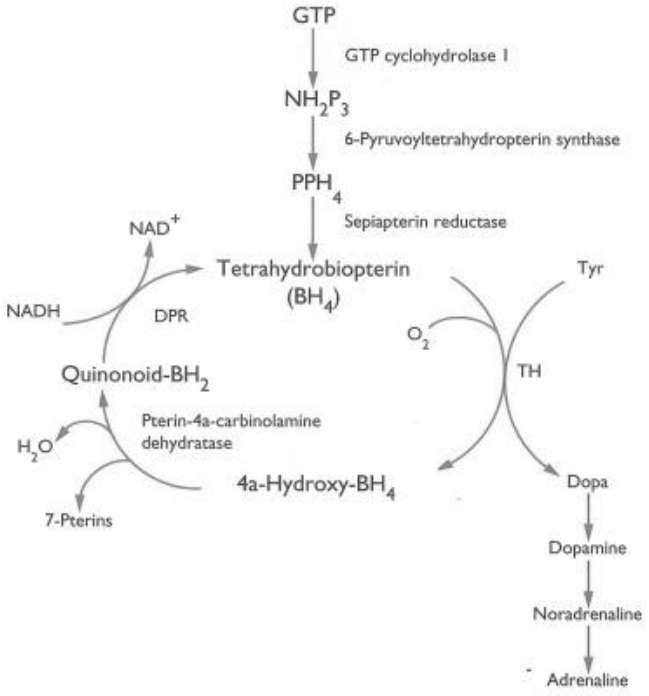

Fig: 8. BH_4 pathway and involvement in the biosynthesis of catecholamines (Nagatsu 1995).

TH is subject to two types of feedback inhibition by the catechols. Firstly, TH activity is inhibited by the ability of all of the catechols to compete with BH_4 for binding of the ferric iron at the catalytic site of the enzymes thus inhibiting cofactor interaction; secondly, catechols can bind almost irreversibly with the ferric iron at the TH catalytic site (Kumer and Vrana 1996). Loss of CA binding allows the Fe^{3+} to be reduced by BH_4, thereby returning the enzyme to the fully active state. TH is also subject to inhibition by the substrate L-tyrosine and by excess BH_4 (Dunkley et al. 2004).

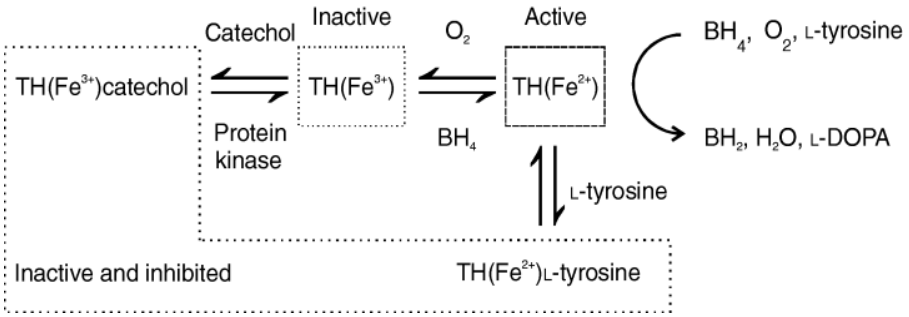

Fig: 9. Active and inactive form of tyrosine hydroxylase (Dunkley et al. 2004).

The product of the enzymatic reaction, L-DOPA, can be transformed to dopamine by the enzyme DOPA decarboxylase. Dopamine may be converted into norepinephrine by the enzyme dopamine β-hydroxylase, which can be further modified by the enzyme phenylethanol N-methyltransferase to obtain epinephrine (Nagatsu et al. 1964).

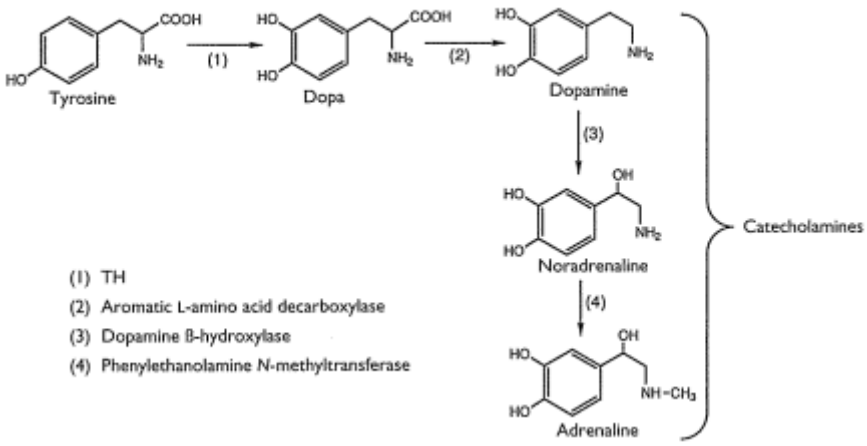

Fig: 10. Pathway of the biosynthesis of catecholamines (Nagatsu 1995).

The TH gene

The human TH gene is located on the short arm of chromosome 11 in band 15.5, a highly gene-rich region (Craig et al. 1986). In humans it consists of 14 exons, interrupted by 13 introns, spanning approximatively 8,5 Kb, while it has 13 exons in animals. In subprimates, a single form of tyrosine hydroxylase (TH) is expressed (Haycock 2002), whereas two TH protein isoforms have been identified in monkeys (Ichinose et al. 1993) and four isoforms have been demonstrated in humans. The four isoforms are produced from a single gene by alternative mRNA splicing in the N-terminus (Kobayashi et al. 1988) and they differ only in the inclusion of 12, 81 or 93 base pairs sequences between nucleotide 90 and 91 of the human TH mRNA. There are two modes of alternative splicing: the alternate use of two donor sites in exon 1, whereby the selection of the two donor sites determines the insertion of the 12bp sequence; and the insertion of an entire exon 2 (Nagatsu 1995).

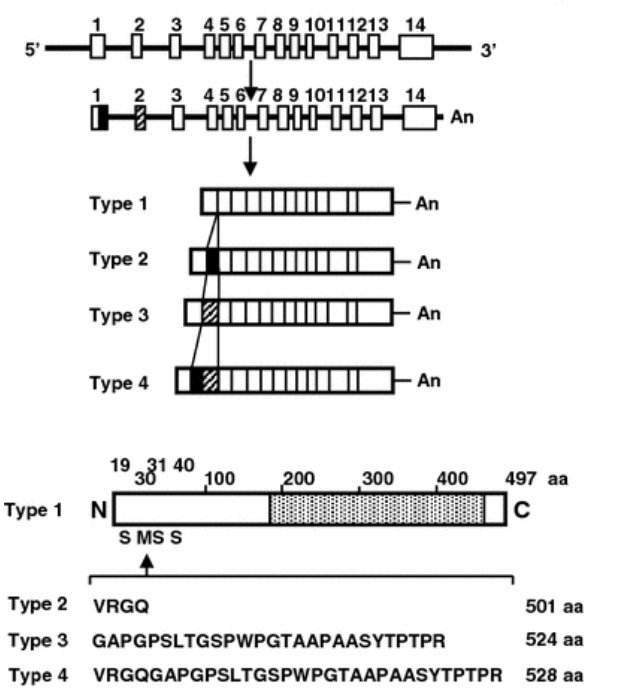

Fig: 11. Structure of the human TH gene and schematic illustration of the pathway of alternative splicing producing four isoforms of mRNA and proteins (adapted from Nakashima et al. 2009).

Tyrosine hydroxylase is found in the brain, gut and retina, the sympathetic nervous system and the adrenal medulla. The protein exists both in cytosolic and membrane-associated forms (Kuhn et al. 1990). The distribution of the two forms seems to be region-specific, with soluble TH predominating in the substantia nigra and locus coeruleus, while in nerve endings or axons the enzyme it seems to be associated with microtubules and membranes (Pickel et al. 1975). The membrane association seems to be related with the packaging of transmitter into synaptic vesicles (Chen et al. 2003). The binding of tyrosine hydroxylase to membranes involves the N-terminal region of the enzyme, and may be regulated by a three-way interaction between 14-3-3 proteins, the N-terminal region of tyrosine hydroxylase, and negatively charged membranes (Halskau et al. 2009).

The TH structure

Tyrosine hydroxylase is a tetrameric protein of about 240KDa, each subunit having a mass of approximatively 60 KDa. It is constituted of 498 amino acids and is highly conserved among species. Tyrosine hydroxylases shares a lot of structural features with the others member of the aromatic amino acid hydroxylases (AAAHs) phenylalanine hydroxylase (PheH) and tryptophan hydroxylase (TrpH). Each enzyme has a multi-domain structure, with an amino-terminal regulatory domain of varying size from 100–160 amino acid residues, and a carboxyl terminal domain composed of a catalytic domain of about 330 residues and a coiled-coil domain at the carboxyl

terminus of about 40 amino acids that allows the tetramerization of the protein (Vrana et al. 1994; Daubner et al. 2011). The catalytic core bounds iron atom, which is held in place in the active site cleft by two histidine residues and a glutamate residue, and it must be in the ferrous state to carry out catalysis. While there is a fine crystal structure of the C-terminus domain of the protein (Goodwill et al. 1997), the N-terminus has never been crystallized, presumably due to its flexibility and also attempts to crystallize it with ligands have been unsuccessful (Daubner et al. 2011).

Fig: 12. Crystal structure of human tyrosine hydroxylase catalytic domain (PDB ID: 2XSN).

TH regulation

Since tyrosine hydroxylase catalyses the rate limiting step in the biosynthesis of catecholamines, it is regulated in a very complex way. In the short term, TH activity is mainly regulated by phophorylation of serine residues in the N-terminus regulatory domain by various protein kinases; in the long term, such as under stress, TH is regulated at the transcriptional level resulting in the induction of the enzyme.

In the short term, TH is subject to two types of feedback inhibition by the catechols. Firstly, TH activity is inhibited by the ability of all of the catechols to compete with BH 4 for binding of the ferric iron at the catalytic site of the enzymes thus inhibiting cofactor interaction. This is a classic kinetic-mediated, readily reversible inhibition and acts as a sensor of the local concentrations of the catechols. Secondly, catechols can bind almost irreversibly with the ferric iron at the TH catalytic site. This decreases enzyme activity and stabilizes the enzyme (Kumer and Vrana 1996). Phosphorylation of TH alters the enzyme's conformation leading to a form of TH that is still inhibited but one in which dissociation of bound catechols is now reversible (Ramsey and

Fitzpatrick 1998). Loss of catechols binding allows the Fe^{3+} to be reduced by BH_4, thereby returning the enzyme to the fully active state. TH is subject to feedback inhibition by a range of catechols but the physiologically relevant catecholamines dopamine, noradrenaline and adrenaline all have the highest affinity. Catecholamines inhibit TH activity by competing with BH_4 for the catalytic binding site. The effect of phosphorylation of TH is to cause a conformational change in TH and decrease the affinity of the bound catechols and therefore increase their rates of dissociation. (Ramsey and Fitzpatrick 1998; Ramsey and Fitzpatrick 2000, Dunkley et al. 2004).

The most important short term mechanism for regulation of TH is activation by phosphorylation via protein kinases and deactivation by dephophorylation by protein phosphatases. Rat TH can be phosphorylated at serine residues (Ser) 8, 19, 31 and 40 by a variety of protein kinases (Haycock and Wakade 1992). The human isoforms undergo phophorylation also at Thr8 (Grima et al. 1987). The regulation of the phosphorylation of these sites and the consequences in terms of TH activity *in vitro* have been extensively investigated, while *in vivo* mechanisms are less clear. Tyrosine hydroxylase can be phosphorylated at Ser40 *in vitro* by eight different protein kinases and dephosphorylated at Ser40 by two protein phosphatase. The protein kinases include protein kinase A (PKA), protein kinase C (PKC), calcium- and calmodulin- stimulated protein kinase (CaMPK) II, protein kinase G (PKG), MAPK-activated protein kinases (MAPKAPKs) 1 and 2 , p38-regulated/activated kinase (PRAK) and mitogen- and stress-activated protein kinase (MSK) 1. Ser40 is phosphorylated mainly by PKA that is able to phosphorylate Ser40 of all four subunits of the enzyme molecule, causing a marked activation, whereas PKC and CaMPK phosphorylate only two of the four subunits. MAPKAPK2 had a preference for Ser40 and phosphorylated Ser19 at about half the rate while CaMPKII and PRAK had a preference for Ser19. Ser40 is dephosphorylated by protein phosphatase 2A and 2C (PP2A and PP2C).

Ser31 is phosphorylated by the extracellular signal-regulated kinase 1 and 2 (ERK1 and ERK2), two microtubule associated protein kinases. The phosphorylation of TH at Ser31 is much slower and increased the enzyme activity to a lesser extent than that of both Ser19 and Ser40 and often occurs at the time when Ser19 phosphorylation is already declining. Ser31 is dephosphorylated by PP2A.

TH is mainly phosphorylated at Ser19 by the CaMPKII in response to depolarizing agents and increases in intracellular calcium. Ser19 is also phosphorylated by MAPKAPK2 and PRAK. Ser19 is dephosphorylated by PP2A and PP2C.

Ser8 is phosphorylated by PDPK and can also be phosphorylated by ERK *in vitro* but at a ninefold lower rate than Ser31. The phosphorylation of TH at Ser8 has been shown to be increased by EGF

(Haycock 1990, Sutherland et al. 1993, Nagatsu 1995, Dunkley et al. 2004, Lehmann et al. 2006, Daubner et al. 2011).

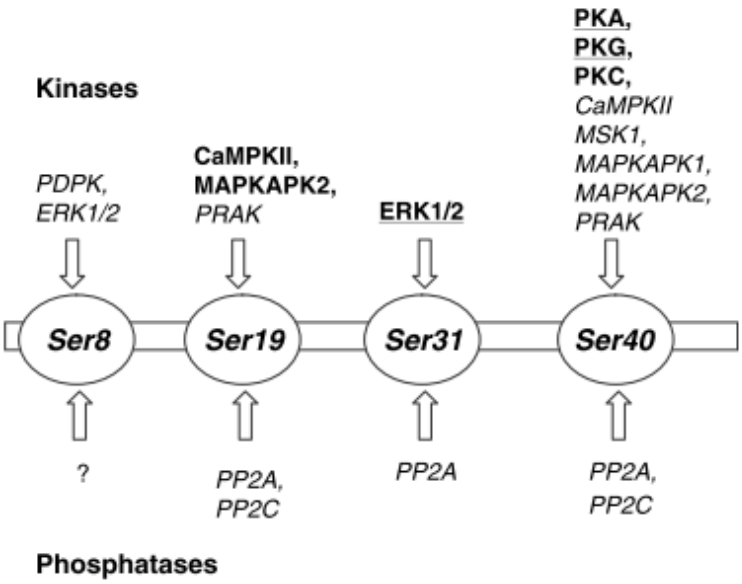

Fig: 13. Kinases and phosphatases acting on TH serine residues (Dunkley et al. 2004).

In the presence of NO and superoxide TH is nitrated at three tyrosine residues with resulting loss of activity. Nitration may be a mode of regulation of TH activity in the cell. Oxidizing conditions also result in the modification of six of the seven cysteine residues of TH by thiolation.

TH is, also, regulated by the interaction with other proteins. In 1987, Ichimura et al. found that 14-3-3 protein, an acidic neuronal protein, activates the enzyme. Only in the presence of 14-3-3 protein, TH is activated by phosphorylation of Ser19 (Ichimura et al. 1987). Also α-synuclein, shown to shares physical and functional homology with 14-3-3 protein (Ostrerova et al. 1999), can modulate the activity of TH. α-synuclein has been shown to bind to TH and to diminish TH phosphorylation and DOPA production (Perez et al. 2002).

TH can also be regulated in the long term, such as under chronic stress, by regulation of gene expression (enzyme stability, transcriptional regulation, RNA stability, alternative RNA splicing and translational regulation). Protein kinases, that activate the enzyme in the short term, can also induce TH protein in the long term, having a dual regulatory role. The expression of TH can also be regulated in the long term by various first messengers such as dopamine, dopamine agonist and antagonist, angiotensin II and by PKA and PKC signal transduction pathways (Nagatsu 1995).

TH in diseases

Since catecholamines are closely related to the pathogenesis of neuropsychiatric and cardiovascular disorders, TH has been suggested to play an important role in a number of diseases. TH seems to be particularly involved in the pathogenesis of Parkinson's disease, a common neurodegenerative disorder that is clinically characterized by tremor, bradykinesia, rigidity, and loss of postural reflexes. It is believed that these symptoms are caused by a dopamine deficiency due to degeneration of dopaminergic neurons probably accompanied by a decrease dopamine biosynthetic capacity in the surviving cells. A direct pathogenic role of TH has also been suggested as the enzyme is a source of reactive oxygen species (ROS). These compounds can cause oxidative damage to cellular macromolecules (lipids, protein, nucleic acids and carbohydrates) leading to cellular death (Haavik and Toska 1998). TH expression and activity have also been related to mental diseases, especially bipolar affective disorders and schizophrenia. To better understand TH alteration consequences, genetically modified mice carrying targeted mutation in the TH gene were generated. Knockout mice lacking the TH gene (homozygous mutation) die at a late stage of embryonic development or soon after birth. Lack of TH activity in these mice causes severe depletion of dopamine, noradrenaline, and adrenaline in tissues. These changes do not affect gross development of the cells that normally produce catecholamines. However, surviving newborn mutants display abnormal electrocardiograms characterized by reduced heart rate and prolonged P–Q interval, suggesting alterations in cardiovascular function in the mutant mice. Knockout of TH function causes perinatal lethality probably because of cardiovascular failure (Kobayashi et al. 1995, Zhou et al. 1995, Kobayashi and Nagatsu 2005).

Mice heterozygous for the TH mutation show a reduced TH activity in the tissues (approximately 40% of the wild type), although they are apparently normal in development and gross behavior. In these mice, noradrenaline accumulation in the brain regions is moderately reduced to 73–80% of the wild type levels and the reduction in TH activity causes defects in some neuropsychological functions at least associated with noradrenaline transmission in the brain (Kobayashi et al. 2000).

Mutations in the human TH gene have been reported in some inherited neurological diseases. Lüdecke et al. identified a point mutation in exon 11 of the tyrosine hydroxylase gene, resulting in an amino acid exchange of Gln381 to Lys381, in a Segawa's syndrome affected family (Lüdecke et al. 1995). When expressed by a coupled *in vitro* transcription-translation system and in *E.coli*, the mutant enzyme represents a kinetic variant form, with a reduced affinity for L-tyrosine. The 'residual activity' of about 15% of the corresponding wild-type hTH is compatible with the clinical phenotype of the two Q381K homozygote patients carrying this recessively inherited mutation

(Knappskog et al. 1995). Another mutation in the tyrosine hydroxylase gene was found in three patients originating from three unrelated Dutch families with autosomal recessive L-DOPA-responsive dystonia (DRD). An A698G transition in the exon six resulted in the substitution of the evolutionary conserved arginine 233 by a histidine (R233H) (Van den Heuvel et al. 1998). Moreover, a deletion of a single nucleotide C at the nucleotide 291 in the exon three, that generates a truncated form of TH protein, was identified in the patient who is compound heterozygous for this mutation and the mutation A to G at the nucleotide 698 (Wevers et al. 1999). Lüdecke et al. also identified a T614C transition in exon 5 resulting in a leucine to proline transition (L205P) in a girl presenting parkinsonian symptoms in early infancy and a very low level of the dopamine metabolite homovanillic acid in the CSF. The recombinant mutant enzyme had a low homospecific activity, approximately 1.5% of wilde type hTH in *E.coli* and approximately 16% in a cell-free in vitro transcription-translation system (Lüdecke et al. 1996).

All these data together seems to indicate TH as a potential molecular target for the treatment of catecholamines-related diseases. Cell transplantation or gene terapy may restore the TH activity, compensating for decreased levels of catecholamines in neurological and cardiovascular diseases, for example, for supplementation of dopamine in Parkinson's diseases.

HSPB8

A living cell responds to the different environmental stresses such as increased temperatures, pH extremes, osmotic pressure variation, hypoxia and noxious chemicals, by selectively inducing or overexpressing genes that code for protective proteins called HSPs (heat-shock proteins). HSFs (heat-shock factors) bind to HSEs (heat-shock elements) upstream of the HSP genes and bring about their increased expression, conferring tolerance to stress (Chowdary et al. 2004). Under stress conditions or as a result of genetic mutations, proteins tend to expose hydrophobic regions which are normally buried inside the molecule and become unstable. As a consequence of these novel acquired biophysical properties, these proteins will interact with each other through their hydrophobic regions, leading to protein aggregation which can also lead to the formation of highly ordered fibrillar aggregate called amyloid (Hartl et al. 2009, Hartl et al 2011, Carra et al. 2012). In such conditions, HSPs play a fundamental role acting as molecular chaperones. They recognize and bind to misfolded proteins and participate in either their refolding or, alternatively, assist their degradation via the major degradative systems (ubiquitine/proteosome and autophagy) (Carra et al. 2012). The modern classification of the human heat shock proteins, based on their molecular masses, contains the following main groups: HSPH (former name HSP110), HSPC (HSP90), HSPA (HSP70), HSPD/E (HSP60/HSP10) and CCT (TRiC), DNAJ (HSP40), and HSPB (small HSP) (Mymrikov et al. 2011, Vos et al. 2008).

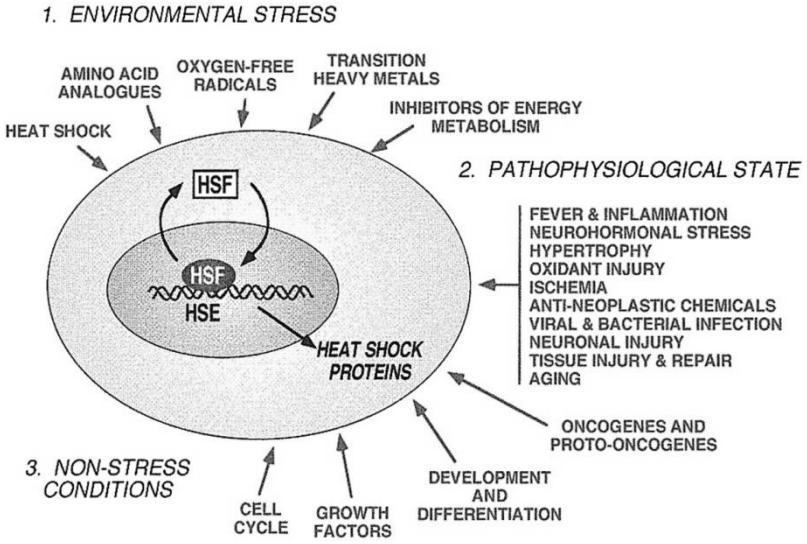

Fig: 14. Conditions that induce heat shock response (Morimoto 1998).

sHSPs perform many physiological functions including the maintenance of the cellular cytoskeleton, the regulation of protein aggregation and the modulation of cell survival in a number of cell types including glial and neuronal cells (Quraishe et al. 2008). The members of this family

share some important features: they form the conserved structure 'alpha-crystallin domain' with about 80-100 residues in the C-terminal part of the proteins; they have monomeric molecular masses ranging in 12-43 kDa; they associate into large oligomers consisting in many cases of subunits; they increase expression under stress conditions; they exhibit a highly dynamic structure and they play a chaperone-like role. Ten mammalian sHSPs have been identified so far (HSPB1-HSPB10), of which αβ-crystallin, HSP20 and HSP27 are the most extensively studied (Hu et al. 2007).

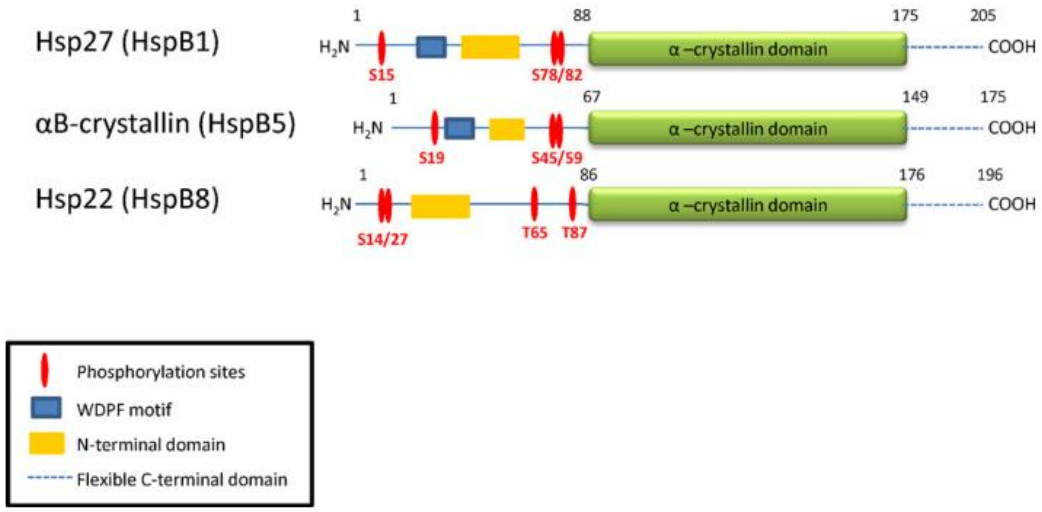

Fig: 15. Structural domains of HSP27, HSP22 and αB-crystallin human proteins (Acunzo et al. 2012).

Among them, HSPB8 (also named HSP22, H11, E2IG1) is of special interest because it seems to have an important role in a series of physiological and pathological process and because mutations in its sequence (K141E and K141N) correlate with the development of distal motor neuropathy type II and Charcot-Marie-Tooth disease type 2 (Irobi et al. 2004b, Tang et al. 2005). Moreover, recent studies showed that HSPB8 is trapped within inclusions formed by proteins with polyglutamine tails and is able to prevent formation of aggregates formed by this protein. HSPB8 was detected in senile plaques and cerebral amyloid angiopathy which are pathological lesions of Alzheimer's disease and hereditary cerebral hemorrhage with amyloidosis of the Dutch type (Carra et al. 2005, Wilhelmus et al. 2006, Wilhelmus et al. 2009). All these data together seem to suggest a protective role in the cell both by preventing aggregation and/or promoting degradation of improperly folded proteins and make HSPB8 a very promising target for understanding and cure neurodegenerative disease.

Different names of the HSPB8

The different names attributed to HSPB8 derive from independent works which describe novel-identified genes, subsequently found to have the same sequence.

Smith et al. reported the isolation and characterization of a novel gene, designated H11, that contains an open reading frame of 588 nucleotides, which encodes a protein similar to ICP10, the large subunit of herpes simplex virus type 2 ribonucleotide reductase which is a multifunctional protein that contains a serine-threonine protein kinase (PK) activity (Smith et al. 2000b). The H11 gene maps at chromosome site 12q24.1-12q24.31 (Yu et al 2001) and consists of 1835bp. A search for heat-shock elements revealed two heat-shock factor–binding sites upstream of ATG of the gene (Chowdary et al. 2004). The gene encodes a protein of 196 amino acids with a calculated molecular weight of 21.6 kDa. The protein shared a 40% identity to the small heat shock protein HSP27 (Aurelian et al. 2001). In the same year Charpentier et al. cloned five novel genes (E2IG1-5), which were observed up-regulated by hormonal treatment. Of these the most highly induced transcript, E2IG1, appeared to be a novel member of the family of small heat shock proteins, showing a 54% homology to HSP27 (Charpentier et al. 2000). In 2001 Benndorf et al performed a yeast two-hybrid screen of a human heart cDNA library for HSP27-interacting proteins. In this way they identified a protein with a molecular mass of 21.6 kDa containing the α-crystallin domain in its C-terminal half, a hallmark of the superfamily of small stress proteins. Thus, the new protein itself was considered a member of this protein superfamily, and consequently designated as HSP22 (Benndorf et al. 2001). Being the eighth known human sHSP it was named also HSPB8 (Kappé et al. 2001).

HSPB8 in Drosophila

In a review by Hu et al. HSPB8 gene is related to the Drosophila melanogaster HSP22 gene (Hu et al. 2007). The HSP22 gene was first described in 1980 by Craig and McCarthy which isolated a 11Kb region of the 67B locus of the Drosophila melanogaster genome including the 27K, 26k, 23K and 22K heat shock proteins. The DmHSP22 gene is approximately 1.1Kb in length and the RNAs encoding the heat shock proteins are transcribed from the same DNA strand (Craig and McCarthy 1980). Each of the four genes contains on their 5' flanking regions an A-T rich sequence, either TATAAATA or TATAAAAG, which is flanked by a G-C rich region. This A-T rich sequence ends about 23bp upstream from the proposed site of initiation of transcription. This sequence is also found in the gene for the major heat shock protein, HSP70 (Ingolia and Craig 1981). The gene encoding HSP22 has three heat shock element (HSE) upstream of the transcribed region and two of them are closely spaced and only 26 and 46bp from the TATA box (Klemenz and Gehring 1986). DmHSP22 was found to localize in the mitochondrial matrix where it tends to form oligomers *in*

vivo and it was shown to be a key player in cell-protection mechanisms against oxidative injuries and aging, playing a positive role in lifespan determination (Morrow et al. 2000,Morrow et al. 2004a-b, Tao et al. 2004, Wadhwa et al. 2010, Chen et al. 2011). Immunoprecipitation results indicate that there is no interaction between DmHSP22 and the other small heat shock proteins (Morrow et al. 2000). Moreover, it was shown that DmHSP22 expression in human cancer cells increased their malignant properties including anchorage-independent growth, tumor formation in nude mice, and resistance to a variety of anticancer drugs interacting and inactivating wild type tumor suppressor protein p53 (Wadhwa et al. 2010)

This direct relation between mammalian and Drosophila melanogaster HSP22 was, however, argued by Shemetov et al. in a more recent review. The authors sustain that it is inappropriate to directly compare DmHSP22 with mammalian HSP22 in the absence of a detailed phylogenetic analysis. A BLASTP structural comparison between human HSP22 and four sHSP of Drosophila (DmHSP22, DmHSP23, DmHSP26, DmHSP27), indeed, revealed that human HSP22 is more similar to DmHSP27 than to DmHSP22 (Shemetov et al. 2008b).

In 2010 Carra et al. finally suggested the Drosophila melanogaster HSP67Bc (Dm-HSP67Bc) as the closest ortholog of human HSPB8 on the basis of a functional analysis. Dm-HSP67Bc is, like human HSPB8, able to induces autophagy via the eIF2α pathway and has the in *vitro* potential to protect against mutated ataxin-3-mediated toxicity and decrease the aggregation of a mutated form of HSPB1 (P182L-HSPB1) associated with peripheral neuropathy (Carra et al. 2010).

Tissue distribution and cellular localization

Lots of laboratories focused their attention on the tissue distribution of HSPB8.

Verschuure et al. studied expression of sHSP in porcine lens, brain, heart, liver, kidney, lung, skeletal muscle, stomach, and colon, and found a ubiquitous expression of HSPB8. During development, the sHSPs tend to temporarily increase in stomach, liver, lung, kidney, hippocampus, and striatum, while expression in heart is more or less constant, and a large variation is found in sHSP expression patterns in skeletal muscle. In cerebellum and cortex a temporary decrease of HSP20 and HSPB8 is observed directly after birth (Verschuure et al. 2003).

Analysis of abundance of human HSP22 mRNA (Northern blotting) reveals a single signal in several tissues with a size of ~1.8 kilobase pairs. The highest expression of hHSP22 was found in skeletal and smooth muscles, heart, and brain. Expression was moderate in cervix, prostate, lung, and kidneys, whereas virtually no signal was seen in ovaries, testis, liver, pancreas, spleen and blood (Benndorf et al. 2001, Kappé et al. 2001).

The HSP22 expression in the brain has been intensively investigated. Quraishe et al. analyzed its expression in mouse brain by reverse-transcriptase polymerase chain reaction (RT-PCR), in situ hybridization and Western blotting. The results demonstrate a ubiquitous expression of HSPB8 involving the dorsal 3rd (d3v) and later ventricles (lv) of the brain, but also the synaptosomal fraction (Quraishe et al. 2008). Using in situ hybridization and quantitative real-time RT-PCR, Kirbach et al. showed HSPB8 to be expressed in all rat brain regions. The expression is low in embryonic and postnatal hippocampus while increase significantly in adult hippocampus. Heat shock in cultured hippocampal neurons lead to a significant induction of *HSPB1* and *HSPB8* but not of the other sHSPs (Kirbach et al. 2011).

In a recent work Ramìrez-Rodrìguez and colleagues found that expression of HSPB8 increases during differentiation *in vitro* and is particularly associated with later stages (48-96 h) of differentiation. In the dentate gyrus of adult mice *in vivo*, lentiviral overexpression of HSPB8 doubles the surviving cells and concomitantly promotes differentiation and net neurogenesis without affecting precursor cell proliferation through a mechanism involving the α-crystallin domain of the protein (Ramírez-Rodríguez et al. 2013).

All these data suggest that HSPB8 might be a very important modulator of brain growth, being involved in both neuron cell cycle and neuroprotection under stress conditions.

The cellular localization of HSPB8 is, to date, not well characterized. The data of size-exclusion chromatography of extracts of estrogen receptor-positive breast cancer cells indicate that HSPB8 is detected predominantly in cytoplasm and is eluted in the fractions containing proteins with apparent molecular masses in the range of 30–670 kDa (Sun et al. 2007). However, other studies indicate that it may interact with the membrane or proteins associated with the inner surface of the membrane (Yu et al. 2001). Immunolocalization studies in a human neuroblastoma cell line, SK-N-SH, using confocal microscopy show that a significant fraction of HSP22 is localized to the plasma membrane. *In vitro* studies show that HSP22 binds stably with lipid vesicles; the extent of binding depends on the nature of the lipid. HSP22 binds more strongly to vesicles made of lipids containing a phosphatidic acid, phosphatidylinositol or phosphatidylserine headgroup (known to be present in the inner leaflet of plasma membrane) compared with lipid vesicles made of a phosphatidylcholine head-group alone and this binding can lead to conformational changes of the protein suggesting an important role of the interaction in the cellular function of the protein (Chowdary et al. 2007).

HSPB8 physicochemical properties and interaction with sHSPs and other ligands

Up to now all attempts to obtain structural data of full size mammalian sHSP were predominantly unsuccessful, and most investigations were performed on isolated crystallin domains of these proteins (Kasakov et al. 2007, Datskevich et al. 2012b).

HSP22 was categorized as a sHSP based on the presence of the conserved α-crystallin domain in this protein. In HSP22, the N-terminal domain extends from residues 1–85 while the α-crystallin domain comprises residues 86–176. The calculated mass of HSP22 is 21.6KDa. It has an acidic pI of 4.9 and it is more stable at pH 8.0 than at neutral pH (Benndorf et al. 2001, Chowdary et al. 2004, Hu et al. 2007).

The far-UV CD spectra and predictions of secondary structure indicate that the protein belongs to the group of the so-called "intrinsically disordered proteins" and this is one of the reasons for its unusual high thermal stability. The protein contains very small quantities of α-helices (5%) and is enriched in unordered structure (58%) and β-strands (36%). According to the predictions, residues 153–155 of HSP22 tend to form a α-helix, whereas residues 156 and 157 tend to form a short β-strand that might correspond to the β8 strand of the other sHSP (Chowdary et al. 2004, Kim et al. 2004b, Chowdary et al. 2007, Kasakov et al. 2007, Kasakov et al. 2009). The sequence of HSP22 shows the presence of three cysteine residues not being involved in any disulphide bond, according with the fact that the occurrence of disulphide bonds in the HSPs is very rare (Chowdary et al. 2004).

The available literature indicates that HSP22 is highly susceptible to proteolysis (Benndorf et al. 2001, Chowdary et al. 2004, Kim et al. 2006).

The data on oligomeric structure of HSPB8 remain controversial.

Quaternary structure analyses by glycerol density-gradient centrifugation and gel filtration chromatography showed that HSP22 exists as a monomer in vitro, unlike other members of the sHSP family (Chowdary et al. 2004). However, most studies do not agree with this view. Two-dimensional gels of cell extracts showed signals at an apparent molecular mass of ~50 kDa indicating the existence of hHSP22 dimers similar to what has been described for other sHSPs such as hHSP27 (Benndorf et al. 2001). If the cell extract is subjected to glycerol gradient ultracentrifugation, HSPB8 sediments as a dimer (or even as a tetramer) (Chávez Zobel et al. 2003). Data from size exclusion chromatography and chemical crosslinking with dimethylsuberimidate indicate that HSP22 forms stable dimers (Kim et al. 2004b, Kim et al. 2006), while yeast two-hybrid assays showed that HSPB8 not only forms dimmers but also high-order oligomers and that HSP22 homo-dimers are formed through N-N and N-C interactions (Sun et al. 2004). More recent

works suggested that wild type HSPB8 forms a mixture of monomers and dimers depending on concentration (Kasakov et al. 2007, Datskevich et al. 2012a) and that rat HSPB8 exists in a dynamic equilibrium between various oligomers mainly forming tetramer in physiological condition (pH 7.4) or octamers in non physiological solution (Yang et al. 2012).

Benndorf et al. firstly described, performing yeast two hybrid system screen, HSPB8 as a interaction partner of a triple aspartate mutant of HSP27 (Benndorf et al. 2001). Since then, numerous studies have focused on possible interaction between HSPB8 and other members of the small heat shock proteins family. Using various techniques Sun and colleagues showed that HSP22 interacts not only with itself, but also with cvHSP (HSPB7), MKBP (HSPB2) and HSP27. HSP22-cvHSP hetero-dimers are formed through C-C interaction while HSP22-MKBP and HSP22-HSP27 hetero-dimers involve the N and C termini of HSP22 and HSP27, respectively, but appear to require full-length protein as a binding partner (Sun et al. 2004). Subsequently it was shown that HSP can interact also with HSPB6, αβ-crystallin and HSPB3 and (Fontaine et al. 2005, Fontaine et al. 2006, Mymrikov et al. 2012) even if some studies report that HSPB8 fail to interact with HSPB3 and HSPB1 (Fontaine et al. 2005, Datskevich et al. 2012a). It is possible that the creation of a binding between the proteins and its strength depends on the techniques and the condition used to study the interaction.

Several factors or modifications can affect the physicochemical properties of the protein. Mutations associated with the development of neuropathies, for instance, can modulate HSP22 homo- and hetero-oligomerization. These mutations do not dramatically affect the quaternary structure but, at the same time, induce destabilization of the overall structure of the sHSP (Kim et al. 2006, Kasakov et al. 2007). The data suggest aberrantly increased interactions of mutant HSP22 forms with themselves, αB-crystallin and HSP27. It seems that each mutant form of HSP22 has a characteristic pattern of abnormal interaction properties. Increased interactions involving mutant sHSPs may be the molecular basis for their increased tendency to form cytoplasmic protein aggregates, and for the occurrence of the associated neuropathies (Fontaine et al. 2006). Yeast two hybrid assay and intracellular FRET showed that the interaction of neuropathies-associated HSPB8 mutants with HSPB5 is stronger than the interaction of the wild-type protein with HSPB5 (Datskevich et al. 2012a). Moreover, Kasakov et al. revealed that mutation K137E and especially a double mutant K137,141E lead to an increase in unordered structure in HSP22 and increase susceptibility to trypsinolysis. Both mutations decrease the probability of dissociation of small oligomers of HSP22 and mutation K137E increase the probability of HSP22 crosslinking (Kasakov et al. 2007). Another study using phosphomimicking mutant showed that phosphomimicking mutation affect the tertiary

structure of the protein, promote concentration-dependent association of HSPB8 subunits and protect the protein from proteolysis (Shemetov et al. 2011). It has also been suggested that mild oxidation may increase the portion of unordered structure in the protein (Sun et al. 2004).

HSPB8 has been shown to interact not only with other members of the small heat shock proteins family, but also with a discrete number of other proteins. For instance, using two hybrid screen, HSP22 was found to interact with the RNA helicase Ddx20, a component of the survival-of-motor-neurons complex (SMN complex) involved in spliceosome assembly and pre-mRNA processing. Neuropathies-associated mutations have increased interaction stoichiometry with Ddx20, suggesting a potential role of HSPB8 in ribonucleoprotein processing (Sun et al. 2010). An exhaustive review by Arrigo et al. (Arrigo et al. 2013) reports all the known binding partner of HSP22, most of which are involved in the HSPB8 mechanisms of action (regulators of authophagy, protein aggregation and apoptosis regulators) related to neurodegenerative diseases and other diseases.

HSPB8 kinase activity and phosphorilation

Smith et al. were the first to describe the autophosphorylation activity of HSP22. Recombinant fusion GST-HSP22 purified from bacteria as well as immunocomplexes of HSP22 obtained from human cells possess autophosphorylating activity. The H11 protein has Mn^{2+} dependent serine-threonine-specific PK activity and it has been shown that mutation of Lys-113 located in the presumptive ATP-binding site results in complete ablation of autophosphorylation activity, whereas mutation of Lys-115 located outside of putative conservative protein kinase domains had no effect on the autophosphorylation of HSP22 (Smith et al. 2000b). Further experiment by Kim et al. showed using two different protein substrates (α-casein and histone IIIS), that HSP22 has very low or no kinase activity and that the activity recorded by Smith et al. was due to the presence of trace amounts of exogenous protein kinases contaminating immunocomplexes used in the experiments (Kim et al. 2004b). These finding were argued by Gober and colleagues that criticized the absence of a negative control (a protein that is known to lack kinase activity) and the lack of a construct mutated in the invariant lysine required for ATP binding (catalytic domain II). They indeed sustained that the data presented by Kim at al. together with the result showed by Chowdary et al., which evidenced that HSP22 can phosphorylate myelin basic protein (Chowdary et al. 2004), can prove the specificity of HSP22 kinase activity (Gober et al. 2004).

In a later work Kim and colleagues suggested that HSP22 contains only seven out of 11 motifs characteristic to protein kinases and even these seven motifs are not completely preserved.

Therefore, it is difficult to expect that isolated HSP22 will possess significant protein kinase activity (Kim et al. 2004a).
Anyway, the autokinase/kinase activity of HSP22 is still under investigation and it is not possible to surely state which of the two way of thinking is the right one.

Belonging to the group of intrinsically disordered proteins, HSPB8 seems to be a good substrate for different protein kinases (Mymrikov et al. 2011). *In vitro,* HSP22 is phosphorylated by protein kinase C (at residues Ser^{14} and Thr^{63}), by p44 mitogen-activated protein kinase (ERK1) (at residues Ser^{27} and Thr^{87}) and by casein kinase 2 but not by MAPKAPK-2 (Benndorf et al. 2001). Other *in vitro* experiments revealed that HSP22 is effectively phosphorylated by cAMP-dependent protein kinase and that Ser^{57} is the primary site of phosphorylation. Mutations S57D or S24,57D prevent phosphorylation of HSP22 and result in changes of the local environment of tryptophan residues and increase HSP22 susceptibility to chymotrypsinolysis (Shemetov et al. 2008a).
Modern proteomic methods provide important information on HSPB8 phosphorylation *in vivo*. Recently published data indicate that HSPB8 is phosphorylated at Ser^{24} (Cantin et al. 2008, Dephoure et al. 2008) and $Ser(Thr)^{87}$ (Villén et al. 2007). In addition, Tyr^{118} of HSPB8 was found to be phosphorylated in non-small-cell lung cancer cells (Rikova et al. 2007). Phosphomimicking mutants experiments showed that mutation S159D does not affect phosphorylation, whereas mutations S24D and S27D equally moderately inhibit phosphorylation and mutation T87D strongly inhibit phosphorylation of HSPB8. The double mutations S24D/T87D and S27D/T87D induce very strong inhibitory effect and the triple mutations S24D/S27D/T87D completely prevente phosphorylation catalyzed by ERK1. Phosphorylation promotes concentration-dependent association of HSPB8 subunits and affects the structure and chaperone-like activity of HSPB8 (Shemetov et al. 2011).

HSPB8 chaperone activity

Like the other members of the small heat shock protein, HSPB8 prevents aggregation of partially unfolded or denatured proteins *in vitro*. HSP22 was found to decrease heat-induced aggregation of citrate synthase, to retard or completely prevent aggregation of yeast alcohol dehydrogenase (ADH) and heat-induced aggregation of bovine liver rhodanese, and to prevent dithiothreitol-induced aggregation of insulin (Morrow et al. 2006, Sun et al. 2004, Chowdary et al. 2004). The chaperone-like activity is temperature and concentration dependent (Chowdary et al. 2004, Benndorf et al. 2001, Sun et al. 2004). Neuropathies-associated mutations have lower chaperone-like activity than

the wild type protein and the chaperone activity can also be influenced by phosphomimiking mutations and phosphorilation (Kasakov et al. 2007, Shemetov et al. 2011).

The most important and innovative results, anyway, are linked to the *in vivo* ability to prevent or decrease the accumulation of misfolded protein. This peculiarity property of the HSP22 is at the base of a large number of studies aimed at understanding the role of this protein in preventing protein aggregation, a hallmark of many neurodegenerative disorder.

HSPB8 and apoptosis

HSPB8 seems to play an important role in the regulation of apoptosis, an irreversible process resulting in cell death and particularly implicated in tumor growth and therapy. First results on HSPB8 regulation of apoptosis were a little bit controversial. Gober et al. first reported of a heat shock protein with proapoptotic activity. The H11 mRNA and protein levels were reduced in various tumor tissues and cell lines (melanoma, prostate cancer and sarcoma). In these cells, expression was not restored by heat shock, but rather by the demethylating agent 5-aza-2'-deoxycytidine (Aza-C). Forced H11 expression by Aza-C treatment triggered apoptosis. A single site mutant (H11-W51C) had cytoprotective activity related to MEK/ERK activation, and it blocked H11-induced apoptosis in co-transfected and Aza-C-treated cells, indicating that it is a dominant negative mutant (Gober et al. 2003). However, other studies reported anti-apoptotic effects. In these studies the ICP10 PK domain of herpes simplex virus type two HSV-2, homologue of H11/HSPB8 sharing with it 32% sequence identity and a number of functional properties (Aurelian et al. 2012), was able to protect HEK293 and PC12 cells from apoptosis activating the Ras/MEK/MAPK mitogenic pathway through a mechanism dependent on the protein kinase activity of the protein and leading to a Bag-1 upregulation (Perkins et al. 2002, Perkins et al. 2003, Smith et al. 2000a). Putting all these data together it seems reasonable that HSPB8 can exert both pro- and anti-apoptotic activity depending on the cell type (Gober et al. 2003, Shemetov et al. 2004b).

HSPB8 in the heart

Depre et al. firstly showed that H11 kinase gene expression is increased in a swine model of ischemia/reperfusion and in response to long-term pressure overload with hypertrophy, thus indicating possible involvement of this protein in cell survival. Adenoviral-mediated overexpression of H11 kinase, resulting in average 7-fold increase in protein expression, in isolated neonatal rat cardiac myocytes leads to a 37% increase in protein/DNA ratio, reflecting hypertrophy. This phenotype was accompanied by a dose-dependent activation of Akt/PKB and $p70^{S6}$ kinase, whereas the MAP kinase pathway was unaffected. These data showed a new mechanism by which the cardiac response to stress (both acute ischemia/reperfusion and chronic pressure overload) is

coupled to a stimulation of cell growth (Depre et al. 2001, Depre et al 2002). It was also proposed that H11 is a dual function kinase in cardiac rat cell: it induces hypertrophy at low doses through kinase-independent activation of Akt, whereas it causes apoptosis at high doses through protein kinase-dependent mechanisms, in particular by physical interaction and inhibition of CK2 (Hase et al. 2005). A study on metabolic adaptation to cardiac hypertrophy and ischemia revealed that H11 promotes the synthesis of glycogen, an essential fuel for the stressed heart in both conditions of overload and ischemia. In transgenic mice, overexpression of H11 gene resulted in an improve interaction of the protein with phosphoglucomutase (PGM), the enzyme converting glucose 6-phosphate into glucose 1-phosphate, and in 3-fold increase in the protein expression of the glucose transporter GLUT1 in plasma membrane, leading to an increase of glycogen content. Transgenic mice are characterized by increased phosphorylation (activation) of the α-catalytic subunit of AMPK, he major regulator of glucose utilization in the ischemic heart (Wang et al. 2004, Depre et al. 2006). Experimental data on transgenic mice also evidenced that the cardioprotection conferred by H11K is quantitatively comparable to the protection of preconditioning, a condition in which short episodes of ischemia/reperfusion activate survival kinases that will protect the heart against myocardial infarction during subsequent ischemia. This results is achieved through two mechanism of cardioprotection activated downstream of phosphatidylinositol 3-kinase (PI3K): on one way activation of Akt promotes the phosphorylation of several downstream effectors, including GSK-3β, Bad, the endothelial isoform of NO synthase (eNOS), and the transcription factor Foxo. Akt inhibits GSK-3β, an activator of cell death and the proapoptotic effector Bad while it activates the cytoprotective eNOS. In the nucleus, Akt phosphorylates the proapoptotic transcription factors of the Foxo family, which is followed by their inhibition, and increases the expression of heat shock proteins. On the other way H11K activates PKCε wich triggers the expression of the inducible isoform of NOS (iNOS), which is particularly important in activating the delayed mechanisms of myocardial protection after ischemia/reperfusion (Depre et al. 2006). Thus, H11K is responsible for the activation of two antagonistic pathways for cell growth, the Akt pathway, which stimulates protein synthesis through mTOR, and the AMPK pathway, which inhibits it. TG mice are characterized by an increased interaction between Akt and AMPK specifically in the nucleus. Both the AMPK and Akt pathways stabilize the hypoxia-inducible factor-1α (HIF-1α). HIF-1α results in an increased expression of genes encoding enzymes regulating anaerobic metabolism and growth factors. It was, therefore, proposed that the subcellular translocation of AMPK and Akt to the nuclear periphery prevents this paradox, thereby allowing AMPK to play its cytoprotective role without interfering with cell growth (Danan et al. 2007). More recently studies elucidated the signal pathways activated by the expression of HSPB8 in cardiac cells. H11K promotes the formation of

the BMP receptor complex, upregulating the BMP receptors Alk3 and BMPR-II, and their ligand BMP4. Activation of the BMP pathway in transgenic mice was confirmed by increased phosphorylation of the "canonical" BMP effectors Smad 1/5/8 leading to an increase in PI3K activity. H11K increased both the association of Alk3 and BMPR-II together, and their interaction with the transforming growth factor-beta-activated kinase (TAK)1, a "noncanonical" mediator of the BMP receptor signaling which mediates the activation of the PI3K/Akt pathway responsible for the physiological effects of H11K on cardiac cell growth and survival (Sui et al. 2009). *In vitro* and *in vivo* studies involving knockout mouse model deleted for HSP22 gene also demonstrate that HSP22 activates STAT3 via production of interleukin-6 by the transcription factor nuclear factor-κB leading to an increase iNOS expression. The increased nitric oxide production stimulates oxidative phosphorylation in normoxia and decreases oxidative phosphorylation and reactive oxygen species production after anoxia (Chen et al. 2011, Qiu et al. 2011, Laure et al. 2012). A recent experiment in mouse model of infarction showed that HSPB8, at least in part, plays an important role in the development of the impaired mitochondrial energy-producing ability that leads to heart failure after a myocardial infarction (Marunouchi et al. 2013). All these data suggest HSP22 as a potential tool for prophylactic protection of mitochondrial function during ischemia.

Moreover, characterization of the proteasome in hearts from TG mice overespressing HSPB8 revealed an increased expression of both 19S and 20S subunits, a doubling in 20S catalytic activity, a redistribution of both subunits from the cytosol to the nuclear periphery and a four-fold increase in nuclear-associated 20S catalytic activity (Hedhli et al. 2008). Taken together, these results demonstrate that H11K is responsible for the activation of a genomic program of cell survival that is involved in an antiapoptotic response via the Akt pathway, a preconditioning survival response by PKCε, a metabolic survival response via AMPK, and a growth response mediated by mTOR.

An arg120gly (R120G) missense mutation in HSPB5 (alpha-beta-crystallin) causes desmin-related cardiomyopathy (DRM), a muscle disease that is characterized by the formation of inclusion bodies, which can contain pre-amyloid oligomer intermediates. *In vitro* studies showed that HSPB8 can directly interrupt oligomer formation by the CryAB R120G protein. Blockade of amyloid oligomer formation by HSP25 and HSP22 recovered the ubiquitin proteosomal activity and cellular viability (Chávez Zobel et al. 2003, Sanbe et al. 2007). These previous results were extended *in vivo* by oral administration of geranylgeranylacetone (GGA), a potent HSPs inducer, in R120G transgenic (R120G TG) mice. Overexpression of HSPB8 led to a reduction in amyloid oligomer and aggregate formation, resulting in improved cardiac function and survival (Sanbe et al. 2009).

HSPB8 was also shown to protect against atrial fibrillation (AF), the most common sustained and progressive clinical tachycardia in the population, by attenuation of the RhoA GTPase pathway at different levels (Ke et al. 2011).

In *in vitro* studies, expression of HSPB8 K141N by adenoviral infection resulted in increased HSPB8-positive aggregates around nuclei and cardiac-specific HSPB8 K141N transgenic mice exhibited mild hypertrophy and apical fibrosis as well as slightly reduced cardiac function (Sanbe et al. 2013).

All these results, confer to HSPB8 a major role in preventing and fighting a series of cardiac disease. Even thought additional investigations have to be done to better understand HSP22 role in physiological and pathological conditions, its important role seems to be also confirmed by the fact that a single point mutation of HSPB8, such as K141N, can cause cardiac disease.

HSPB8 and Immune Response

A study by Roelofs et al. demonstrated that HSPB8 is involved in the activation of dendritic cells (DCs) through a mechanism dependent on its newly identified ligand toll-like receptor 4. The maturation of DCs induced by HSPB8 coincided with an increased production of the inflammatory mediators TNF-α, IL-6, IL-10, and IL-12p70. HSPB8 is abundantly expressed in synovial tissue from rheumatoid arthritis (RA) patients, suggesting a role during the inflammatory process in autoimmune diseases (Roelofs et al. 2006). Moreover, it was found that HSPB8 induced interleukin-6 production in cultured pericytes and astrocytes, thus it is supposed that HSPB8 might be among key mediators of local inflammation associated with hereditary cerebral hemorrhage with amyloidosis of the Dutch type (Wilhelmus et al. 2009)

HSPB8 and tumor

HSPB8 involvement in tumors has been extensively investigated but the exact role of the protein in this kind of pathologies remains not easy to understand. To date, it is thought that HSPB8 has divergent properties in tumors, exerting both pro- or- anti-proliferative effects depending on the cells.

The proliferative effect of HSPB8 was first suggested by Morrow and co-workers. They found that endogenous H11 RNA and protein are expressed in melanoma cell lines and primary melanoma tissues at levels higher than in normal melanocytes and in benign nevi, indicating that H11 expression is associated with cell growth (Smith et al. 2000b, Yu et al. 2001). Previous studies showed that treatment of human breast cancer cell line MCF-7 with 17β-estradiol results in up-regulation of the HSP22 gene (Charpentier et al. 2000). HSPB8 expression in also induced in

estrogen receptor-positive breast cancer cells. First, it was shown that in breast tumors induced by *erbB2* and *cyclin D1* HSPB8 displayed higher expression levels in invasive lesions than in preinvasive lesions using samples obtained by laser capture microdissection (LCM) from transgenic erbB2, ras, and cyclin D1 mice (Yang et al. 2006). Later, it was demonstrated that treatment of estrogen receptor-positive MCF-7 breast cancer cells with both estrogen (E2) and cadmium (Cd) is able to induce HSP22 showing also that in cytosolic extracts of MCF-7 cells, most of the E2- and Cd-induced HSP22 was incorporated into high-molecular mass complexes (Shemetov et al. 2008a). HSPB8 expression confers resistance to tamoxifen in breast cancer patients preventing the induction of autophagy and giving a proliferative advantage to the treated cells (Gonzalez-Malerva et al. 2011, Clarke 2011).

Despite these results, a lot of studies seem to suggest an anti-proliferative effect of the protein. Gober et al. showed that the H11 mRNA and protein levels were reduced in various tumor tissues and cell lines (melanoma, prostate cancer and sarcoma). In these cells, forced H11 expression by demethylating agent 5-aza-2'-deoxycytidine (Aza-C) triggered apoptosis. A single site mutant (H11-W51C) had cytoprotective activity related to MEK/ERK activation, and it blocked H11-induced apoptosis in co-transfected and Aza-C-treated cells, indicating that it is a dominant negative mutant (Gober et al. 2003). Other studies revealed that H11 is silenced by aberrant DNA methylation in 60-75% of melanoma and atypical nevi, but not in normal skin or most benign nevi. Methylation is inversely correlated with H11 expression. Aza-C induced H11/HSPB8 overload induces apoptosis in 55% of examined melanoma cultures. Apoptosis was determined by activation of caspases-9 and -3 and TUNEL, and was not seen in normal melanocytes. It was associated with H11/HSPB8 complexation with TAK1 and activation of TAK1 and p38MAPK. TAK1 was not bound, nor activated by the H11/HSPB8 mutant W51C, which has dominant anti-apoptotic activity. β-catenin was phosphorylated at Ser^{552} by activated TAK1, inhibiting its nuclear accumulation and MITF and CyclinE/CDK2 expression. The activation of TAK1 also lead to caspase-1 activation and beclin-1 upregulation. The data indicate that H11/HSPB8 overload causes melanoma growth arrest and apoptosis through TAK1 activation and suggest that H11/HSPB8 is a promising molecular therapy target (Li et al. 2007,Smith et al. 2011, Smith et al. 2012). Other works showed that HSPB8 overexpression markedly increase the effect of cyclin D1 which is paradoxically known to enhance radiation sensitivity (Trent et al. 2007). HSPB8 is known to interact *in vitro* and *in vivo* with Sam68 (Src-associated protein in mitosis 68kDa), a multifunctional protein, known to govern cellular signal transduction, transcription, RNA metabolism, proliferation, apoptosis, and HIV-1 replication. The critical domain of HSP*22* that interacts with Sam68 resides between amino acids 62 and 133. HSPB8 overexpression significantly inhibits Sam68 while HSP22 knockdown dramatically

increased both Sam68 mRNA and protein, altered cellular morphology, and enhanced cell proliferation. These results demonstrated for the first time that HSP22 regulates Sam68 expression and the ratio of Sam68 to HSP22 may determine the proliferative potential of glioblastoma cells (Modem et al. 2011, Badri et al. 2006). Promoter DNA methylation of HSPB8 was observed in hematopoietic tumor cell lines. HSPB8 expression could be restored after demethylation treatment with 5-aza-2′-deoxycytidine. Overexpression of HSPB8 reduced colony formation of both K562 and Namalwa cell lines, inhibited the cell growth of Namalwa in vitro, and suppressed tumor formation of K562 cells in vivo demonstrating that overexpression of HSPB8 may have an antitumor activity in chronic myelogenous leukemia and lymphoma (Cui et al. 2012).

HSPB8 in inherited peripheral neuropathies

The distal hereditary motor neuropathies (dHMN) are a genetically heterogeneous group of diseases affecting the peripheral nervous system, characterized by distal lower-motor-neuron weakness. This is in contrast to Charcot–Marie–Tooth disease (CMT) and the hereditary sensory neuropathies where sensory involvement forms a significant component of the disease. Nevertheless, many forms of dHMN have minor sensory abnormalities, and there is an overlap between the axonal forms of CMT (CMT2) and dHMN. However, even when the phenotype is classified as CMT2, motor signs and symptoms predominate. Similarly, minor sensory involvement is also recognized in other motor syndromes including amyotrophic lateral sclerosis (ALS), Kennedy's disease and spinal muscular atrophy (SMA) (Irobi et al. 2004a, Fontaine et al. 2006, James et al. 2006, Rossor et al. 2012).

Mutations in *HSPB8* were first identified as a cause of dHMN by Irobi et al. which identified in four separate families two missense mutations targeting the same amino acid: a K141N, c.423G→C (Lys141Asn) in Belgian and Czech families; and a K141E, c.421A→G (Lys141Glu) in English and Bulgarian families (Irobi et al. 2004b). Subsequently, a K141N, c.423G→T (Lys141Asn) was reported in a large Chinese family with Charcot–Marie–Tooth disease type 2 (CMT2) (Tang et al. 2005, Zhang et al. 2005). As said, the missense mutations K141N and K141E affect the same amino acid, a highly conserved lysine residue located in the central α-crystallin domain of HSPB8. This Lys141 residue corresponds to the residue Arg120 that is mutated in αB-crystallin, causing a familial desmin-related myopathy (DRM) (Irobi et al. 2004b). Recently, Nakhro and colleagues identified a fourth novel mutation K141T, c.422A→C (Lys141Thr) in the HSPB8 gene in a Korean axonal CMT patient who presented distal limb atrophy, sensory loss, areflexia, and axonal loss of large myelinated fibers (Nakhro et al. 2013). The mutation involves once again the same amino acid, suggesting Lys141 as a mutational hot spot for peripheral neuropathy development.

Despite the identification of these mutations, low mutation frequency is observed in the gene, with some works reporting low rate or no one mutations in the pedigrees studied (Rohkamm et al. 2007, Dierick et al. 2008, Capponi et al. 2011) and the pathological mechanisms of the diseases are not so well understood. Intriguingly, despite the ubiquitous presence of HSPB8, the motor signs and symptoms are much greater than the sensory manifestations and only motor neurons appear to be affected by the K141N and K141E mutations which explain the predominant motor neuron phenotype in distal HMN and CMT2 (Irobi et al. 2010, Züchner et al. 2006). It was proposed that mutations in the HSPB8 gene can result in a loss of function phenotype as suggested by the aggregation of the mutant protein into large formations leading to a reduction in the mitochondrial membrane potential in primary fibroblast of dHMN patients and the inhibited autophagy of misfolded protein in motor neuron-like NSC34 cells (Irobi et al. 2012, Kwok et al. 2011). Moreover, the last years have seen a growing list of evidence demonstrating that the mutations lead to dysfunctional intracellular trafficking and mitochondrial dynamics in CMT2 (Gentil et al. 2012). If these statements are correct, components that upregulate HSP-expression will be useful for hereditary peripheral neuropathies. However, if mutant small HSPs act as toxic components that induce neuronal cell death, an upregulation of these mutant proteins could make the pathology even worse. Therefore, the ideal therapeutic strategy would be to selectively inhibit the expression of the mutant protein and maintain the expression of wild-type proteins (Dierick et al. 2005).

HSPB8 in neurodegenerative diseases

Many neurodegenerative disorders are characterized by conformational changes in proteins that result in misfolding, aggregation and intra- or extra-neuronal accumulation of amyloid fibrils. Molecular chaperones provide a first line of defense against misfolded, aggregation-prone proteins and are among the most potent suppressors of neurodegeneration known for animal models of human disease. Recent studies have investigated the role of molecular chaperones in amyotrophic lateral sclerosis, Alzheimer's disease, Parkinson's disease and polyglutamine diseases (Muchowski and Wacker 2005). Some members of the small heat shock proteins family, including HSPB8, have been shown to be up-regulated and involved in the protection of neurons from various stress condition (Bartelt-Kirbach and Golenhofen 2013).

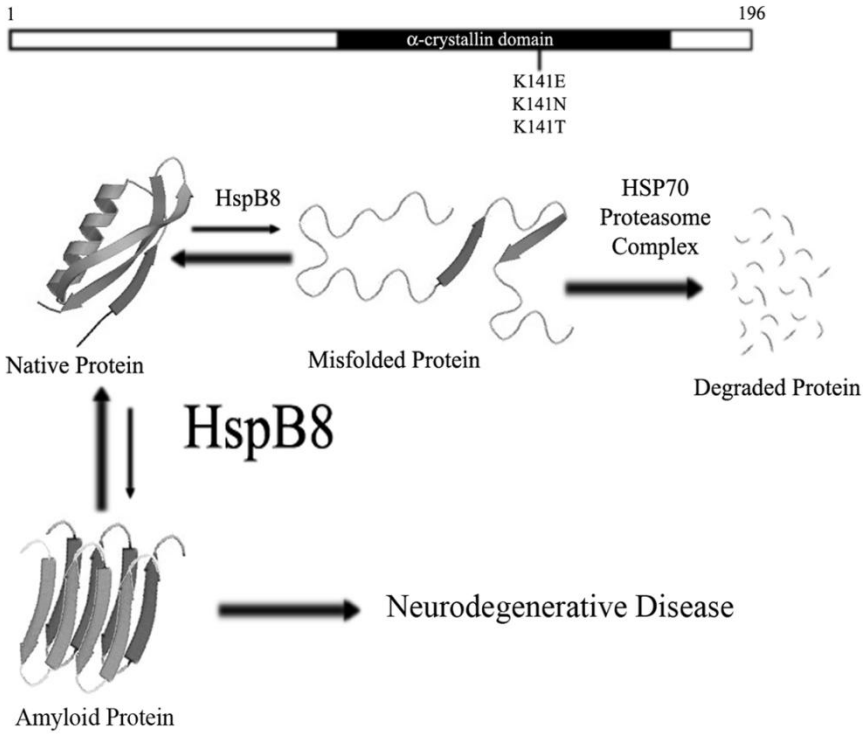

Fig: 16. The small heat shock protein HSPB8: a pathway to clear misfolded proteins in nervous system disease.

In 2005 Carra et al. investigated the capacity of HSP22, to prevent protein aggregation in the CCL39 cells using the polyglutamine protein Htt43Q, a pathogenic form of huntingtin responsible for Huntington's disease. In control conditions, Htt43Q accumulated in perinuclear inclusions composed of SDS-insoluble aggregates. Co-transfected with Htt43Q, HSPB8 became occasionally trapped within the inclusions; however, in most cells, it blocked inclusion formation. Biochemical analyses indicated that HSPB8 inhibited the accumulation of SDS-insoluble Htt43Q. This suggested that HSPB8 functions as a molecular chaperone, maintaining Htt43Q in a soluble state competent for rapid degradation. The C-terminal domain of HSPB8 contains the specific sequence necessary for chaperone activity. Neuropethies-associated mutations at Lys141 inhibited chaperone activity contributing to the development of the disease (Carra et al. 2005, Vos et al. 2010). The HSPB8 activity is based on the formation of a stable complex between the protein and Bag3 (Bcl-2-associated athanogene 3), a member of the co-chaperone family of Bag domain-containing proteins. Overexpressing Bag3 or HSPB8 stimulates the formation LC3-II, a key molecule involved in macroautophagy suggesting that the HSPB8-Bag3 complex might stimulate the degradation of Htt43Q by macroautophagy (Carra et al. 2008a). It was proposed that in the HSPB8-Bag3 complex, HSPB8 is responsible for recognizing the misfolded proteins whereas Bag3, through its proline-rich domain, might recruit and activate the macroautophagy machinery in close proximity to the chaperone-loaded substrates (Carra et al. 2008b). Biochemical methods indicate that the wild type HSPB8 forms tight complexes with Bag3 while K141E mutant weaker interact with Bag3 and that

the stoichiometry of complexes formed by HSPB8 and Bag3 is variable and is dependent on concentration of protein partners (Shemetov and Gusev 2011). The formation of the HSPB8–Bag3 complex results from the interaction between the hydrophobic groove in the sHSP and two IPV (Ile-Pro-Val) motifs in Bag3. The same IPV motifs are involved in the binding between Bag3 and wild-type αB-crystallin and the αB-crystallin mutant R120G, and a mutation in one of these IPV motifs (P209L) has recently been associated with a severe dominant childhood muscular dystrophy with experienced development of cardiomyopathy and peripheral neuropathy, suggesting a possible important role for the sHSP–Bag3 complex formation in the development of human congenital diseases (Fuchs et al. 2009, Hishiya et al. 2011). The HSPB8-Bag3 complex is highly upregulated upon viral infection and aging and induce the phosphorylation of the alpha-subunit of the translation initiator factor eIF2, which in turn causes a translational shut-down and stimulates autophagy (Carra 2009, Carra et al. 2009, Behl 2011). In a study aimed to analyze the involvement of NF-κB in basal and heat-stress-induced protein quality control, Nivon and colleagues showed that during heat shock recovery NF-κB activates selective removal of misfolded or aggregated proteins by controlling the expression of BAG3 and HSPB8 and by increasing the level of the BAG3-HSPB8 complex (Nivon et al. 2012). A strong upregulation of HSPB8 and a moderate upregulation of BAG3 specifically in astrocytes in the cerebral areas affected by neuronal damage and degeneration were, finally, found in post-mortem human brain tissue from patients suffering of a series of protein conformation disorders such as Alzheimer's disease, Parkinson's disease, Huntington's disease and spinocerebellar ataxia type 3 (SCA3) (Seidel et al. 2012).

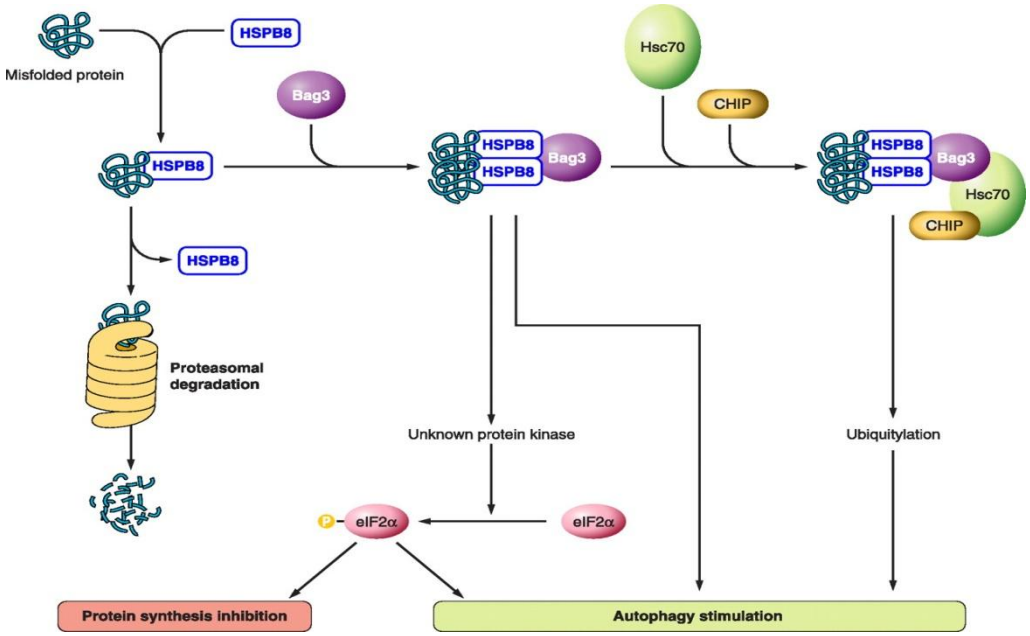

Fig: 17. Participation of HSPB8-Bag3 complex in regulated proteolysis of misfolded proteins (Mymrikov et al. 2011).

A study by Wilhelmus et al. observed HSPB8 expression in senile plaques (SPs), pathological lesions characterizing Alzheimer's disease (AD) and in cerebral amyloid angiopathy (CAA), the major pathological lesion in hereditary cerebral hemorrhage with amyloidosis of the Dutch type (HCHWA-D), caused by a mutation in the gene coding for the Aβ peptide. HSPB8 directly interact with wild-type $A\beta_{1–42}$, wild-type $A\beta_{1–40}$ or D-$A\beta_{1–40}$ having the highest binding affinity with the Dutch mutation. Co-incubation of HspB8 with D-$A\beta_{1–40}$ resulted in the complete inhibition of D-$A\beta_{1–40}$ -mediated death of cerebrovascular cells, likely mediated by a reduction in both the beta-sheet formation of D-$A\beta_{1–40}$ and its accumulation at the cell surface. HSPB8 also induced the production of interleukin-6, interleukin-8, soluble ICAM-1 and monocyte chemoattractant protein 1 in cultured astrocytes, suggesting a role as a mediator of the local inflammatory response associated with HCHWA-D and AD lesions (Wilhelmus et al. 2006, Wilhelmus et al. 2009, Bruinsma et al. 2011b).

HSPB8 expression was found to be significantly increased in amyotrophic lateral sclerosis (ALS), where a mutation in the superoxide dismutase 1 (SOD1) gene leads to the production of a mutant SOD1. The mutant SOD1 misfolds, forms insoluble aggregates and impairs the proteasome. In spinal cord motor neurons, HSPB8 decreases aggregation and increases mutant SOD1 solubility and clearance via autophagy, without affecting wild-type SOD1 turnover (Anagnostou et al. 2010, Crippa et al. 2012a-b).

HSPB8 was also related with Parkinson's diseases. Bruinsma and colleagues showed that HSPB8 was the most potent sHSP in inhibiting mature fibril formation of both wild-type and mutant α-synuclein (A53T, A30P, E46K), suggesting that an optimization of the interaction between HSP22 and α-synuclein may be an interesting target for therapeutic intervention in the pathogenesis of α-synucleinopathies (Bruinsma et al. 2011a).

Spinal and bulbar muscular atrophy (SBMA) is an X-linked motoneuron disease caused by an abnormal expansion of a tandem CAG repeat in exon 1 of the androgen receptor (AR) gene that results in an abnormally long polyglutamine tract (polyQ) in the AR protein. As a result, the mutant AR (ARpolyQ) misfolds, forming cytoplasmic and nuclear aggregates in the affected neurons. HSPB8 was shown to prevent AR65Q aggregation and facilitates the autophagic removal of misfolded aggregating species of ARpolyQ. Trehalose, an autophagy stimulator, induces HSPB8 expression, suggesting that HSPB8 might act as one of the molecular mediators of the proautophagic activity of trehalose (Carra et al. 2005, Rusmini et al. 2013).

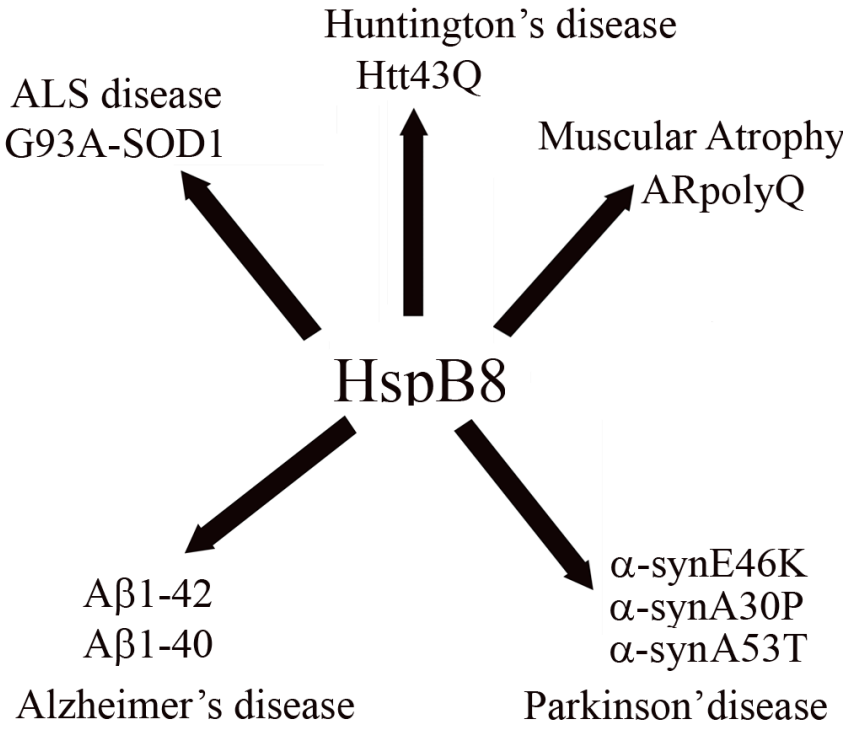

Fig: 18. The small heat shock protein HspB8 has been detected in neurodegenerative disorders such as Alzheimer's disease, Parkinson's disease, Huntington disease and spinocerebellar ataxia type 3, where it may function to protect cells from accumulation of insoluble protein aggregates.

MATHERIALS AND METHODS

Bacterial strains

Top 10: *E.coli* cells ideal for high-efficiency cloning and plasmid propagation. They allow stable replication of high-copy number plasmids and allow a transformation efficiency of 1 x 10^9cfu/µg plasmid DNA.

BL21(DE3) pLysS: *E.coli* cells belonging to a non-pathogenic strain capable of growing even in minimum medium. They allow the synthesis of large amounts of recombinant proteins due to the absence of some proteases. These cells are ideal for use with expression systems based on T7 promoter. They are, in fact, engineered in such a way as to have steadily integrated into their genome the coding gene for T7 RNA polymerase that, when expressed, produces the enzyme T7 RNA polymerase that can bind to T7 promoter and initiate transcription of downstream genes. The gene encoding the T7 RNA polymerase is placed under the control of the lac operon and this leads to an inhibition of gene transcription by the protein encoded by the gene repressor lacI, constitutively expressed in *E.coli*. However, due to the high activity of T7 RNA polymerase, cells can have basal levels of expression of the gene of interest. This can create problems if the gene of interest is toxic to bacteria. In this case, the expression of the toxic gene leads to selection of cells expressing the gene at minor level. These cells are often unable to express high levels of the gene of interest after induction with IPTG. The strain BL21pLysS solves this problem because it has a free plasmid pLysS able to express the enzyme lysozyme, which can inhibit transcription by the little RNA polymerase transcribed at basal level, forming with it a 1: 1 complex that is able to bind the promoter but can only produce abortive transcript (Zhang and Studier, 1997). The repression state of the gene can, however, be removed by adding to the culture medium IPTG (isopropyl-β-D-thiogalactopyranoside), molecule similar to galactose that acts as inductor. The IPTG, take off the repressor lacI from the promoter allowing high levels of expression of T7 RNA polymerase, that is now able to overcome the inhibition of lysozyme. The RNA polymerase produced initiates the transcription from the T7 promoter.

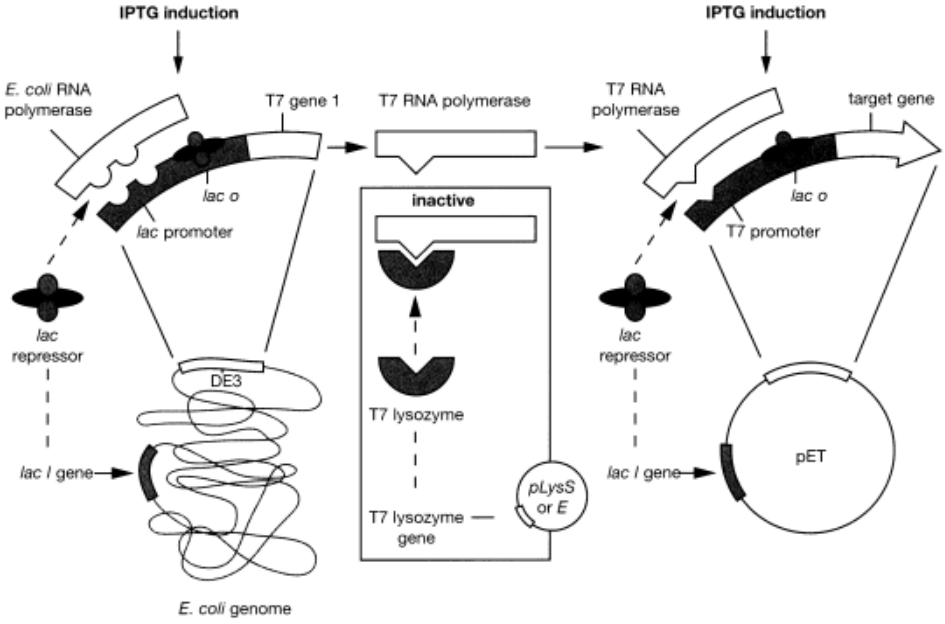

Fig: 19. Mechanism of inhibition of bacteriophage T7 RNA polymerase by T7 lysozyme and induction mediated by IPTG.

Praparation of competent E.coli

Most method for bacterial transformation are based on the observations of Mandel and Higa (1970), who showed that bacteria treated with ice-cold solutions of $CaCl_2$ and the briefly heated could be transfected with bacteriophage λ DNA (Mandel and Higa, 1970). The same method was subsequently used to transform bacteria with plasmid DNA and *E.coli* chromosomal DNA. Apparently, the treatment induces a transient state of competence in the recipient bacteria, during which they are able to take up DNAs derived from a variety of sources. Many variations of this basic technique have since then been described, all directed toward optimizing the efficiency of transformation of different bacterial strains by plasmid. Bacteria treated with the original protocol of Mandel and Higa yield 10^5-10^6 transformed colonies/µg of supercoiled plasmid DNA, but this efficiency can be increased 100 to 1000 fold. To prepare competent *E.coli* cells we used a simple and rapid variation of the technique published by Cohen et al. in 1972, frequently used to prepare batches of competent bacteria that yield $5x10^6$ to $2x10^7$ transformed colonies/µg of supercoiled plasmid DNA. Competent cells made by this procedure may be preserved at -80°C, although there may be some deterioration in the efficiency of transformation during prolonged storage (Cohen et al. 1972).

A single bacterial colony is picked up from a plate that has been incubated overnight at 37°C without antibiotic or with the antibiotic appropriate to the bacterial strain. The colony is transferred

in 50ml of LB and growth overnight at 37°C. The day after 2 ml of the culture are inoculated in 200ml of LB and growth until the O.D. at 600nm reach 0.5. The culture is stored on ice for 30 minutes and then divided into four 50ml falcon and centrifuged at 2200 rpm for 15 minutes at 4°C. The medium is discarded and the pellet resuspended in 50 ml of ice cold 0.1M $CaCl_2$ and subsequently stored on ice for 50 minutes. The culture is centrifuged at 2200 rpm for 15 minutes at 4°C and the pellet resuspended in 5ml of ice cold 0.1M $CaCl_2$. 5ml of 30% glycerol in 0.1M $CaCl_2$ are added to the solution and the tube is inverted to ensure the mix of the two solutions. The competent cells are dispensed into aliquots and freeze in liquid nitrogen.

PCR

The polymerase chain reaction (PCR) is a technique developed in 1986 by Kary Mullis, allowing the multiplication (amplification) of fragments of nucleic acids of which you know the initial nucleotide sequences and terminals. The same method can be used to modify the sequence amplified or add new information and there is no need for this sequence to be present in pure form in the reaction mixture. PCR is used in all those situations where you have to amplify a DNA amount to levels useful for later analysis. PCR is robust, simple, speedy and flexible.

The polymerase chain reaction contains several components:

- A thermostable DNA polymerase to catalyze template-dependent synthesis of DNA
- Deoxinucleoside triphosphates (dNTPs)
- A pair of synthetic oligonucleotydes to prime DNA synthesis
- Monovalent and divalent cations
- Buffer to maintain pH
- Template DNA

A PCR cycle consists of 4 phases:

- Denaturation step, where there is the separation of the DNA strands to be amplified. This phase is carried out at a temperature between 94 and 99 °C therefore using a DNA polymerase that isn't inactivated at high temperatures, such as Taq polymerase from the thermophilic bacterium Thermus aquaticus.
- Annealing, where there is the annealing of primers with their complementary regions on the DNA sequence by lowering the temperature up to 40-55°C.
- Extension phase, conducted at a temperature of 65-72° C, in which the Taq polymerase extends the segment of DNA from the primer using as template the single strand DNA.
- Termination phase.

The cycle is repeated 30-40 times. In each cycle the DNA synthesized is duplicated, resulting in a chain reaction that allows extremely fast multiplication of the genetic material of interest. The length of the cycles and annealing temperature may vary depending on the length and composition of the DNA to be amplified and primer.
At the end of the reaction the DNA is analyzed and recovered by agarose gel electrophoresis.

Restriction enzymes and ligation

The restriction endonuclease, or restriction enzymes, are a very important class of enzymes due to their ability to cut double helix DNA molecules at specific sites. Enzymes recognize, in fact, unique sequences of nucleotides in a very specific way. A DNA molecule that lacks a particular nucleotide sequence cannot be cut by a particular enzyme and this makes the DNA perfectly resistant to it, thereby making it easily recognizable. These enzymes have almost all bacterial origin and their physiological function is to protect bacteria from viral attacks. In recombinant DNA technology, restriction enzymes are used in molecular cloning, which involves the introduction of a gene of interest in a DNA molecule called plasmid, able to replicate in a host system to produce large amounts of the gene or to allow its expression. So that the gene is inserted, both the plasmid DNA and the gene are treated with the same restriction enzyme: at the end of the reaction, both plasmid and gene will have similar terminals. In particular, if the enzyme used produces a staggered cut, cohesive ends produced will tend to associate in the presence of the enzyme DNA ligase, which catalyzes the reaction of ligation. For the digestion with restriction enzymes are usually used 5µl of DNA to digest, 2µl of reaction buffer specific for the enzyme used, 1µl of restriction enzyme and milliQ water until a reaction volume of 20 µl is reached. Digestion is carried out at 37°C for at least an hour. The ligation reaction is, instead, conducted at 15°C overnight and requires 3 µl of carrier DNA, 5 µl of insert DNA, 2 µl of enzyme, 1 µL of DNA ligase and de-ionized water until reaching a volume of 20 µl.

Transformation of competent E.coli

To transform the $CaCl_2$-treated cells, 100µl of the suspension of competent cells are transferred into a 1.5ml eppendorf tube and mixed to no more than 50ng of plasmid DNA. The tube is stored on ice for 30 minutes and subsequently heat shocked for 30 seconds (in the case of BL21pLysS) or 90 seconds (in the case of TOP10) before being rapidly transferred on ice in order to chill the cells for 3 minutes. 1ml of SOC medium is added to the sample and the culture is incubated for 40 minutes at 37°C with vigorous shaking before being centrifuged at 4000 rpm for 5 minutes. The pellet is

resuspended with an appropriate volume of supernatant and transferred into a agar LB medium plate. The plate is incubated overnight at 37°C until the colonies appear.

Agarose gel electrophoresis

Electrophoresis through agarose gel is a simple technique, rapid to perform and capable of resolving fragments of DNA that cannot be separately adequately by other procedures. Furthermore, the location of DNA within the gel can be determinate directly by staining with low concentration of fluorescent intercalating dyes, such as ethidium bromide. Bands containing as little as 20pg of double-stranded DNA can be detected by direct examination of the gel in UV. DNAs from 50 bp to several megabases in length can be separated on agarose gel of various concentrations and configurations. Agarose is a linear polymer composed of alternating residues of $_{D}$- and $_{L}$- galactose joined by α-(1→3) and β-(1→4) glycosidic linkages. Chains of agarose forms helical fibers that aggregate into supercoiled structures with a radius of 20-30nm. Gelation of agarose results in a three dimensional mesh of channels whose diameters range from 50 nm to >200nm. The rate of migration of DNA through agarose gel is determinate by a lot of factors:

- The applied voltage: at low voltage the rate of migration of linear DNA fragments is proportional to the voltage applied;
- The presence of ethidium bromide in the gel: intercalation of ethidium bromide causes a decrease in the negative charge of the double stranded DNA that leads to a retardation of the rate of migration;
- The molecular size of DNA: molecules of double-stranded DNA migrate through gel matrices at rates that are inversely proportional to the $\log_{10}$ of the number of base pairs;
- The conformation of the DNA: supercoiled, circular and linear DNA migrates through agarose gel at different rates;
- The type of agarose;
- The electrophoresis buffer.

The agarose gel electrophoresis is used to check the PCR products, the vectors and the genes necessary for the cloning and to analyze the plasmid DNA extracted from the bacteria. A 1% agarose gel is made by dissolving 0,8g of agarose into 80ml of TAE 1X buffer diluted from a 50X stock solution (2M Tris/HCl, 2M CH_3COONa, 50 mM EDTA). The solution is heated and mixed until the agarose is completely dissolved. When the solution has cooled until 40-50°C, the ethidium bromide is added to a final concentration of 0,5µg/ml. The gel is gently mix and poured into the mold. Once the gel is completely solid (about 30 minutes), it's transferred into electrophoresis tank. The samples are mixed with the DNA gel-loading buffer (0,25% bromophenol blue, 30% glycerol

in H_2O) and loaded into the slots of the gel. The run is conducted for about 30 minutes at 80 volts. If necessary, the bands of DNA can be recovered from the gel for other purposes.

Recovery of DNA from agarose gel

The recovery of DNA from agarose gel is performed with the use of the Illustra GFX PCR DNA and gel band purification kit (GE Healthcare), designed for the purification and concentration of DNA from PCR mixture, restriction enzyme digestions, solutions and agarose gel bands. DNA ranging in size from 50bp up to 100kbp can be purified from gel slices of up to 900mg. The kit uses a chaotropic agent to extract DNA from solution and/or to dissolve agarose and to denature proteins. DNA binds selectively to a silica membrane contained in the Illustra GFX microspin column. The matrix-bound DNA is washed with an ethanolic buffer to remove salts and other contaminants, and the purified DNA is eluted in a low ionic strength buffer. The yield of DNA is in the range of 60-80% and the purity of the sample is very high thanks to the removal of about 95% of the contaminants.

Once the electrophoretic race is over, the agarose band containing the sample of interest is cut out and placed into a 1,5ml eppendorf to measure the weight of the slice. 10µl of capture buffer for each 10mg of gel slice are added, the tube is mixed by inversion and incubated at 55°C until the agarose is completely dissolved. The capture buffer-sample mix is transferred onto the assembled GFX Microspin column and collection tube. The assembled column and collection tube are spin at 14000 rpm for 10 seconds and the flow is discarded by emptying the collection tube. 500µl of the wash buffer are added and the column is spin two times for 10 seconds and subsequently for 1 minute at 14000 rpm. The GFX microspin column is transferred into a fresh 1,5ml microcentrifuge tube and 25µl of elution buffer are added. The DNA is eluted by centrifugation at 14000 rpm for 1 minute.

Miniprep

After the transformation into TOP 10 cells, the DNA is extracted from cells using the miniprep (minipreparation) protocol which allows rapid small-scale isolation of plasmid DNA from bacteria. The method involves a phase of alkaline lysis of bacterial membrane followed by one neutralization step and one plasmid DNA purification step using subsequent high-speed centrifugations. The yield of DNA should be about 2-10μg.

A single bacterial colony is inoculated into 2 ml of LB medium containing the appropriate antibiotic in a 15ml tube. The culture is incubated at 37°C for 5 hours with vigorous shaking.

1,5ml of the culture are poured into a microfuge tube and centrifuged at 10000 rpm for 1 minute.

The medium is removed by aspiration and the pellet is resuspended in 100µl resuspension buffer P1 (50mM Tris -HCl pH 7.5; 10mM EDTA pH 8.0; 100µg/ml RNAse). 200µl lysis buffer P2 for 5 minutes. 150µl of chilled neutralization buffer P3 (3.0 M potassium acetate pH 5.5) are added to the sample and the latter is immediately mixed by vigorously inverting 4-6 times and incubated on ice for 5 minutes and then centrifuged at 12000 rpm for 5 minutes in a microfuge.

After centrifuging the supernatant is transferred to a fresh tube and the double-stranded DNA is precipitated with 2 volumes (800µl) of absolute ethanol at room temperature. After 5 minutes on ice the sample is centrifuged at 12000 rpm for 5 minutes and the supernatant is removed while the pellet is rinsed with 400µl of 70% ethanol at 4°C. The supernatant is discarded and the pellet air dried for 10 minutes and subsequently redissolved in 20µl of milliQ water.

The purified plasmid DNA is analyzed by cleavage with the appropriate restriction enzymes.

Maxiprep

This technique allows us to isolate DNA from the positive colonies in a more pure form and in major yields. To do this we use the Plasmid Purification Kit (QIAGEN), based on a modified alkaline lysis procedure, followed by binding of DNA to an anion exchange resin under appropriate low salt and pH conditions. RNA, proteins, dyes and low molecular weight impurities are removed by a medium salt wash. Plasmid DNA is eluted in a high salt buffer and the concentrated and desalted by isopropanol precipitation. The protocol is designed for preparation of up to 100µg of plasmid.

A culture of 100ml LB medium containing the appropriate selective antibiotic is inoculated with a single colony from a freshly streaked selective plate and growth overnight at 37°C with vigorous shaking (300 rpm). The bacterial cells are harvested by centrifugation at 3800 rpm for 20 minutes at 4°C and the bacterial pellet is resuspended in 5 ml of resuspension buffer P1 (50mM Tris -HCl pH 7.5; 10mM EDTA pH 8.0; 100µg/ml RNAse). 5ml of lysis buffer P2 (200mM NaOH; 1% SDS) are added and the tube is inverted 4-6 times and incubated at room temperature for 5 minutes. 5ml of chilled neutralization buffer P3 (3.0 M potassium acetate pH 5.5) are added to the sample and the latter is immediately mixed by vigorously inverting 4-6 times and incubated on ice for 15 minutes. The precipitation is enhanced by using chilled buffer P3 and incubating on ice. After addiction of buffer P3, a fluffy white materials forms and the lysate becomes less viscous. The precipitated material contains genomic DNA, proteins and cell debris. The sample is centrifuged at 11000 rpm for 30 minutes at 4°C and the supernatant containing plasmid DNA is applied to a Qiagen-tip previously equilibrated with 4ml of equilibration buffer QBT (750mM NaCl; 50mM MOPS pH 7.0; 15% isopropanol; 0.15% Triton X-100). The column is washed two times with 10ml of wash buffer

QC (1.0M NaCl; 50mM MOPS pH 7.0; 15% isopropanol) and the DNA eluted with 5ml of eluition buffer QF (1.25M NaCl; 50mM Tris-HCl pH 8.5; 15% isopropanol). The DNA is precipitated by adding 3.5ml of room temperature isopropanol and by centrifuging at 12000 rpm for 30 minutes at 4°C. The pellet is washed with 2ml of room temperature 70% ethanol and air-dried for 10 minutes before being redissolved in a suitable volume of MilliQ water or buffer.

Large-scale production of proteins

For a larger scale production of proteins, bacterial plate is washed with a few milliliters of LB 1X and the bacteria so resuspended are placed in a 2-liters conical flask with two liters of LB 1X. 1ml of 100 µg/ml antibiotic ampicillin is added to the culture. The 2 liters of culture are divided into 4 flasks (500 ml each) in order to increase the aeration and put at 37°C with vigorous shaking . The bacteria are grown until the optical density at 600 nm reach 0.6 and at this point they are induced with IPTG to a final concentration of 100 µg/ml. After induction culture is left in agitation for 3 hours before being centrifuged for 20 min at 6000 rpm at 4°C. The supernatant is removed while the pellet is resuspended in a few milliliters of PBS.

Proteins purification

The purification of protein engineered to contain a histidine tag is perfomed through IMAC (immobilized metal ion affinity chromatography). This technique has a very high efficiency, capacity, concentrating power and speed. Polyhistidine tracts bind tightly to a resin charged with divalent nickel ions. Contaminating protein can be removed with appropriate washing, and the protein of interest can then be eluted by a soluble competing chelator. Because few natural proteins bind with significant affinities to such matrices, His-tagged proteins can be purified substantially in a single step. Purification can be performed both under native and denaturing conditions. When the proteins are purified in denaturing conditions, bacteria are lysed by sonication in 6 M guanidinium chloride pH 8.0 and then centrifuged at 13000 rpm for 30 min at 4°C. Meanwhile the resin (approx. 3 ml of His-select Nickel resin) is washed with approximately 15 ml of H_2O milliQ to remove ethanol and with 15 ml of sonication buffer. After centrifugation, the supernatant bacteria is put in agitation with the resin in a bottle for about an hour to allow the binding of the protein to the resin. The resin is then put back in the column and washed with 70 ml of 6 M guanidinium chloride at pH 8.0 and 70 ml of urea at pH 8.0. The protein is eluted from the column with urea pH 4.5 and collected in fractions of 1 milliliter. The final concentration is calculated by measuring the absorbance at a wavelength of 280 nm. When the proteins are purified in native conditions, the

same steps are followed but the sonication is performed in the appropriate buffer and the protein is eluted with imidazole.

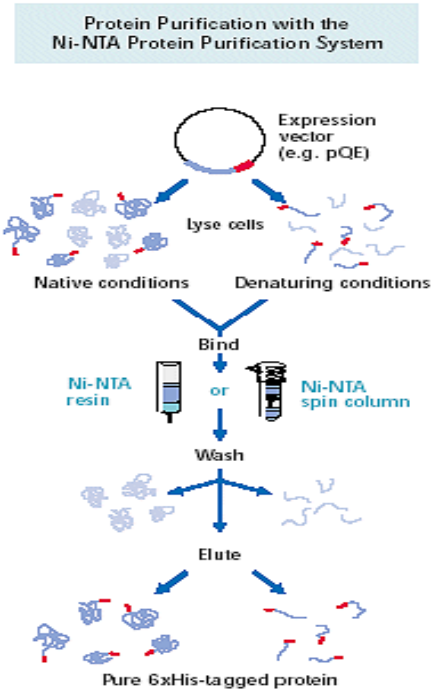

Fig: 20. Scheme of protein purification using the Ni-NTA system.

SDS-Page

The SDS-polyacrylamide gel electrophoresis is carried out in polyacrylamide gels under condition that ensure dissociation of the proteins into their individual polypeptide subunits and that minimize aggregation. This technique is based on the use of the strongly anionic detergent SDS (sodium dodecyl sulfate) in combination with a reducing agent (such as β mercaptoethanol or DTT) and heat to dissociate the protein before they are loaded into the gel. The denatured proteins bind SDS and become negatively charged. Because the amount of SDS bound is almost proportional to the molecular weight of the polypeptide and is independent of its sequence, SDS-protein complexes migrate through the gel in accordance with the size of the polypeptide. By using markers of known molecular weight, it is possible to estimate the molecular weight of the polypeptide. The polyacrylamide gel is composed of two parts: a stacking gel and a resolving gel. Once the proteins have passed the stacking gel of high porosity, they are deposited in a very thin zone on the surface of the resolving gel and they can start the real separation through the gel. Polyacrylamide gels are composed of chains of polymerized acrylamide that are cross-linked by a bifunctional agent such as N, N'-methylene-bis-acrylamide. The effective range of separation depends on the concentration of polyacrylamide used to cast the gel and on the amount of cross-linking. The sieving properties of

the gel are determined by the size of the pores, which is a function of the absolute concentration of acrylamide and bisacrylamide used to cast the gel.

Once the glass plates are assembled, the resolving gel (30% acrylamide-bisacrylamide solution, 1,5M Tris HCl pH 8,8, 10% SDS, 10% ammonium persulfate, H_2O milliQ, TEMED) is poured into the gap between the glass plates. Few microlitres of isopropanol are used to overlay the polyacrylamide solution. After polymerization is complete (30 minutes), the overlay is poured off and the top of the gel is washed several times with deionized H_2O to ensure the removal of any unpolymerized acrylamide. The stacking gel (30% acrylamide-bisacrylamide solution, 1M Tris HCl pH 6,8, 10% SDS, 10% ammonium persulfate, H_2O milliQ, TEMED) is poured directly onto the surface of the polymerized resolving gel and a comb is inserted to form the slots in the gel. Before the run the sample is resuspended in an appropriate volume of 1X SDS gel loading buffer (50mM Tris HCl pH 6,8, 100mM DTT, 2% SDS, 0,2% bromophenol blue, 10 % glycerol). The run is performed in a 1X Tris-glycine electrophoresis buffer (25mM Tris base, 250mM glycine, 0,1% SDS) at 25 mA and maximum voltage until the bromophenol blue reaches the bottom of the resolving gel. Once the run is over, the gel is stained with Coomassie Brilliant Blue R-250 and destained by soaking in methanol: acetic acid solution.

Western blotting

Western blotting was introduced by Towbin et al. in 1979 and is now a routine technique for protein analysis (Towbin et al. 1992). Western blotting, also called protein blotting or immunoblotting, uses antibodies to identify specific protein targets bound to a membrane; the specificity of the antibody-antigen interaction enables a target protein to be identified in the midst of a complex protein mixture. Western blotting can produce qualitative and semi-quantitative data on a protein of interest. After electrophoresis, the separated proteins are transferred, or "blotted", onto a solid support matrix, which is generally a nitrocellulose or polyvinylidene difluoride (PVDF) membrane. PVDF membranes are highly hydrophobic and must be pre-wetted with methanol or ethanol prior to submersion in transfer buffer. The gel to be blotted is briefly wetted with the transfer buffer (39 mM glycine, 48 mM Tris base, 0.037% SDS, 20% methanol) and then put on the PVDF membrane sheet and care is taken to remove all air bubbles. The gel and the PVDF membrane are placed between two sheets of Whatman 3MM paper and the assembly is put into an electrophoretic chamber with the PVDF sheet facing the cathode.

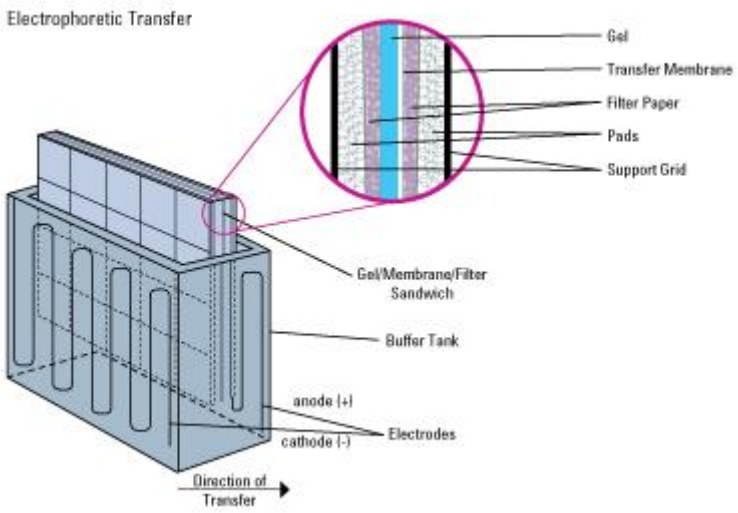

Fig: 21. Schematic representation of an electrophoretic chamber.

The transfer of the protein is performed at 350 mA for 1 hour.

The membrane supports used in Western blotting have a high affinity for proteins. Therefore, after the transfer of the proteins from the gel, it is important to block the remaining surface of the membrane to prevent nonspecific binding of the detection antibodies during subsequent steps. In order to achieve the saturation of the PVDF membrane, the latter is placed in TBS (50 mM Tris HCl, 150 mM NaCl, pH 8.0) + 3% BSA (Bovine serum albumin) for 1 hour or overnight at room temperature with gentle agitation on a platform shaker. The membrane is, then, incubated with the primary antibody (diluted at the right concentration), that is able to recognize the target protein, for 1 hour or overnight and then washed twice with TBS + 1% BSA + 0,1% Tween 20 for 15 minutes in order to remove nonspecifically bound material and unbound primary antibody. At this point the membrane is exposed to a secondary antibody, directed at a species-specific portion of the primary antibody, that is linked to biotin or to a reporter enzyme such as alkaline phosphatase or horseradish peroxidase. After the unbound probes is washed away, by incubating twice with TBS + 1% BSA + 0,1% Tween 20 for 15 minutes, the western blot is ready for detection of the probes that are labeled and bound to the protein of interest. The detection is made through ECL (enhanced chemiluminescence) in the case of the horseradish peroxidase and through NBT (Nitro blue tetrazolium chloride) / BCIP (5-Bromo-4-chloro-3indolyl phosphate) when the alkaline phosphatase is used.

Circular dichroism

Circular dichroism (CD) is the difference in the absorption of left-handed circularly polarised light (L-CPL) and right-handed circularly polarised light (R-CPL) and occurs when a molecule contains one or more chiral chromophores (light-absorbing groups).

Circular dichroism = $\Delta A(\lambda) = A(\lambda)_{LCPL} - A(\lambda)_{RCPL}$, where λ is the wavelength

Circular dichroism (CD) spectroscopy is a spectroscopic technique where the CD of molecules is measured over a range of wavelengths. CD spectroscopy is used extensively to study chiral molecules of all types and sizes, but it is in the study of large biological molecules where it finds its most important applications. The vast majority of biological molecules, in fact, are chiral. For instance, 19 of the 20 common amino acids that form proteins are themselves chiral, as are a host of other biologically important molecules, together with the higher structures of proteins, DNA and RNA. The highly chiral chemistry of biological molecules lends itself well to analysis by circular dichroism. A primary use is in analysing the secondary structure or conformation of macromolecules, particularly proteins. As secondary structure is sensitive to its environment, temperature or pH, circular dichroism can be used to observe how secondary structure changes with environmental conditions or on interaction with other molecules. Structural, kinetic and thermodynamic information about macromolecules can be derived from circular dichroism spectroscopy.

Measurements carried out in the visible and ultra-violet region of the electro-magnetic spectrum monitor electronic transitions, and, if the molecule under study contains chiral chromophores then one CPL state will be absorbed to a greater extent than the other and the CD signal over the corresponding wavelengths will be non-zero. A circular dichroism signal can be positive or negative, depending on whether L-CPL is absorbed to a greater extent than R-CPL (CD signal positive) or to a lesser extent (CD signal negative). Circular dichroism spectra are measured using a circular dichroism spectrometer. CD spectrometers measure alternately the absorption of L- and R-CPL, usually at a frequency of 50kHz, and then calculate the circular dichroism signal.

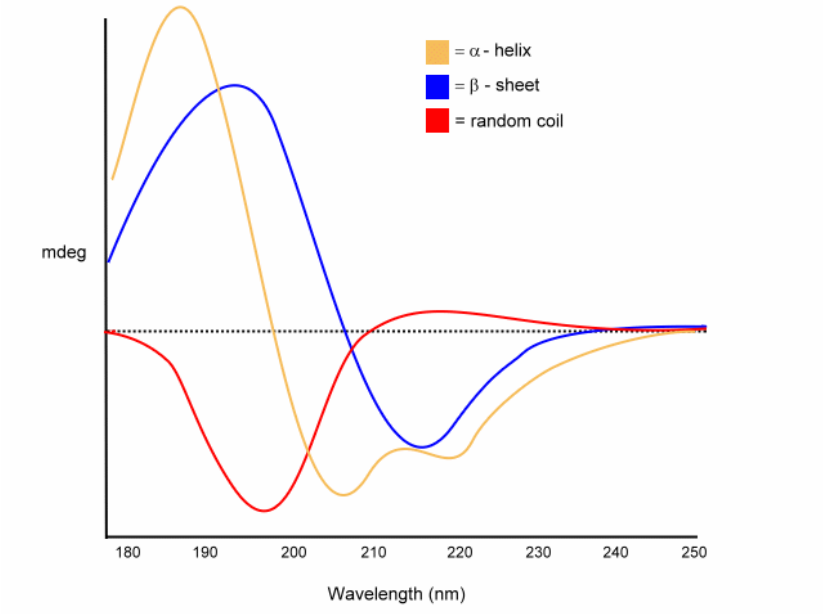

Fig: 22. Standard circular dichroism spectra of α-helix, β-sheet and random coil structures.

Interaction analysis on Biacore via surface plasmon resonance (SPR)

SPR experiments are performed using a Biacore 3000 system (GE Healthcare, Uppsala, Sweden) setting both sensor and sample temperature at 25°C and using 10 mmol/L Hepes (pH 7.4), 150 mmol/L NaCl, 3 mmol/L EDTA, and 0.05% v/v surfactant P20 as running buffer. Three flow cell surfaces are activated by 1:1 mixture of N-hydroxysuccinimide and N-ethyl-N-(dimethylaminopropyl) carbodiimide for 7 min (flow rate 5 µL/min). Afterwards, all proteins are immobilized on parallel channels of the sensor chip CM5, using amine coupling chemistry according to the manufacturer's protocol. Residual binding sites on the sensor chip surface are blocked with a 7 min injection of 1 mol/L ethanolamine, pH 8.0. A reference cell is always prepare in parallel by the same immobilization procedure (activation/deactivation step) without protein addiction. After the binding experiment the sensor chip is regenerated by a 1 minute injection with 10nm/L glycine pH 2,5. Response time at start of injection is always reported as the difference between signals arising from the active and the reference cell which, if necessary, was additionally corrected for baseline drift and bulk refractive index contribution. The observed curves are fitted assuming single phase kinetics (single phase dissociation/association). The kinetic and thermodynamic parameters were calculated from the fits using BIA evaluation software (version 4.1 BIACORE, GE Healthcare).

Cell cultures and transfection

Experiments are carried out with Chinese hamster ovary (CHO), HeLa or SKNBE cells, cultured in 75-cm^2 flasks (37°C, 5% CO_2 atmosphere), using Ham's F12 medium (for CHO) or DMEM

medium (for HeLa and SKNBE) supplemented with 10% fetal calf serum, penicillin (100 U/mL), and streptomycin (100 µg/mL). The cells, seeded onto glass coverslips at $4.5x10^4$ cells/cm^2 were transiently transfected with the Lipofectamine Plus reagent (Invitrogen). DNA is diluted and mix with Plus reagent. The mix is incubated at room temperature for 15 minutes. Lipofectamine reagent is diluted in a second tube with OPTIMEM medium without serum and then mixed with the pre-complexed DNA. The mix is incubated at room temperature for 15 minutes and then added to each well of cells containing fresh OPTIMEM medium. To optimize proteins expression, 6 hours after transfection the medium was changed, and cells were kept at 30°C for 48h for immunolabeling assays. For image analysis cells are cultured on coverslips and transfected as above, washed with PBS (phosphate saline buffer), permeabilized with Triton X-100 and fixed with 2% paraformaldeyde followed by incubation with the antibody of interest. Coverslips are mounted onto glass microscope slides and analyzed with fluorescence microscopy. For western blot analysis, cells are transiently transfected. Two days after transfection, $2–3 \times 10^6$ cells are collected with PBS and one quarter of the sample is resolved by SDS-Page, blotted onto a PVDF membrane and probed with the appropriate antibody.

Co-immunoprecipitation

Co-immunoprecipitation (Co-IP) is a popular technique to identify physiologically relevant protein-protein interactions by using target protein-specific antibodies to indirectly capture proteins that are bound to a specific target protein. These protein complexes can then be analyzed to identify new binding partners, binding affinities, the kinetics of binding and the function of the target protein.

$3×10^6$ cells are transiently transfected with the appropriate plasmid. Two days after transfection the cells are treated with the protein of interest and after 4 h lysed in 250 µL of 50 mmol/L Tris-HCl, pH 7,5, 150 mmol/L NaCl, and 1% v/v Triton X-100, plus protease inhibitors for 15 min on ice, followed by two sonication pulses. Protein extracts (800 µg) are incubated with 20 µL of NinTA beads (Sigma) for 8 h at 4°C. Beads are washed three times with wash buffer (50 mmol/L Tris-HCl, 150 mmol/L NaCl, pH 7,4), and proteins are eluted by incubating the beads with 8 mol/L urea, 50 mmol/L Tris-HCl pH 8 for 10 min at room temperature. The eluted is resolved by SDS-PAGE, blotted onto a PVDF membrane and probed with the antibodies of interest.

RESULTS

Prion protein-Tyrosine hydroxylase interaction

Construction of plasmids for PrP

The expression plasmids encoding recombinant *E.coli*-derived human (hu: 23-230), mouse (mu: 23-231), hamster (ha: 29-231), bovine (bo: 25-242) and ovine PrP (sh: 25-234) and human doppel (Dpl: 28-152) were already present in our laboratory (described in Negro et al. 1997; Negro et al. 2000 and Cereghetti et al. 2004). The human PrP deletion mutants 23-90 and 94-230 were constructed in the same way using the following primers:

5'ggcggatccaagaagcgcccgaagcctggagga 3', 5' ggcggatccggcacccacagtcagtggaacaag 3'

5'gcggaattcaaccccagccaccaccatgaggct 3', 5' gcggaattcacgatcctctctggtaataggcctg 3'

A TAT-PrP fusion protein was produced by introducing the DNA sequence coding for the 23-230 amino acid sequence for huPrP in plasmid pTAT-Neuroglobin (described in Peroni et al. 2007) between *NheI* and *EcoRI* restriction sites using the following primers:

5'gtagctagcaagaagcgcccgaagcctggagga 3', 5' agtgaattcacgatcctctctggtaataggcctg 3'

Construction of plasmids for TH

The TH human gene was amplified by PCR from a template (kindly provided by Prof. J. Haavick, University of Bergen, Bergen, Norway) containing the full-length coding sequence of human TH isoform 1 using the following primer:

5' cacgctagatgcccacccccgacgccacca 3', 5' cggaattctagccaatggcactcagcgcatg 3'

The PCR product was cut with *NheI* and *EcoRI*, and cloned into pRSETA (Invitrogen), pTAT-Neuroglobin and pEGPF (Clontech) plasmids to give, respectively pRSET-TH, pTAT-TH and pcDNA-TH. pEYFP-TH was produced by cloning TH in pEYFP between *NheI* and *EcoRI*. The TH sequences 1-497 and 150-497 were also sub-cloned into pPROEX vector (Invitrogen) using the following primers:

5' aattcggcgccatgcccacccccgac 3', 5' ggacgccgggtacctagccaatggca 3' for 1-497;

5' aattcggcgccatgtcagaggacgtgc 3', 5' ggacgccgggtacctagccaatggca 3' for 150-497.

The PCR product was cut with *NarI* and *KpnI* and cloned in the same sites of plasmid pPROEX to give plasmids pRPROEX TH(1-497) and pRPROEX TH(150-497). TH(1-152) cDNA was sub-

cloned into pET28 and pET3a vectors (Novagen), with *NdeI* and *BamHI* sites for expression with or without the His-tag, respectively, using the following primers:
5’ ggagatatacatatgcccacccc 3’, 5’cggggatccgcacgtcctatgac 3’

The TH amino acid coding sequences 1-497, 1-184 and 150-497 were also sub-cloned in pcDNA-mRuby2 (Addgene) using the following primers:
5’cccaagcttatgcccacccccgacgccaccacg 3’, 5’cgtggatccgagccaatggcactcagcgcatgg 3’ for 1-497;

5’cccaagcttatgcccacccccgacgccaccacg 3’, 5’ gctggatcctctgacacctggcgcacacaccactg 3’ for 1-184;

5’ cccaagcttatgaggccgcgagctgggggcccca 3’, 5’cgtggatccgagccaatggcactcagcgcatgg 3’for 150-497.

Each amplified product was cut with *HindIII* and *BamHI* and cloned in the same restriction site of plasmid pCDNA-mRuby2 (Addgene) in order to give plasmids pTH(1-497)-Ruby2, pTH(1-184)-Ruby2 and pTH(150-497)-Ruby2, respectively.

The nucleotide sequences of the plasmids were analyzed for correctness by BMR genomics (Padova, Italy).

Recombinant protein expression and purification

Plasmids pRPROEX TH(1-497), pRPROEX TH(150-497), pRSET-TH, pET28 TH(1-152), pET3a TH(1-152) and pTAT-TH were introduced in BL21(DE3) *E.coli*. TH(1-497) was produced overnight at 16°C, while TH(150-497), pRSET-TH and pTAT-TH expression was carried out at 28°C for 5 h. All proteins were expressed with an N-terminal His-tag and purified following established procedures by HisTrap immobilized metal affinity chromatography (IMAC) FF (GE Healthcare) and Superdex 200 HR 10/30 gel-filtration chromatography (Amersham Bioscience). The His-tag was removed by incubation with TEV protease and by an additional IMAC step. For activity assay, TH(1-497) and TH(150-497) were dialyzed against 50 mmol/L HEPES (pH 7.0), 100 mmol/L KCl and 2 mmol/L dithiothreitol (DTT), concentrated to 1-2 mg/mL by ultrafiltration (Vivaspin) and frozen in liquid nitrogen in the presence of 30% v/v glycerol. For binding experiments, TH buffer was exchanged for 20 mmol/L sodium phosphate (pH 7.4), 100 mmol/L NaCl. TH(1-152) protein from plasmids pET28 and pET3a was purified from inclusion bodies by a series of 30-min stirred washes at room temperature (RT), with centrifugation at 10,000g for 30 min at 4°C. The first wash was with 20 mmol/L Tris-HCl (pH 7.4) containing 150 mmol/L NaCl, 2 mmol/L $MgCl_2$, 0.5 mmol/L $CaCl_2$ and 50 U of DNase /RNase per liter of culture, followed by 20 mmol/L Tris-HCl (pH 8.0), 200 mmol/L NaCl, 1% v/v sodium deoxycholate and 2 mmol/L EDTA.

The resulting pellet was taken up in 20 mmol/L Tris-HCl (pH 8.0), 1 mmol/L EDTA and 0.25% v/v sodium deoxycholate, and this step performed twice. The insoluble fraction was then solubilized in 20 mmol/L sodium phosphate (pH 7.4), with 500 mM NaCl and 5 M urea, the suspension stirred for another 30 min, then centrifuged for 20 min at 28,000g. The urea was gradually removed by step dialysis over 48 h at 4°C against 20 mmol/L sodium phosphate (pH 7.4) buffer containing 100 mmol/L NaCl. The successfully refolded protein was separated by centrifugation (28,000g, 30 min at 4°C) and concentrated with an Amicon device (Millipore). TAT-TH was solubilized from the bacterial pellet in 8 mol/L urea, 100 mmol/L NaCl, 10 mmol/L imidazole and 20 mmol/L Tris–HCl (pH 8.0), and applied onto the pre-equilibrated Ni–NTA column at RT (Wu *et al*. 2006). After extensive washing the fusion protein was eluted from the Ni–NTA column with 500 mmol/L imidazole, pH 6.3. The purified fractions were pooled and dialyzed in 0.1 mmol/L reduced glutathione, 0.01 mmol/L GSSG, 100 mmol/L NaCl, and 20 mmol/L Tris–HCl, pH 8.0 to remove the urea, and then dialyzed against phosphate-buffered saline (PBS). All purified proteins were aliquoted and stored at 80°C until used.

SDS- PAGE, Western blotting and dot-blot assay

Mini SDS-PAGE was performed using the electrophoresis MiniVE (Amersham) system according to the manufacturer's instructions. Protein samples were diluted in Laemmli sample buffer (50 mmol/L Tris-HCl pH 6.8, 100 mmol/L DTT, 2% (w/v) SDS, 0.05% (w/v) bromphenol blue) and heated for 5 min at 100°C. Each well of a 12% SDS-PAGE was loaded with 1 μg total proteins. Separated proteins were electrotransferred onto Immobilon-P polyvinylidene difluoride (PVDF) membranes (Millipore) with the mini VE System Blot Module (Amersham). For TH and its deletion mutants the proteins were directly blotted onto the Bio-Dot Apparatus Microfiltration (Biorad) following the manufacturer's instructions. Non-specific binding sites on the membrane were blocked with PBS containing 5% (w/v) bovine serum albumin (BSA) (Sigma-Aldrich) and 50 mol/L Tris/HCl, 150 mmol/L NaCl. For Far Western blots the membrane was incubated with 10 mL of TH (10 μg/mL) or its deletion mutants in blocking buffer. Dot blot membranes were incubated with 10 mL of 10 μg/mL recombinant HuPrP. Membranes were washed 3 x 5 min with PBS/1% BSA, 0.1% Tween 20. TH bound to PrP or vice versa was detected by incubation with 0.4 mg/mL of anti-TH monoclonal antibody (MMS-503P) (Covance, CA) or 0.5 mg/mL of anti-PrP mAb 3F4 (DAKO, Glostrup, Denmark) in blocking buffer for 1 h at room temperature followed by incubation with 50 ng/mL horseradish peroxidase-conjugated goat anti-mouse IgG mAb (Sigma-Aldrich) for 45 min at room temperature. The blot was developed using the NBT/BCIP (Roche).

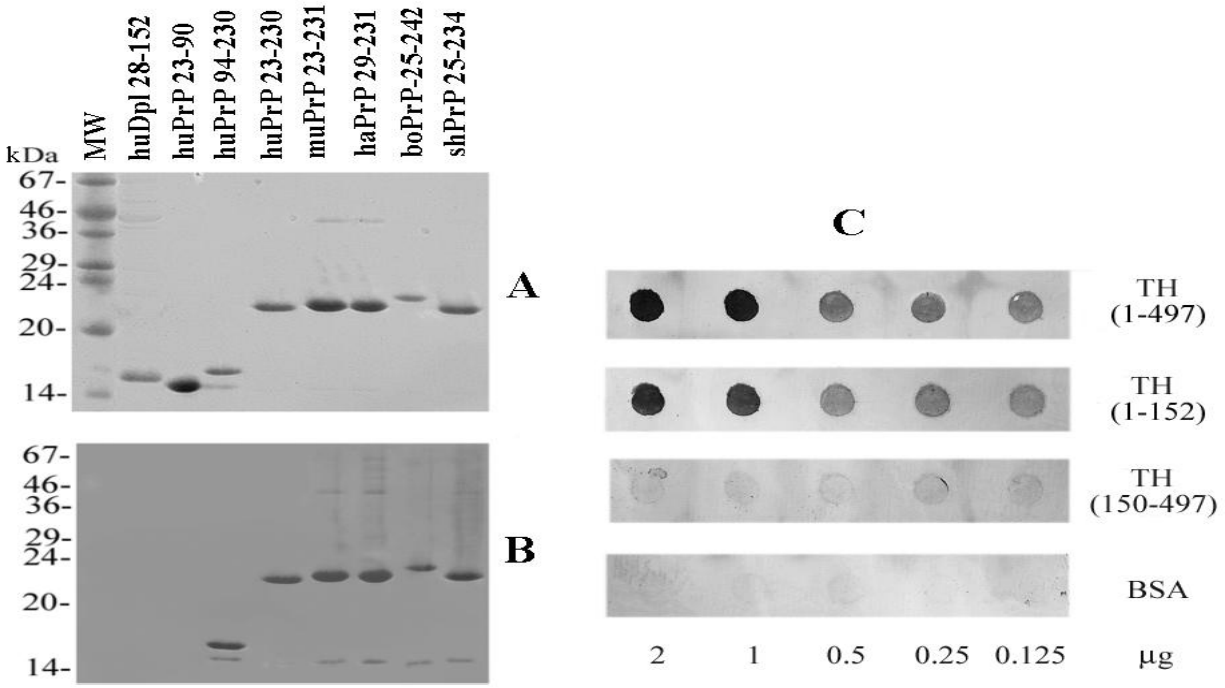

Fig: 23. **Far Western blot and dot blot analyses of prion proteins with tyrosine hydroxylase**.
Panel (A) Recombinant human Dpl, the deletion forms huPrP(23-90) and huPrP(94-230), the full length huPrP(23-230), muPrP(23-231), haPrP(29-231), bovine PrP(25-242), and sheep PrP(25-234) were separated by 13% SDS-PAGE. The same proteins in panel B after transfer on nitrocellulose were probed with 25 µg/mL recombinant human TH(1-497) and developed with an anti-TH antibody. See text for details. Note that TH is unable to recognize the N-terminal un-structured domain of huPrP(23-90), as well as human Dpl protein. Panel (C) Dot blot analyses of TH interaction with human PrP. Serial dilutions (µg) of full length TH(1-497)and its deleted mutants TH(1-152) and TH(150-497),were blotted onto nitrocellulose before probing with 20 µg/mL huPrP(23-230) followed by development with antibodies against huPrP (3F4).

The results obtained from western blot and dot blot analyses reveal that PrP of mouse, hamster, bovine and ovine origin showed similar behaviors, all being involved in the interaction with TH. Human Dpl, which adopts the same secondary/tertiary structure as PrP, was not recognized by TH, indicating that sequence recognition is essential for an effective binding of PrP to TH. Moreover, huPrP(23-90) was not recognized by TH, suggesting that TH recognized the structured C-terminal sequence of PrP but failed to recognize its N-terminal un-structured domain. The TH deletion mutant 1-152 also recognized PrP albeit less robustly than full-length TH, while the C-terminal catalytic and tetramerization domains of TH(150-497) did not recognize PrP at all (data not shown).

Binding specificity was further validated by the fact that TH did not indiscriminately recognize proteins of similar molecular weight that were transferred onto the PVDF membrane. Far Western blotting was effective only with PrP bound to the PVDF membrane and using TH as analyte; no TH-PrP interaction was observed when TH was bound to the PVDF membrane and PrP used as analyte. Indeed, PrP was able to refold after SDS-driven denaturation at 100°C (provided that SDS is removed), while subjecting TH to such treatment resulted in loss of structure, as TH denaturation is an irreversible process (Gahn et al. 1995). The dot blot assay, which does not require a protein

denaturation step, was therefore used. The results show that huPrP(23-230) recognizes full-length TH and its deletion mutant (1-152) but not the catalytic domain (150-497) mutant. Collectively these data provide evidence for the N-terminal regulatory domain TH(1-150) interacting with the PrP C-terminal domain.

Interaction analysis on Biacore via surface plasmon resonance (SPR)

SPR experiments were performed using a Biacore 3000 system (GE Healthcare, Uppsala, Sweden) setting both sensor and sample temperature at 25°C and using 10 mmol/L Hepes (pH 7.4), 150 mmol/L NaCl, 3 mmol/L EDTA, and 0.05% v/v surfactant P20 as running buffer. Three flow cell surfaces were activated by 1:1 mixture of *N*-hydroxysuccinimide and *N*-ethyl-*N*-(dimethylaminopropyl) carbodiimide for 7 min (flow rate 5 μL/min). Afterwards, all proteins were immobilized on parallel channels of the sensor chip CM5, using amine coupling chemistry according to the manufacturer's protocol. Specifically, the PrP forms huPrP(94-230), haPrP(29-231) and haPrP(90-231), diluted in 10 mmol/L sodium acetate buffer (pH 5.0) and TH diluted in 10 mmol/L sodium acetate buffer (pH 4.0), were injected for 8-10 min at a flow rate of 5 μL/min. Residual binding sites on the sensor chip surface were blocked with a 7 min injection of 1 mol/L ethanolamine, pH 8.0. A reference cell was always prepared in parallel by the same immobilization procedure (activation/deactivation steps) without protein addition.

All binding experiments between TH and PrP proteins were carried out at a constant flow rate of 30 μL/min running buffer, unless otherwise specified. To determine the affinity of TH toward PrP, 60 μL aliquots of TH(1-497) and TH(150-497), as analyte, at various concentrations (within the range 0.1 μmol/L to 1.0 μmol/L, were injected over the three PrP-immobilized sensor chips (association phase), followed by a 10-min washing step with the running buffer (dissociation phase). The sensor surface was then regenerated by a 1-min injection with 10 mmol/L glycine, pH 2.5, to remove TH.

The N-terminus TH(1-152) was not examined by SPR, owing to its intrinsic instability and insolubility that hampered protein immobilization on sensor chips. Response time at start of injection was always reported as the difference between signals arising from the active and the reference cell which – if necessary – was additionally corrected for baseline drift and bulk refractive index contribution. The observed curves were fitted assuming single phase kinetics (single phase dissociation/association). The kinetic and thermodynamic parameters were calculated from the fits using BIA evaluation software (version 4.1 BIACORE, GE Healthcare, Uppsala, Sweden).

The catalytic domain of TH(150-497) did not interact with any of the PrP forms, whereas a strong interaction between TH(1-497) and both human and hamster PrPs was recorded. The kinetic and thermodynamic association and dissociation constants obtained are shown in table

Immobilized Protein	Ligand	k_a (1/Ms)	k_d (1/s)	Rmax (RU)	K_D (M)
TH(1-497)	huPrP(94-230)	$(7.41\pm6.8)\ 10^{3}$	$(2.62\pm1.9)\ 10^{-4}$	1137	$(4.64\pm4.8)\ 10^{-8}$
TH(1-497)	haPrP(90-231)	$(7.14\pm2.8)\ 10^{3}$	$(7.57\pm5.7)10^{-4}$	610	$(1.08\pm0.9)\ 10^{-7}$
TH(1-497)	haPrP(29-231)	$(3.79\pm3.6)\ 10^{3}$	$(2.79\pm1.8)\ 10^{-3}$	1950	$(9.50\pm6.9)10^{-8}$
huPrP(94-230)	TH(1-497)	$(9.67\pm9.0)\ 10^{4}$	$(1.38\pm1.6)\ 10^{-5}$	2500	$(4.96\pm2.8)\ 10^{-9}$
haPrP(90-231)	TH(1-497)	$(1.95\pm1.5)\ 10^{5}$	$(3.53\pm2.0)\ 10^{-4}$	845	$(2.77\pm1.3)\ 10^{-9}$
haPrP(29-231)	TH(1-497)	$(2.23\pm1.5)10^{5}$	$(2.51\pm1.9)\ 10^{-4}$	640	$(2.16\pm1.4)\ 10^{-9}$

Fig: 24. Kinetic parameters and dissociation constants for interaction between TH(1-497) and PrP.

Thermodynamic evaluation of the interaction between TH(1-497) and PrP yielded equilibrium dissociation constants (*K*D) of 2.2 nM, 2.8 nM and 5.0 nM for hamster full-length haPrP(23-231), truncated haPrP(90-231) and huPrP(90-230), respectively. The experiments were repeated by injecting the selected PrP (as analyte) at concentrations of 0.5-10.0 μM (in running buffer) over TH(1-497) immobilized on the sensor chip. Sensorgrams for the interaction of TH(1-497) with haPrP(90-231) and haPrP(29-231) are shown in fig. 25A and 25C, respectively, while fig. 25B and 25D show the dose-response SPR signal *versus* the concentration of haPrP(90-231) and haPrP(29-231), respectively. These latter curves are indicative of a specific interaction. Applying global fitting to evaluate the interaction parameters of PrP with TH(1-497) immobilized on the sensor chip revealed high-affinity binding, with *K*D values of 95.0 nM, 108.0 nM and 46.4 nM for haPrP(29-231), haPrP(90-231) and huPrP (23-230), respectively. The kinetic and thermodynamic binding constants of TH to the three forms of PrP were roughly comparable. The three PrP proteins share the same C-terminal domain, suggesting that interaction mainly occurs through the structured C-terminal region of PrP, spanning residues 94-230, rather than the N-terminus. On the other hand, the SPR experiments demonstrate that TH(150-497) does not interact at all with any of the various forms of PrP. The SPR results support high-affinity binding between the C-terminal structured domain of PrP and the N-terminal regulatory domain of TH.

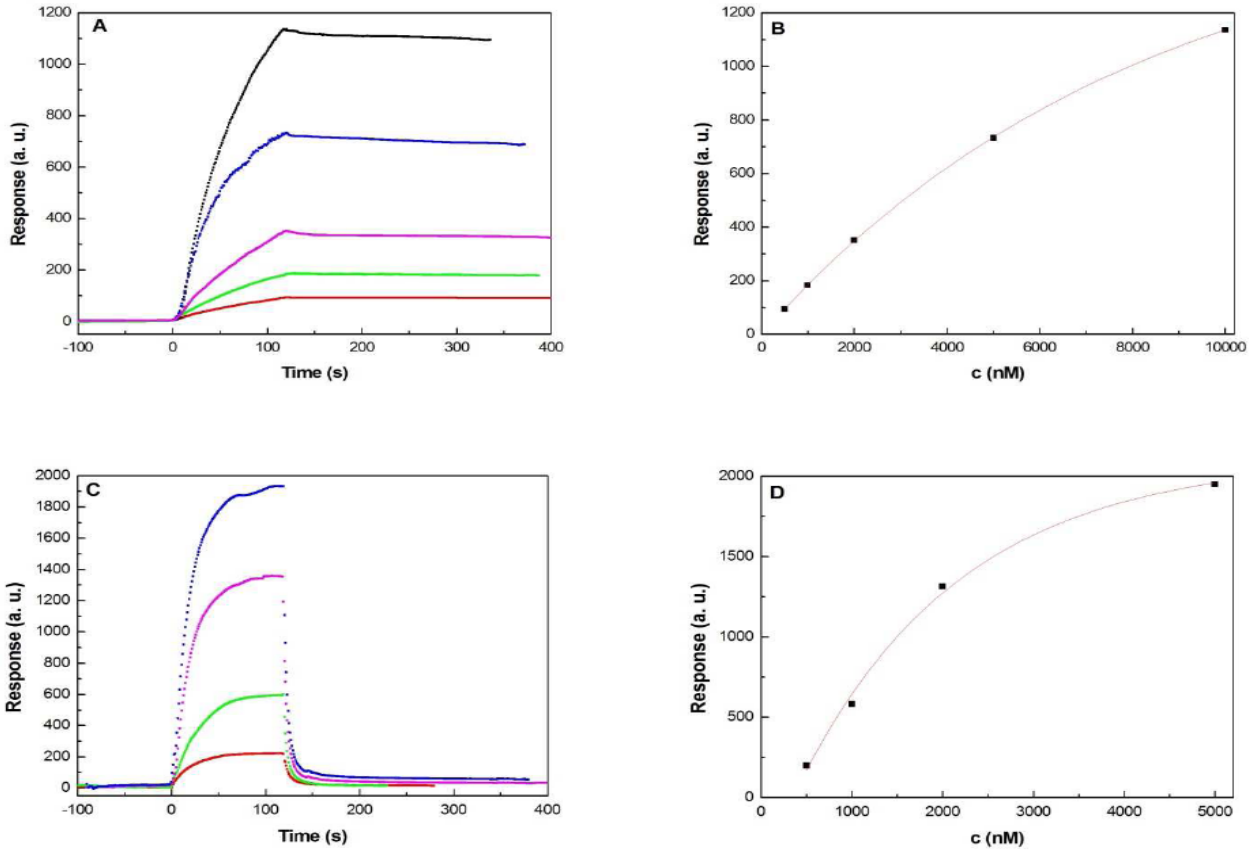

Fig: 25. **SPR interaction between prion protein (PrP) and TH(1-497).** (A) Association and dissociation curves over the TH-immobilized chip at various huPrP(94-230) concentrations (red 0.5 µM, green 1.0 µM, magenta 2.0 µM, blue 5.0 µM and black 10 µM, respectively). (B) SPR response (in arbitrary units) *versus* concentration of huPrP(94-230). (C) Association and dissociation curves over the TH-immobilized chip at various concentrations of haPrP(29-231) (same colour code as in panel A). (D) SPR response (in arbitrary units) *versus* concentration of full-length haPrP(29-231).

Cellular distribution of PrP and TH

Interaction between PrP and TH in intact cells was evaluated by co-transfecting HeLa and CHO cells with expression plasmids for TH and human PrP chimeric proteins linked to yellow and cyan versions of the basic fluorescent protein. Not surprisingly, HeLa cells transfected with pcDNA3-PrP showed a predominantly plasma membrane expression, given that PrP is normally exported and linked to the plasma membrane via a GPI anchor after its translation (fig. 26A). When HeLa cells were transfected instead with pcDNA3-TH, the majority of TH expression was intracellular (fig. 26B). Co-expression of these two proteins resulted in a strong decrease in plasma membrane PrP expression, along with an increased intracellular expression (fig. 26C). TH showed a similar topological localization (fig. 26D) and co-localization of the two proteins (fig. 26E). Analogous results were obtained with a fluorescent chimeric protein linking TH and human PrP, thus

confirming the observed decrease of plasma PrP expression and increased intracellular expression (fig. 27E).

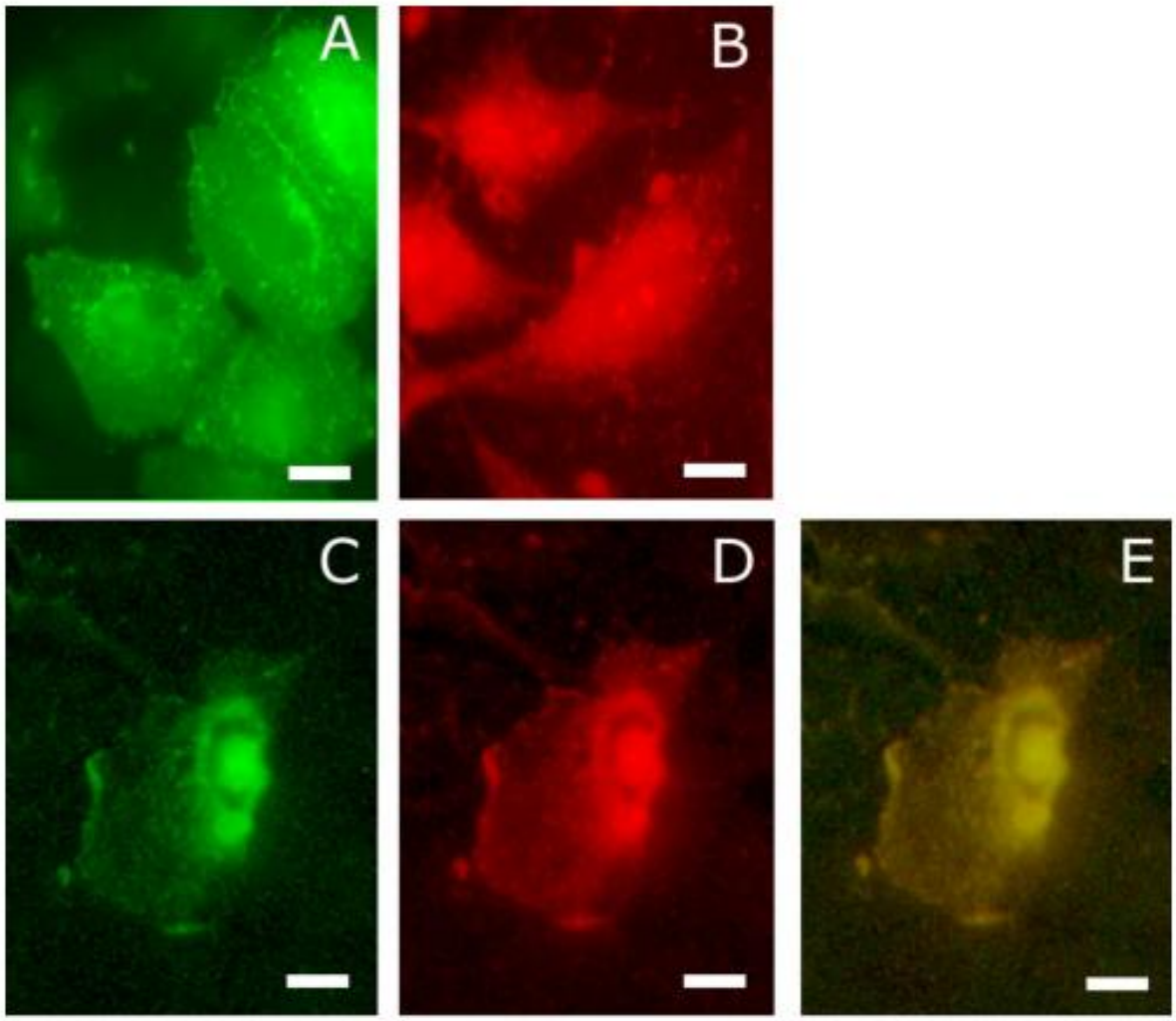

Fig: 26. **Co-localization of huPrP and TH.** Hela cells were transfected with pcDNA3-huPrP (A,C,D,) or with pcDNA3-huTH (B,C,D). After transfection the cells were incubated with anti-huPrP (3F4) and developed with FITC (A,C) or antibodies anti-TH and developed with TRIC (B, D) and developed with FITC and TRIC. Panel E: merged panels C and D.

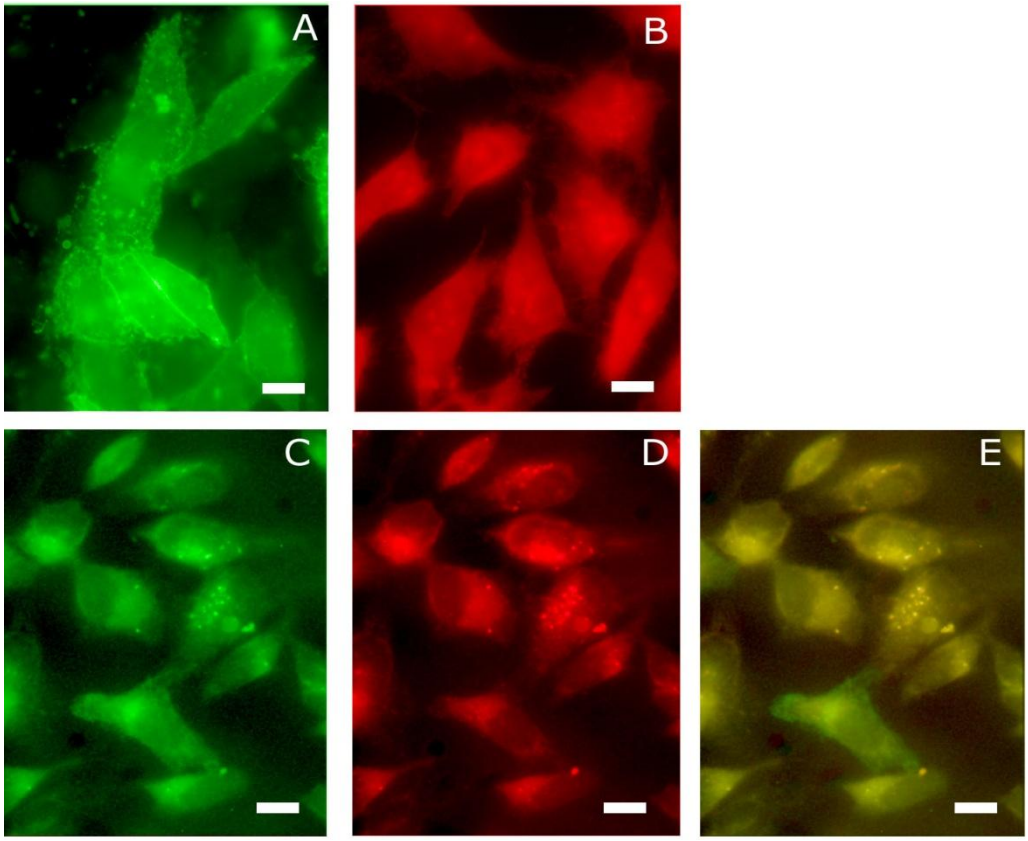

Fig: 27. **Co-localization of CFP-hPrP with YFP-TH.** CHO cells were transfected with pECFP-hPrP (A,C,D) and wih pEYFP-TH (B,C,D). Panel E: merged panels C and D.

Co-localization of the two proteins was also tested by transfecting CHO cells with pEGFP-PrP and pTH(1-497)-Ruby2, pTH(1-184)-Ruby2 or pTH(150-497)-Ruby2. We observed a clear co-localization of GFP-PrP and TH(1-184)-Ruby2 or TH(1-497)-Ruby2 with an aincrease intracellular exspression of the prion protein, while no co-localization was evident for cells transfected to express PrP-GFP and TH(150-497)-Ruby2. In this case, the prion protein still localized to the plasma membrane.

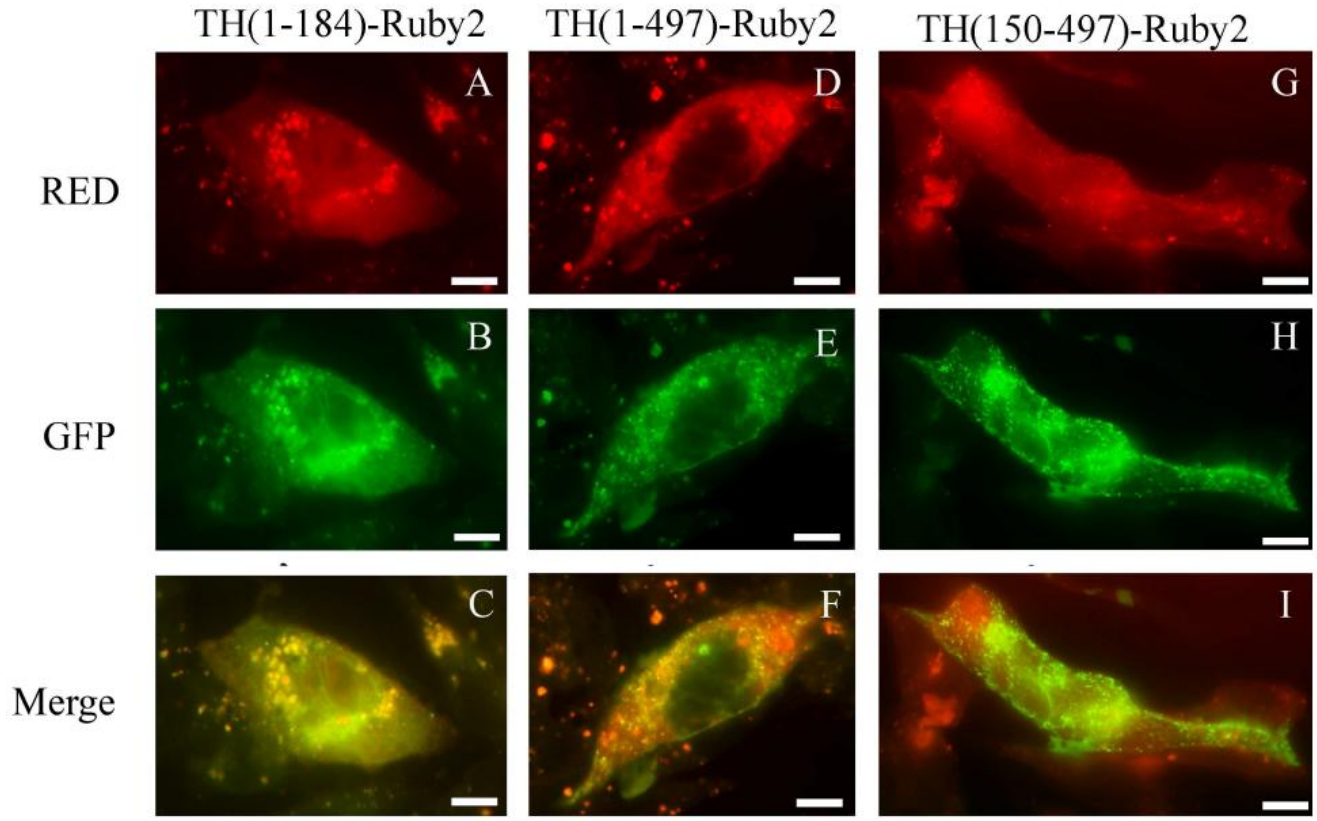

Fig: 28. **Co-localization of GFP-PrP with TH(1-184)-Ruby2, TH(1-497)-Ruby2 and TH(150-497)-Ruby2 fusion proteins.** CHO cells were transfected with plasmids pEGFP-PrP (all panels) and plasmids pTH(1-184)-Ruby2 (A,B), pTH(1-497)-Ruby2 (D,E) and pTH(150-497)-Ruby2 (G,H). After fixation cells were visualized using a TRIC filter for mRuby2 fusion proteins (red) and a FITC filter for GFP (green). Panel C: merged panels A and B. Panel F: merged panels D and E. Panel I: merged panels G and H. Scale bar: 20 μm.

Moreover, when cells were transfected with a PrP tagged to green fluorescent fusion prion protein (GFP-PrP), that normally localized to the plasma membrane of HeLa cells (fig. 29A), and were incubated with 50 mg/mL of TH recombinant protein, GFP-PrP translocated into the cells, indicating a cell surface interaction between these two proteins (fig. 29B).

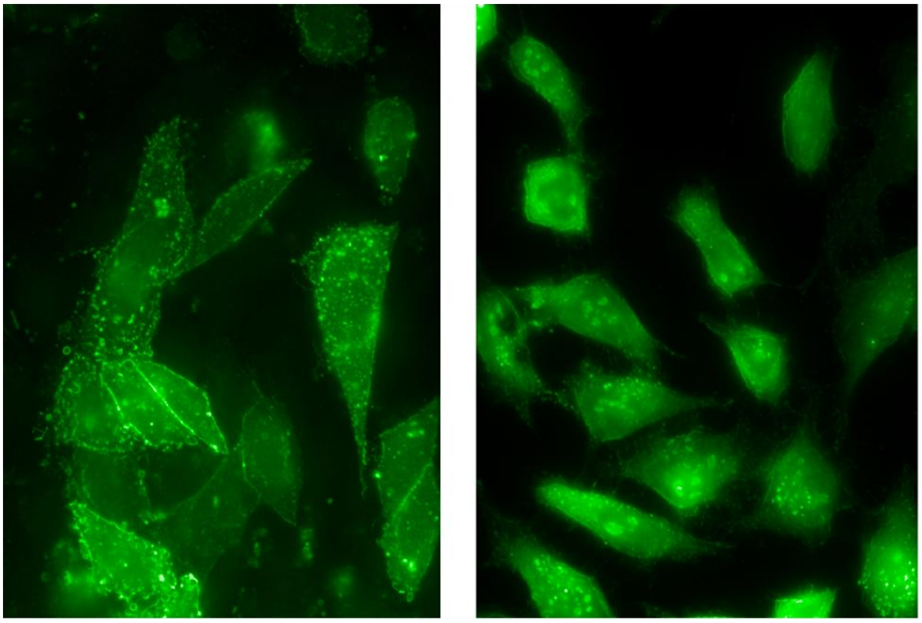

Fig: 29. **Tyrosine hydroxylase (TH) internalized GFP-hPrP.**
Hela cells were transfected with pEGFP-PrP control (A) and also treated with 50 ug/mL of rhTH (B) for 4 h.

In CHO cells transfected with pcDNA-TH and pcDNA-PrP, TH migrated as a 52 kDa species on immunoblots (fig. 30A). Its expression was not influenced by the presence of PrP. The minor bands at 28 kDa and 30 kDa represent degradation products of TH. Using the 3F4 antibody against PrP, lysates from PrP expressing cells showed a series of protein bands representing glycosylation state and the GPI anchor (fig. 30A). Co-expression of TH strongly decreased the presence of all PrP forms, in accord with the immunocytochemical data (fig. 30A).

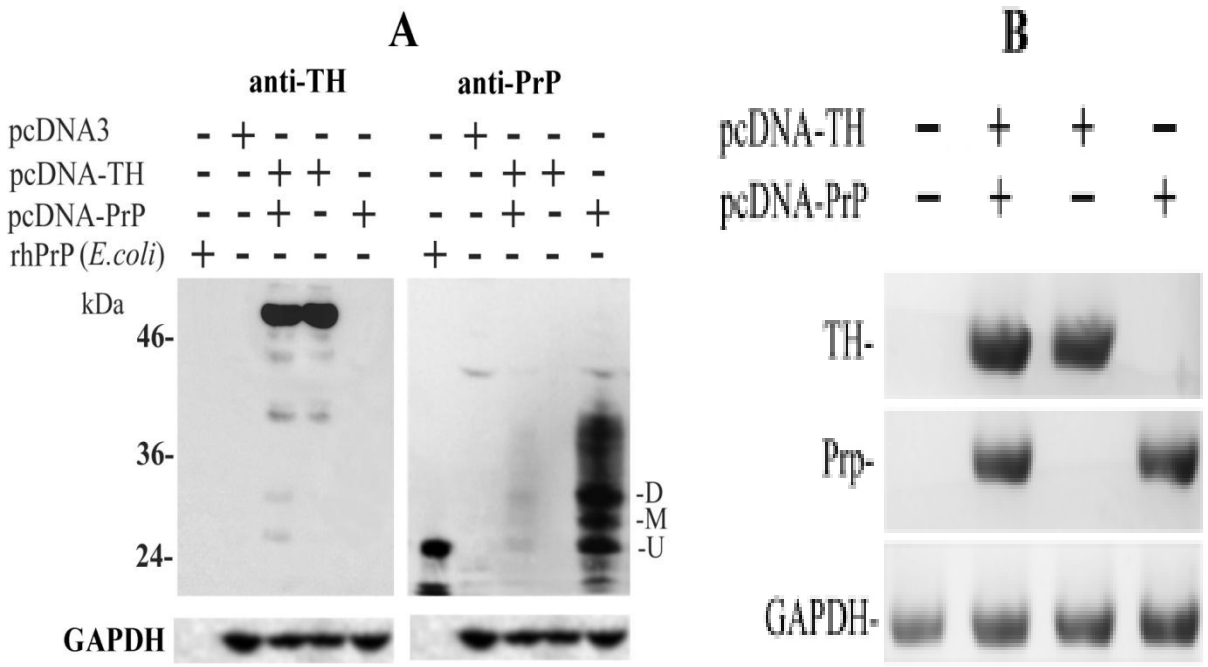

Fig: 30. **Gene and protein expression of tyrosine hydroxylase (TH) and prion protein (Prp).** CHO cells were transfected with pcDNA (control) pcDNA-TH or pcDNA-PrP. A) Western blot was developed with anti-TH, or anti-PrP, and anti-GADPH. rhPrP (*E.coli*): reference standard of huPrP (23-230) produced and purified from E coli. B) RT-PCR of mRNA for TH, PrP and glyceraldehyde-3 phosphate dehydrogenase (GAPDH; control). CHO cells were transfected with pDNA (control), pcDNA-TH or pcDNA-PrP

To verify if also the mRNA levels were affected by the co-transfection of plasmids encoding the two proteins, a Real-Time polymerase chain reaction **(**RT-PCR) was performed using the Qiagen one step RT-PCR kit and the following primers:

417bp for human PrP: 5'cacccacagtcagtggaacaagccgag 3'and 5'accatgctcgatcctctctggtaatag 3';

407bp for human TH: 5'acgctgcctcgcccatgcactcccctg 3'and 5' atgcgtgaggcatagctcctgagcttg 3';

401bp for hamster GAPDH: 5'tctgctgatgccccatgtttgtgatg 3'and 5' atgtcctcatacttggcaggtttctc 3'.

The data obtained showed that the level of PrP mRNA did not change in the presence of plasmid expressing TH, indicating that modulation of PrP level is a post-translational event. PrP did not alter TH mRNA levels (fig. 30B)

Co-precipitation assay

Co-precipitation assay was performed as described in materials and methods transfecting the cells with pcDNA-TH or pcDNA-PrP. The sample were resolved by 12% SDS-PAGE, blotted onto a PVDF membrane and probed with anti-TH (1:1000) and anti-PrP (3F4) (1:1000) antibodies. However, attempts to recover TH and PrP by co-immunoprecipitation using these vector plasmids were unsuccessful, perhaps owing to only low amounts of PrP when the two proteins are co-expressed. Co-immunoprecipitation, however, could be achieved when TAT-PrP was added to the cells (fig. 31A). Note the absence of immunoreactivity when primary antibody is omitted (fig. 31B).

In this manner TH could be recovered from cell lysates bound to PrP, confirming a strong interaction between these two proteins also *ex vivo*.

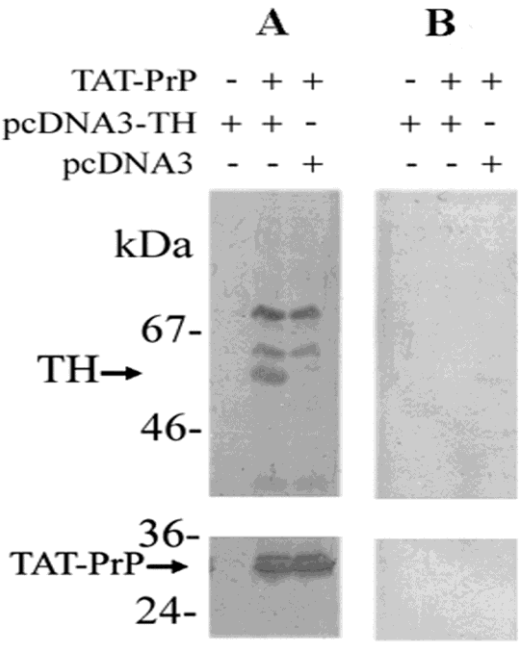

Fig: 31. **Co-immunoprecipitation of TH and TAT-His-Prp.**
CHO cells were transfected with pcDNA-TH or pcDNA3 (control) then treated for 4 h with 50 µg/mL of TAT-PrP. A) Cell lysates were prepared and incubated with NiTA-resin to sequester the His-tagged protein, and the purified proteins subjected to SDS-PAGE and immunoblotting with anti-TH (upper panel) and anti-PrP (lower panel) antibodies. B) Primary antibody omitted.

TH activity assay

The purified enzyme was first incubated to a final concentration of 600 nM, in a solution composed of 50 mmol/L HEPES (pH 7.0), 200 mmol/L $(NH_4)_2SO_4$, 7 mmol/L DTT, 25 µg/mL catalase (Sigma-Aldrich) and 25 µmol/L $(NH_4)_2Fe(SO_4)_2 \cdot 6H_2O$. After 15 min equilibration at RT, the cofactor BH4 (Sigma-Aldrich) was added to 30 µmol/L. In the experiment with PrP, the latter (1:1 molar ratio) was included from the middle of this equilibration time. The reaction was started by adding 50 µmol/L L-tyrosine (Sigma-Aldrich) from a 2.5 mmol/L stock solution. Incubation was carried out at 36°C for 2.5, 5, 10 or 20 min. Assays were stopped by adding 6 µL of 40% v/v trichloroacetic acid per 300 µL of reaction mixture, followed by incubation on ice. After centrifugation at 14000g for 10 min at 4°C, 100 µL of supernatant was injected into a C-18 column (Phenomenex) connected to an HPLC system (Agilent Technology). This was done to separate the reaction product L-DOPA (Sigma-Aldrich) from L-tyrosine. The mobile phase was 50 mmol/L sodium citrate, 50 mmol/L sodium acetate, 8% (v/v) methanol (pH 3.1); runs were performed at RT

with an isocratic flow of 0.2 ml/min. Elution was followed by UV absorbance (280nm). Product formation was also followed by fluorescence (excitation at 294 nm, emission at 330 nm). A standard curve, made with known concentrations of L-DOPA, allowed calculation of the yield of product formation from the intensity of fluorescence emission in the enzymatic reaction. The data obtained showed that incubation of both TH(1-497) and TH(150-497) forms in the presence of full-length muPrP(23-231) or its TH interacting domain 90-231 did not affect TH catalytic activity

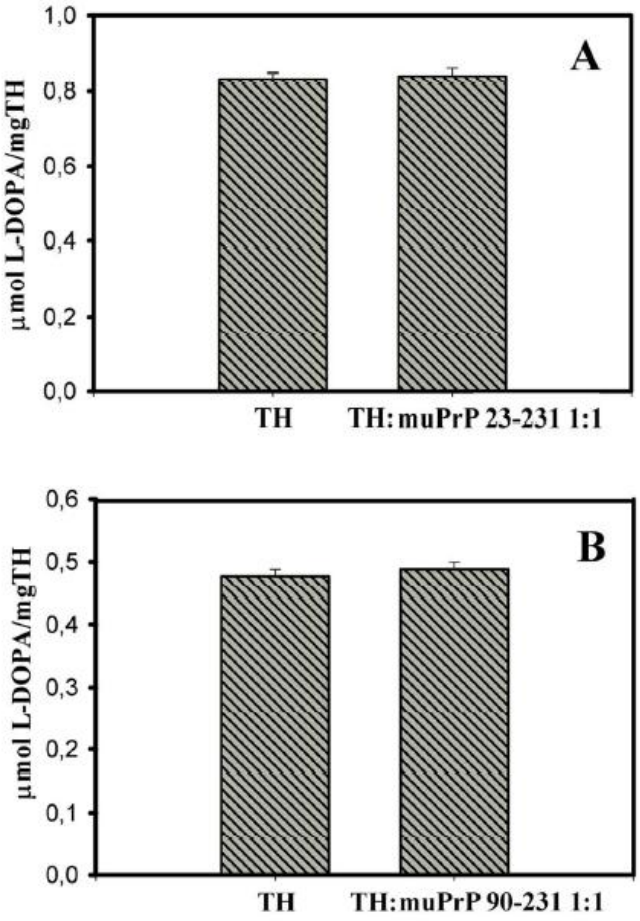

Fig: 32. **Neither the terminal domain nor full-length mouse prion prptein (PrP) affecttyrosine hydroxylase (TH) activity.** (A) L-DOPA formation catalyzed by TH(1-497) with (ratio 1:1) or without (ratio 1:0) the C-terminal domain of mouse PrP (90-231). The reaction was stopped after 10 min. Error bars derive from propagation of three-measurement standard deviation. (B) L-DOPA formation catalyzed by TH(1-497) with (ratio 1:1) or without (ratio 1:0) full-length mouse PrP(23-231). The assay conditions differ from the standard one by the absence of DTT and the use of a higher concentration of BH4 (0.12 mM) and catalase (100 µg/mL). The reaction was stopped after 2.5 min. Error bars values derive from propagation of three-measurement standard deviation.

Prion protein-Heat shock protein B8 interaction

Construction of plasmids for HSPB8

The eukaryotic expression plasmids encoding the human heat shock protein B8 wild type and the two mutants forms were kindly provided by Prof. A. Poletti, University of Milan, Milan, Italy. The HSPB8 human genes were amplified from the template using the following primers:
5' gcagctagcatggctgacggtcagatgcccttc 3', 5' gcagaattcactggtacaggtgacttccttgg 3'

The PCR products were cut with *NheI* and *EcoRI* and cloned into pRSETA (Invitrogen) and pTAT-syn (already present in our laboratory) using the same restriction sites, to give respectively pRSET-HSPB8 and pTAT-HSPB8. The HSPB8 and its mutant from plasmid pRSETA were also sub-cloned in pcDNA-mRuby2 (Addgene) using the following primers:
5' atagatctcactggtacaggtgacttccttgg 3', 5' acaagcttatggctgacggtcagatgcccttc 3'

The amplified product was cut with HindIII and EcoRI before cloning in the same restriction sites of pcDNA-mRuby2. In this way the nucleotide sequence encoding for fluorescent protein mRuby2 was replaced by HSPB8 sequence with N-terminal histidine tag.
The HSPB8 and its mutants was also cloned in plasmid pcDNA-mRuby2 between HindIII and BamHI using the following primers:
5' acaagcttatggctgacggtcagatgcccttc 3', 5' atagatcttgactggtacaggtgacttccttgg 3'.

In this way we have obtained a fusion protein between the nucleotide sequence encoding for HSPB8 with nucleotide sequence for mRuby2.

Recombinant protein expression and purification

Plasmids pRSET-HSPB8wt, pRSET-HSPB8K141E, pRSET-HSPB8K141N, pTAT-HSPB8wt, pTAT-HSPB8K141E and pTAT-HSPB8K141N were introduced in BL21(DE3) *E.coli* cells. Expression of all recombinant proteins was carried out at 37°C for 3 hours after induction with IPTG.

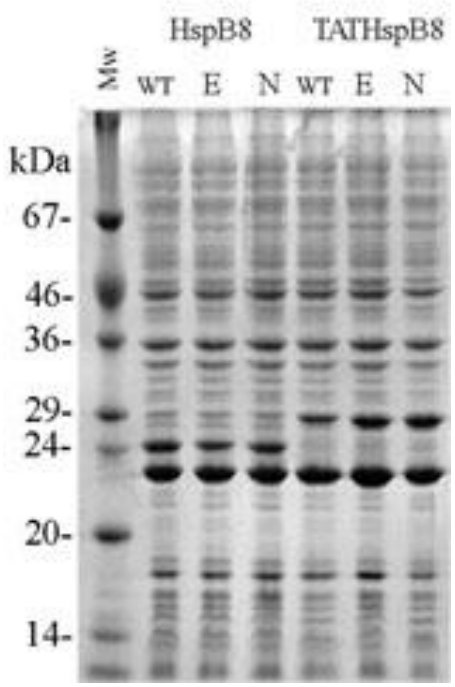

Fig: 33. **Protein expression of HSPB8, TATHSPB8 and their mutants.**
Plasmids were introduced in BL21(DE3) *E.coli* cells. Cells were grown at 37°C for three hours after IPTG induction. Samples were were diluted in Laemmli sample buffer (50 mmol/L Tris-HCl pH 6.8, 100 mmol/L DTT, 2% (w/v) SDS, 0.05% (w/v) bromphenol blue), heated for 5 min at 100°C and resolved by 13,5% SDS-page.

All proteins were expressed with an N-terminal His-tag and purified following established procedures by HisTrap immobilized metal affinity chromatography (IMAC) FF (GE Healthcare). HSPB8wt, HSPB8K141E and HSPB8K141N proteins were purified using a sonication buffer composed of 100mM Tris-HCl, 20% glycerol, 274mM NaCl, 0,1% Pluronic acid, 0,02% Tween 20, 10mM β-mercaptoethanol pH 8. The proteins were eluted in the same buffer plus 250mM imidazole and subsequently dialyzed against the same buffer without imidazole.

TATHSPB8wt, TATHSPB8K141E and TATHSPB8K141N proteins were, instead, purified in denaturant conditions and dialyzed against 50mM phosphate buffer, 274mM NaCl, 20% Glycerol, 0,1% Pluronic acid, 0,02% Tween 80, 10mm DTT pH 5,82.

All purified proteins were aliquoted and stored at 80°C until used.

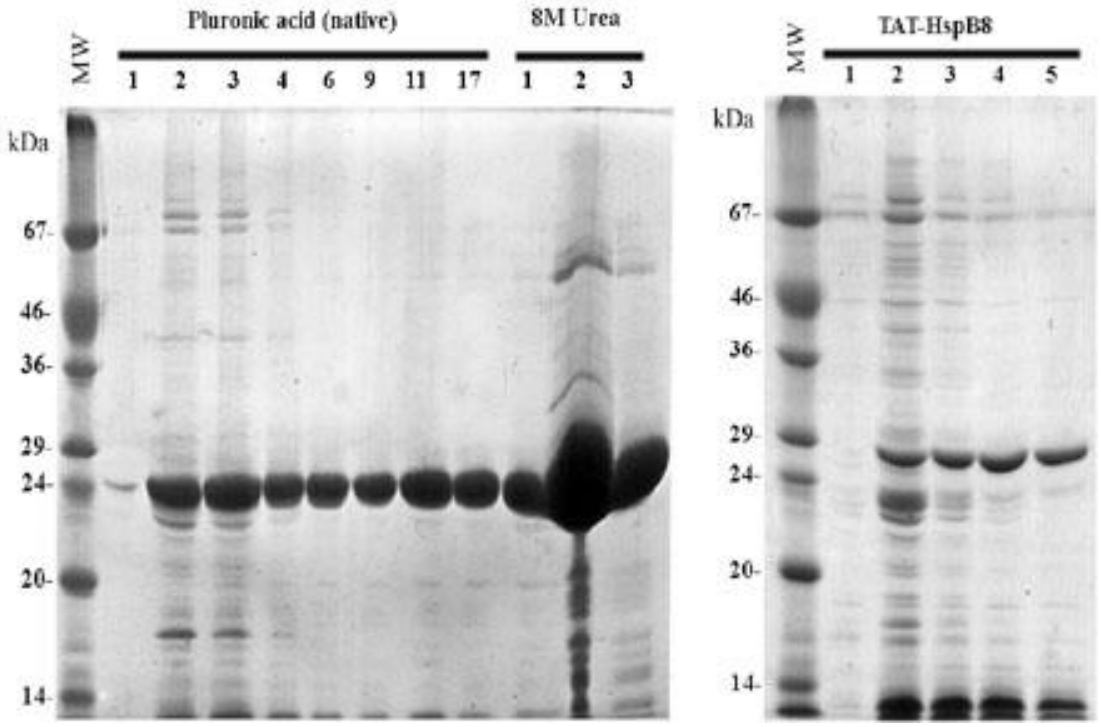

Fig: 34. SDS-page of the recombinant proteins purified in native conditions (left) for HSPB8wt and mutants, and in denaturant conditions for TATHSPB8wt and mutants (right).

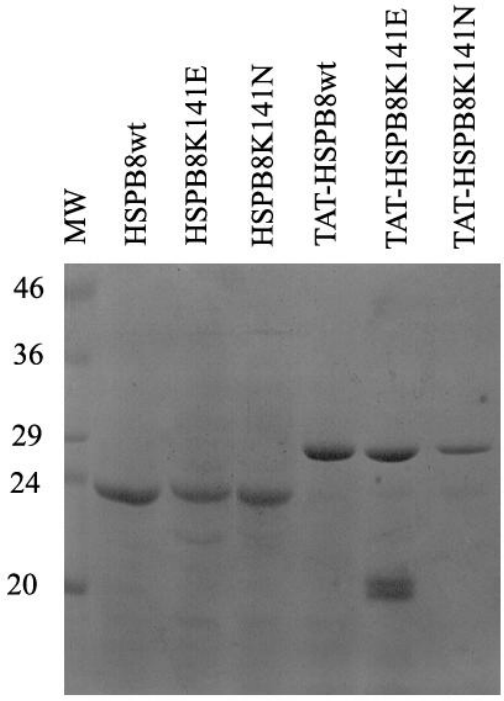

Fig: 35, SDS-page of the recombinant proteins dialyzed against 100mM Tris-HCl, 20% glycerol, 274mM NaCl, 0,1% Pluronic acid, 0,02% Tween 20, 10mM β-mercaptoethanol pH 8 in the case of HSPB8wt and mutants, and 50mM phosphate buffer, 274mM NaCl, 20% Glycerol, 0,1% Pluronic acid, 0,02% Tween 80, 10mm DTT pH 5,82 in the case of TATHSPB8 and mutants.

SDS-PAGE, Western blotting and dot-blot assay

Mini SDS-PAGE was performed using the electrophoresis MiniVE (Amersham) system according to the manufacturer's instructions. Protein samples were diluted in Laemmli sample buffer (50 mmol/L Tris-HCl pH 6.8, 100 mmol/L DTT, 2% (w/v) SDS, 0.05% (w/v) bromphenol blue) and heated for 5 min at 100°C. Each well of a 13,5% SDS-PAGE was loaded with 1 µg total proteins. Separated proteins were transferred onto Immobilon-P polyvinylidene difluoride (PVDF) membranes (Millipore) with the mini VE System Blot Module (Amersham). For HSPB8 and its mutants the proteins were directly blotted onto the Bio-Dot Apparatus Microfiltration (Biorad) following the manufacturer's instructions. For Far Western blots the membrane was incubated with 10 mL of HSPB8wt (10 µg/mL) or its mutants in blocking buffer. Dot blot membrane was incubated with 10 mL of 10 µg/mL recombinant HuPrP. Membranes were washed 3 x 5 min with PBS/1% BSA, 0.1% Tween 20. HSPB8 bound to PrP or vice versa was detected by incubation with 0.4 mg/mL of anti-his monoclonal antibody (H1029) (Sigma-Aldrich) or 0.5 mg/mL of anti-PrP mAb 3F4 (DAKO, Glostrup, Denmark) in blocking buffer for 1 h at RT followed by incubation with 50 ng/mL horseradish peroxidase-conjugated goat anti-mouse IgG mAb (Sigma-Aldrich) for 45 min at RT. The blot was developed using the NBT/BCIP (Roche).

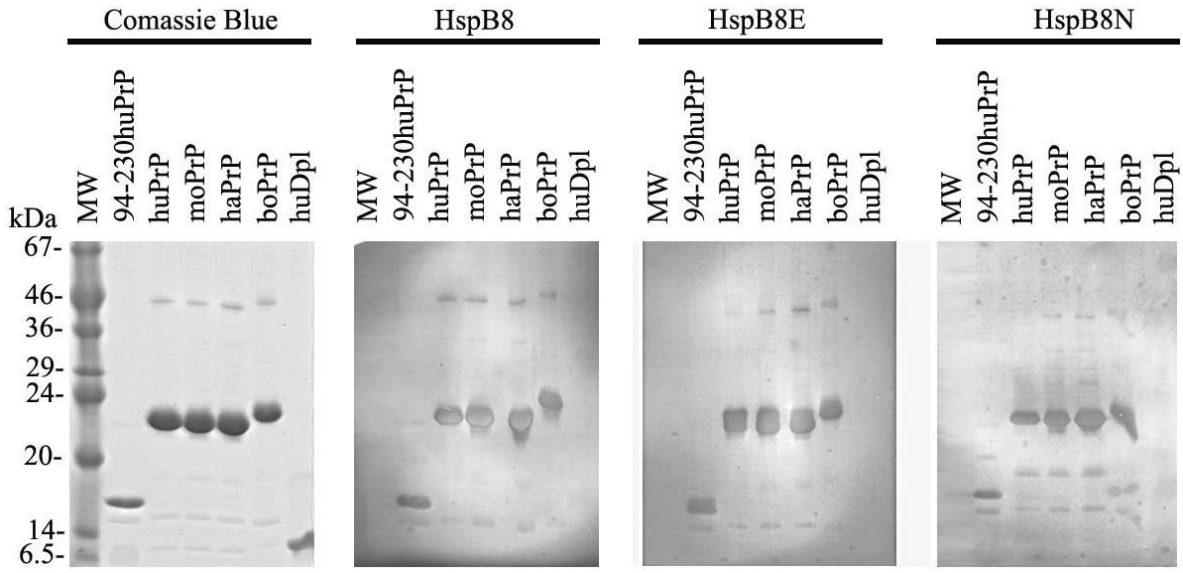

Fig: 36. **Far Western blot analyses of prion proteins with Heat shock porotein B8 and its mutants.**
Recombinant deletion form human PrP(94-230), human PrP, mouse PrP, hamster PrP, bovine PrP and human Dpl were separated by 13% SDS-PAGE. The same proteins are transferred on nitrocellulose and probed with 25 µg/mL recombinant human HSPB8wt, HSPB8K141E or HSPB8K141N and developed with an anti-his antibody.

The data obtained from western blot showed that PrPs from human, mouse, hamster and bovine all interact with HSPB8 wild type and mutants. Human Doppel, instead, is not recognized by none of the three proteins. HSPB8wt and mutants specifically recognized PrP not being able to bind the other protein loaded as molecular weight markers. As for TH, far western blotting was effective only with PrP bound to the PVDF membrane and using HSPB8 as analyte; no interaction was observed when HSPB8 was bound to the PVDF membrane and PrP used as analyte. We, therefore, performed a dot-blot experiment.

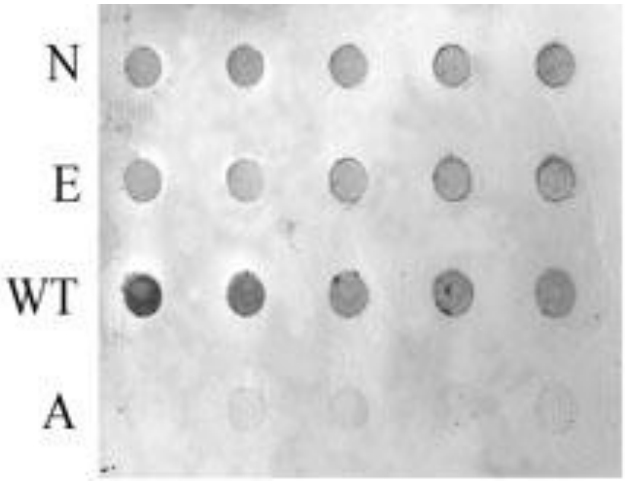

Fig: 37. **Dot blot analyses of prion proteins with Heat shock protein B8 and its mutants**.
Serial dilutions (μg) of recombinant human HSPB8wt, HSPB8K141E, HSPB8K141N and albumin, were blotted onto nitrocellulose before probing with 20 μg/mL huPrP(23-230) followed by development with antibodies against huPrP (3F4).

The results show that PrP is able to bind all the three forms of HSPB8 while it doesn't recognize albumin. The interaction of PrP with HSPB8 wild type seems to be stronger than the interaction of the prion protein with the mutant forms of the heat shock protein.

To further confirm HSPB8-PrP interaction and to identify the region of the prion protein involved in the binding, we performed a far western blot analysis using several deletion mutants of the protein. Sample resolved by SDS-page and blotted onto PVDF membrane, were incubated with 10ml of HSPB8wt (10 μg/ml) in blocking buffer and developed with anti-His antibody.

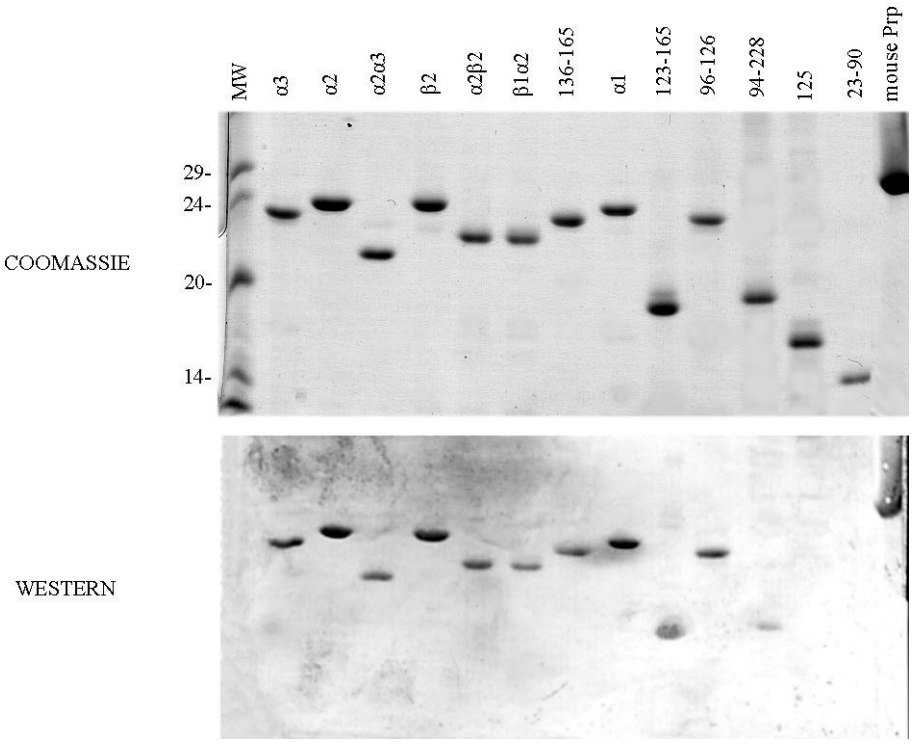

Fig: 38. **Far Western blot analyses of prion protein deletion mutants with Heat shock protein B8.**
Recombinant deletion form of human PrP were resolved by 13% SDS-PAGE. The same proteins were transferred on nitrocellulose, probed with 10 μg/ml recombinant human HSPB8wt and developed with an anti-his antibody.

HSPB8wt is able to recognize almost all the deletion forms of the prion protein, except for PrP125 and PrP(23-90) indicating that the portion of the protein involved in the binding is the structured C-terminal sequence of PrP while the N-terminal un-structured domain is not bound by the heat shock protein.

PrP proteolysis by Proteinase K

To further validate HSPB8-PrP interaction and identify possible in *vitro* consequences of this binding we performed an experiment to analyze PrP susceptibility to degradation mediated by proteinase K in the presence or absence of HSPB8 wild type or its mutants. It is, in fact, known that the cellular isoform of the prion protein (PrP^{C}) has an high susceptibility to proteinase K digestion, while the pathological isoforms of the protein (PrP^{SC}) is resistant to the degradation.

2μg of the murine prion protein were incubated with serial dilution of proteinase K in the presence or absence of 2μg of HSPB8wt and its mutants. The reaction was stopped by adding Laemmli sample buffer to the samples. The reaction products were heated for 5 minutes at 100°C and loaded into a 13,5% polyacrylamide gel.

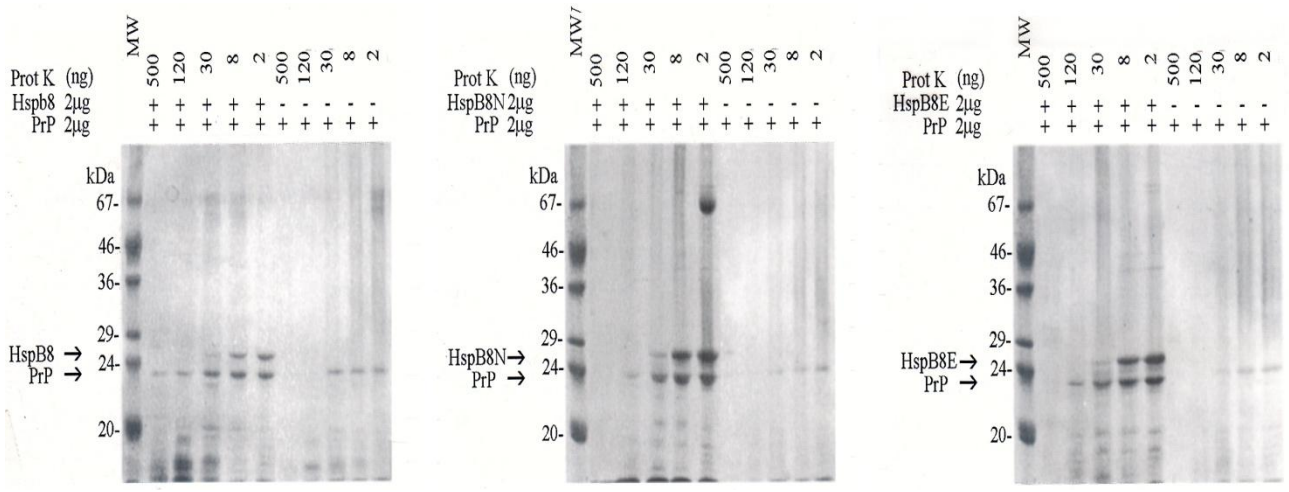

Fig: 39. SDS-page of the proteolysis of the prion protein with proteinase K in the presence or absence of HSPB8wt and mutants form.

The murine PrP is completely degraded after incubation with high concentrations of proteinase K and also lower amount of proteinase K are able to digest the major part of the prion protein. When, instead, the prion protein is incubated in the presence of the heat shock protein it is much less degraded. This protection is almost complete at low doses of proteinase K, but it is also present at higher doses. All the three forms of the HSPB8 are able to protect the prion protein but the mutant forms are less effective as we can see by the fact that at the highest dose of proteinase K they are not able to protect PrP from degradation. All these data together clearly demonstrate a protection from proteolysis by HSPB8 protein in the presence of protease. HSPB8 shows its chaperone activity protecting the prion protein from degradation. The mutant forms of the heat shock protein show a less effective, although present, protective action.

Circular dichroism analyses

A functional consequence of the interaction between the two proteins was evaluated following the denaturation process of the prion protein through circular dichroism in the presence or absence of HSPB8 in wild type form.

As shown in fig. 40 the prion protein spectrum (dashed line) is characterized by two minimum at 211 and 221 nanometers, indicating a prevalent α-helix structure; while the heat shock protein B8 wild type spectrum (solid line) shows a prevalent unorder structur with a little incidence of a β-sheet structure (minimum at 215 nanometers).

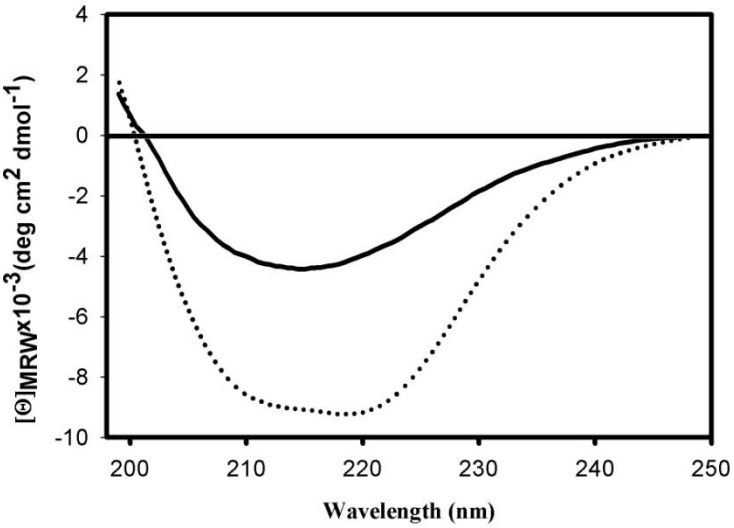

Fig: 40. CD spectra of the prion protein (dashed line) and the small HSPB8WT (solid line).

The thermal denaturation process of the prion protein misured at 220 nanometers show a cooperative transition with a shift around 66°C. When prion protein was incubated in presence of the same molar amount of HSPB8 wild type (dashed line) the process of thermal denaturation occurred at lower temperature it was faster when compared to the prion protein alone (solid line).

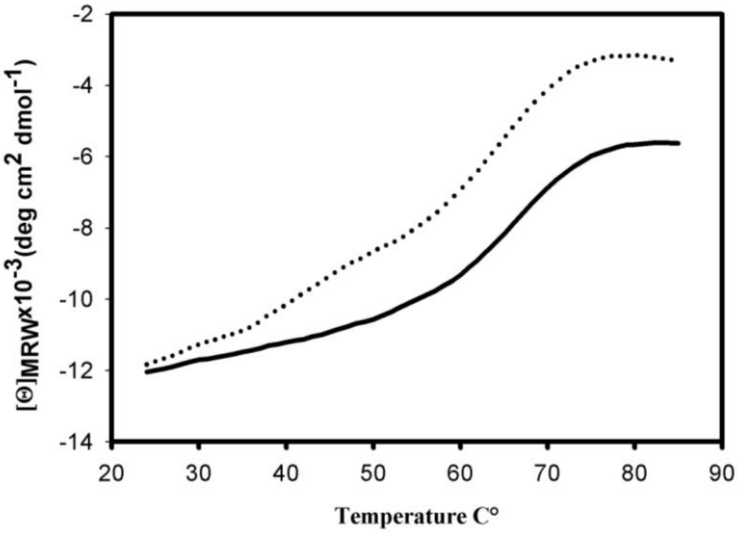

Fig: 41. CD spectra of the prion protein denaturation in the presence (dashed line) or absence (solid line) of the heat shock protein B8 wild type.

This shift in the prion protein denaturation spectrum is attribuible almost entirely to the prion protein with no incidence of the heat shock protein because, as shown in fig. 42, the HSPB8WT doesn't undergo to big changes of structure under thermal denaturation.

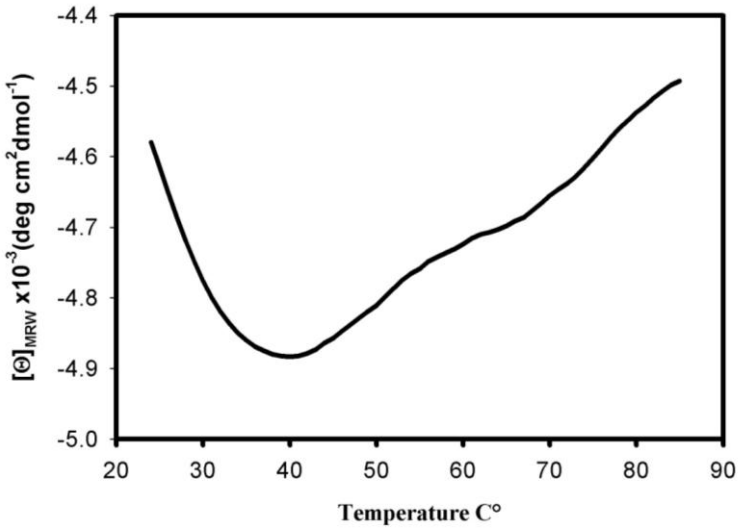

Fig: 42. CD spectrum of heat shock protein B8 wild type denaturation.

Interaction analysis on Biacore via surface plasmon resonance (SPR)

The surface plasmon resonance experiments were conduct in the same conditions used for the PrP-TH interaction evaluation. The huPrP(23-230) was immobilized on the sensor chip while HSPB8wt and its mutant forms were injected, as analyte, at various concentrations (within the range 10nM to 10µM). The kinetic and thermodynamic association and dissociation constants obtained are shown in table:

Ligand	k_a (1/Ms)	k_d (1/s)	K_D (M)	Rmax (RU)	Chi² (RU²)	U-value
HSPB8 WT	7111	0, 00261	$3,67\ 10^{-7}$	606,6	350	2
HSPB8 K141N	6550	0, 00270	$4,12\ 10^{-7}$	667,3	797	3
HSPB8 K141E	5408	0, 00295	$5,46\ 10^{-7}$	693,0	980	4

Fig: 43. Kinetic parameters and dissociation constants for the interaction of HSPB8 wild type and mutants with PrP.

Thermodynamic evaluation of the interaction between HSPB8 and PrP yielded equilibrium dissociation constants (*K*D) of 367nM, 412nM and 546nM for wild type HSPB8, HSPB8K141N and HPB8K141E, respectively. Sensorgrams for the interaction of PrP with HSPB8wt, K141N and K141E are shown in fig. 44, while fig. 45 shows the dose-response SPR signal *versus* the concentration of heat shock proteins.

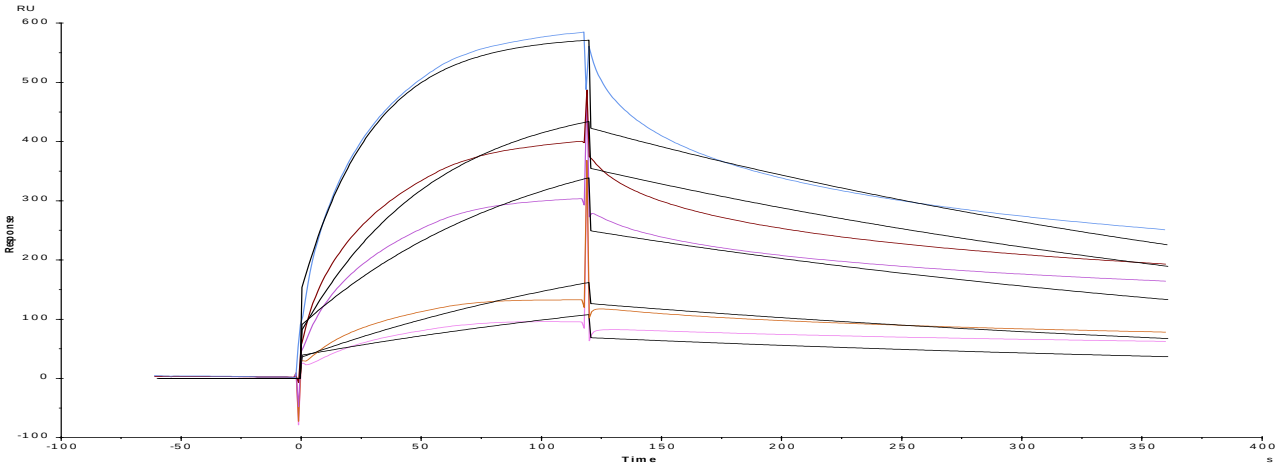

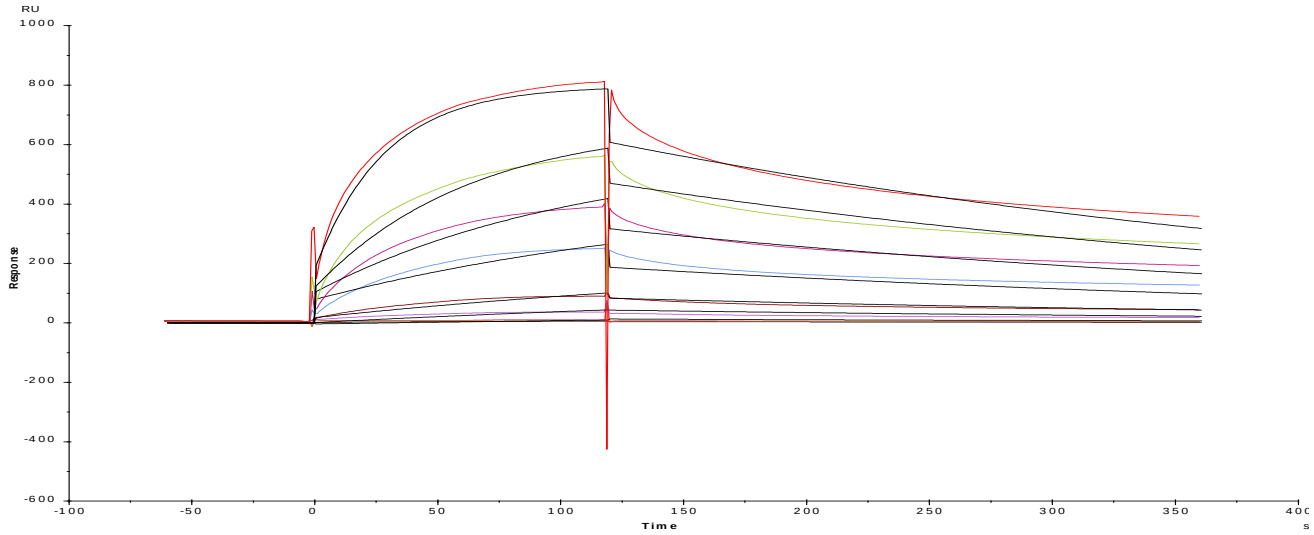

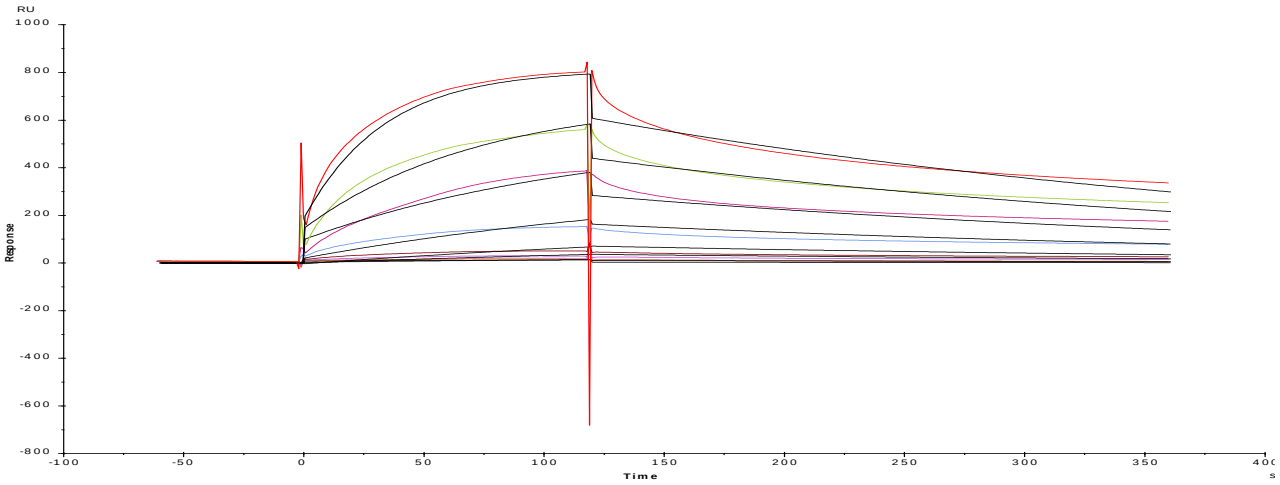

Fig: 44. Association and dissociation curves over the PrP-immobilized chip at various concentrations of HSPB8wt, HSPB8K141N and HSP8K141E (from top to bottom).

The evolution of the response as a function of the concentrations of HSPB8wt and its mutants tends to a plateau at concentrations greater than 5µM, index of specificity in the interaction between the PrP and the HSPB8.

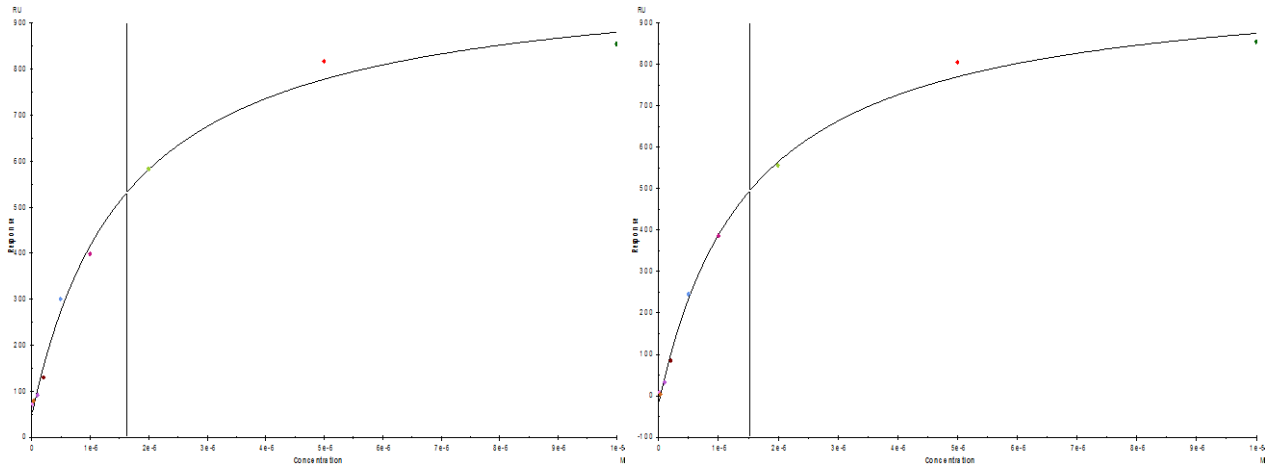

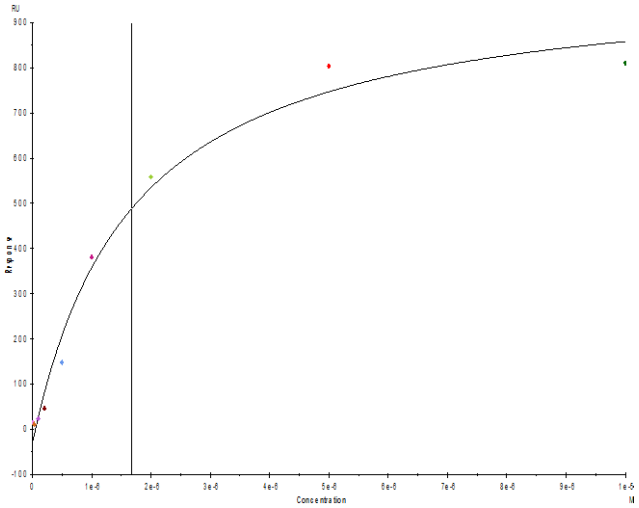

Fig: 45. Response (in arbitrary units) *versus* concentration of HSPB8wt, HSPB8K141N and HSP8K141E, respectively.

The data obtained show a strong interaction between PrP and all the three forms of the small heat shock protein. However, the interaction of the wild type HSPB8 with the prion protein results to be stronger than both the mutants forms, according with the western blot and dot-blot data.

Cellular expression of PrP and HSPB8

Interaction between PrP and TH in intact cells was evaluated by co-transfecting CHO cells with expression plasmids for HSPB8 and human PrP.

In CHO cells transfected with pcDNA-HSPB8 and pcDNA-PrP, HSPB8 migrates as a 29 kDa species on immunoblots because in this case HSPB8 have a N-terminal tail with 14 aminoacids conteining 6 histidine residues necessary for immunoblot assay using His-tag monoclonal antibody. PrP shows different bands corresponding to the various glycosilation states of the protein. Co-expression of HSPB8 strongly decreased the presence of all PrP forms.

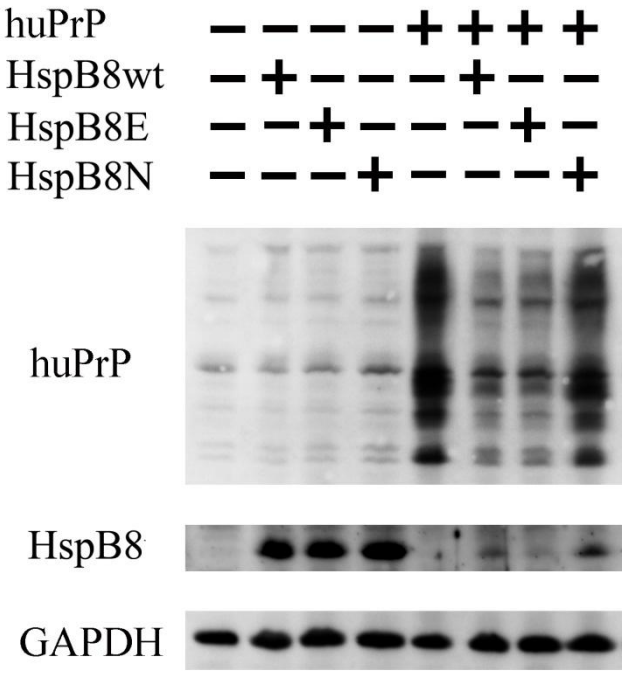

Fig: 46. **Protein expression of heat shock protein (HSPB8) and prion protein (PrP).**
CHO cells were transfected with pcDNA (control), pcDNA-HIS-HSPB8 or pcDNA-PrP. Western blot was developed with anti-His, or anti-PrP, and anti-GADPH.

In particular, it seems that the wild type HSPB8 has an effect on PrP comparable with that of the HSPB8K141E, while the reduction of prion protein expression mediated by HSPB8K141N is much less noticeable. The co-expression of the two protein also strongly reduced the level of expression of all the three forms of the small heat shock protein. Once again the K141N mutated form of the protein is the less affected by the reduction of cellular expression level.

To verify if the effects of the heat shock protein on the prion protein are dependent on the transfection of the plasmid vector, we test if the same effect is reached when CHO cells are treated with TATHSPB8 wild type and mutants. To do this we firstly tested the half life of the protein in the cells. CHO cells were treated with 10µg/ml of recombinant TATHSPB8 wild type and collected 3, 5, 24, 36 and 48 hours after the addition of the protein. Samples were loaded into a 13,5% SDS-page and transferred onto a PVDF membrane developed with anti-His or anti-PrP antibodies.

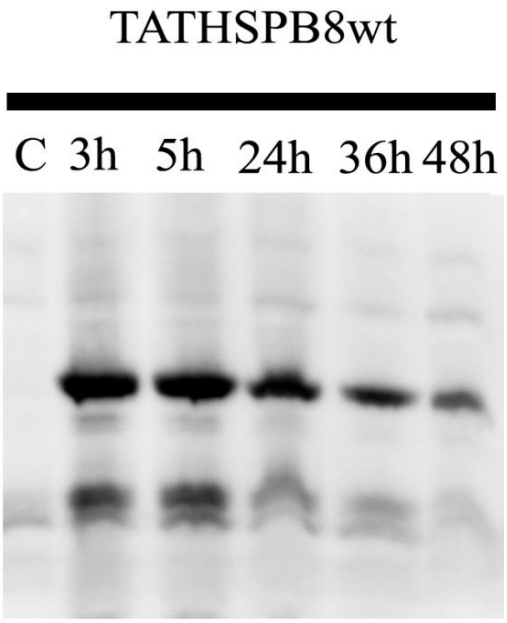

Fig: 47. Time course of the TATHSPB8 wild type in CHO cells.

Our results show that TATHSPB8 wild type is able to enter the cells within three hours after the addiction to the culture medium. The protein remains detectable in the cells for up to 48 hours.

The experiments were repeated treating CHO cells with 10µg/ml of recombinant TATHSPB8 and 10µg/ml of recombinant TATPrPGFP11 or with the same amount of TATPrPGFP11 alone. Samples were colleted after 3, 5, 24, 36 and 48 hours from the addition of the proteins and loaded into a 13,5% SDS-page and transferred onto a PVDF membrane developed with anti-His antibody for the detection of the heat shock protein 3F4 antibody for the detection of the prion protein.

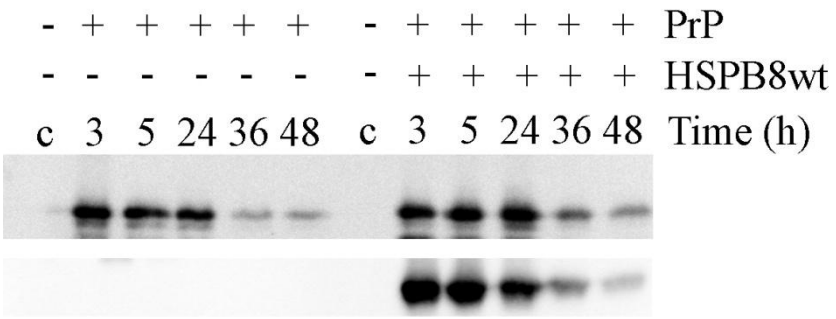

Fig: 48. Time course of the TATHSPB8 wild type and TATPrPGFP11 proteins in CHO cells.

Data from western blot show a slight protection of prion protein degradation mediated by the co-expression of the heat shock protein.

Cellular distribution of PrP and HSPB8

Interaction between PrP and HSPB8 in intact cells was evaluated by co-transfecting CHO cells with expression plasmids for a GFP tagged prion protein (pEGFP-PrP) (Negro et al. 2000) and a mRuby2 tagged human HSPB8 wild type and mutants. Once again, PrP showed a predominantly plasma membrane expression (fig. 49D), while the heat shock proteins seems to accumulate intracellularly and to form small aggregates that are much more evident for the mutant forms K141E and K141N (fig. 49B and C, respectively) than for the wild type protein (fig. 49A).

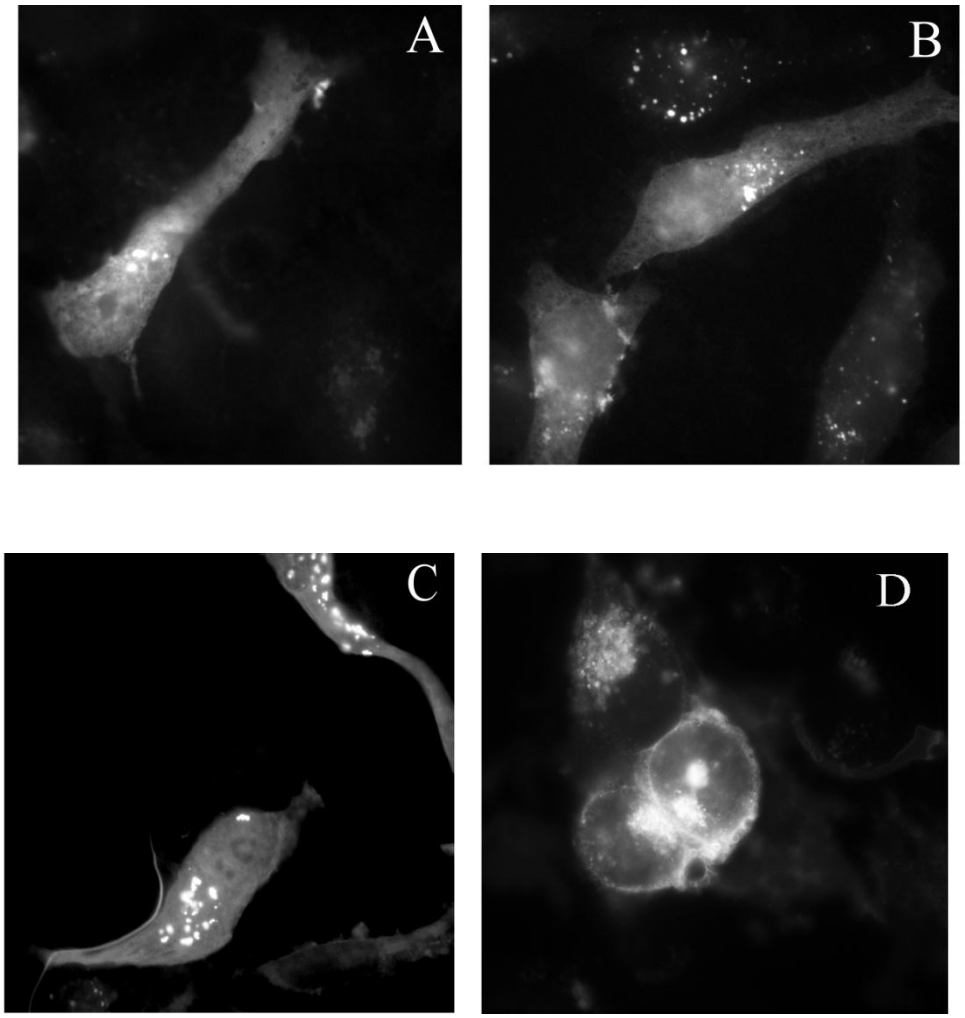

Fig: 49. Cellular localization in CHO cells of HSPB8-mRuby2 wild type, K141E and K141N (panel A,B,C respectively) and GFP-PrP (panel D).

Co-expression of the two proteins resulted in a strong decrease in plasma membrane PrP expression, along with an increased intracellular expression. The switch from a plasma membrane expression to an intracellular expression was particularly evident when the co-expression involved PrP and the wild type form of the small heat shock protein, while it was less clear when the prion

protein was co-expressed with the mutant forms of HSPB8, especially for what concern HSPB8K141N.

The intracellular localization of all forms of the small heat shock protein was unaffected. The co-expression of the two proteins resulted in a strong co-localization of HSPB8 wild type with the prion protein. This co-localization is also present with the mutant forms of the heat shock protein, but with a less extent.

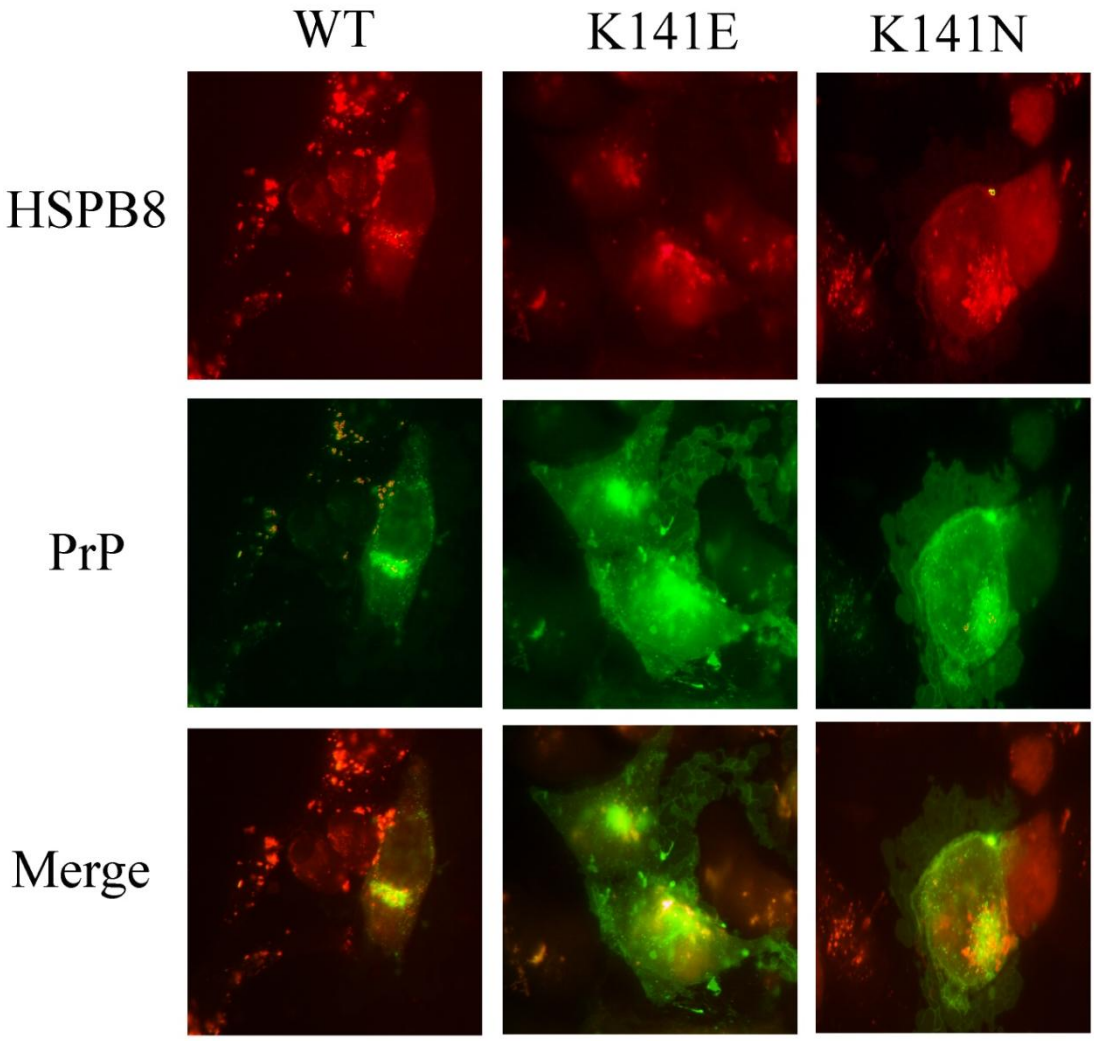

Fig: 50. **Co-localization of GFP-PrP with HSPB8-mRuby2 wild type and mutants.**
CHO cells were co-transfected wih pHSPB8wt-mRuby2, pHSPB8K141E-mRuby2 and pHSPB8K141N-mRuby2 (higher row) and with pcDNAGFP-PrP (middle row). Lower row merges the upper panels.

DISCUSSION AND FUTURE PERSPECTIVE

Our study is the first description of two specific and neurologically relevant interactions involving the prion protein, known to be the major player in a group of diseases involving the central nervous system collectively named transmissible spongiform encephalopathies (TSEs). The novel-identified interaction partners of PrP are tyrosine hydroxylase (TH), enzyme that catalyzes the first and rate limiting step in the biosynthesis of catecholamines, and heat shock protein B8 (HSPB8), member of the small heat shock protein family, that seems to be of special interest in those diseases that, like TSEs, are characterized by the accumulation of misfolded proteins.

Being two cytoplasmatic proteins, TH and HSPB8, would not be expected a priori to be accessible to PrP, prevalently expressed in the cell as a plasma membrane GPI-anchored protein. Anyway, numerous studies report the presence of a cytosolic PrP form in subpopulations of neurons in the hippocampus, neocortex, and thalamus (Mironov et al. 2003, Fioriti et al. 2005, Ma et al. 2002) in a variety of condition including stress (Orsi et al. 2006). Moreover, it is clear from the literature that PrP can interact with numerous intracellular proteins, most of them located in the cytosol. Among them we can find synapsin-1b, neuroglobin, 14-3-3 protein, tubulin and mahogunin (Nieznanski 2010 for review). Thus, it is possible to postulate that particularly at pathologic conditions, intracellular proteins may be exposed to interactions with PrP or that they can cross with the prion protein during its synthesis and translocation to the plasma membrane.

Prion protein-Tyrosine hydroxylase interaction

Western blotting, dot blot and surface plasmon resonance analysis indicate a strong interaction between PrP and tyrosine hydroxylase. The binding occurs with PrP of various species while the human doppel protein, sharing the same structure with PrP, is not recognized by the TH. TH recognizes PrP through its N-terminal regulatory domain TH(1-152), while the catalytic domain is not involved in binding. On the other hand, PrP recognizes TH through its C-terminal domain PrP(90-230), while the N-terminal domain is not involved in binding. The SPR analysis show KD values falling in the range 2.2-5.0 nM when PrP is immobilized on the sensor chip and in the range 46.4-108 nM when TH is immobilized on sensor chip. The two sets of measurements provide strong support for a PrP-TH interaction even though with slightly different affinities. When PrP is covalently immobilized through its -NH_2 groups, its C-terminal interacting domain (94-231) is entirely exposed and hence prone to recognize and bind TH. Likewise, when TH is immobilized, its N-terminus covalently binds to the carboxymethyl

dextran chip-matrix and hence is less exposed to PrP, resulting in a less productive binding. In addition, re-folded PrP is recognized by TH on far Western blot, while PrP recognizes TH only when immobilized by dot-blot technique, indicating that both proteins must be folded for the recognition and binding. All these data together indicate that the interaction between prion protein and tyrosine hydroxylase is characterized by high affinity, is dependent of structured region of the proteins and is both sequence and structure specific.

The interaction between the two proteins is confirmed by the immune-localization data in intact cells, where they show a co-localization pattern. In particular, when TH is co-expressed with PrP, the latter is involved in a switch from a prevalent plasma membrane-expression to a prevalent intracellular expression while the TH topological localization is not affected. Data from western blotting reveal that co-expression of the two proteins significantly reduced the level of expression of all the cellular forms of the prion protein, while the level of expression of tyrosine hydroxylase are not affected. Moreover, RT-PCR analyses show that while the protein expression level of PrP are down-regulated, the mRNA levels don't change after co-transfection with TH, suggesting that the modification of prion protein levels is a post-translational event. The recovery of TH by co-immunoprecipitation supports the evidences of a cellular interaction involving the two protein. The fact that this co-immunoprecipitation is achieved only when TAT-PrP is added to the cell and not when TH and PrP are simply co-transfected, is probably due to the very low amount of PrP in the cell when TH is expressed.

Our finding seems to be supported by previous studies on scrapie infected mice and dopaminergic neurons. Yun et al. found that TH-immunoreactive neurons in the substantia nigra and locus ceruleus are significantly decreased in scrapie-infected mice compared to controls (Yun et al. 1998) while Ford and colleagues showed that while dopaminergic neurons of the substantia nigra express high levels of TH protein, these same cells display a high PrP mRNA content but no detectable PrP^{C} protein (Ford et al. 2002). The reason for this disparity between mRNA and protein level of PrP^{C} within the CNS is not known, although the exceptionally fast turnover of Prp^{C} in cerebellar granule cells has been suggested to account for this disparity (Parizek et al. 2001). This finding is in line with the altered cellular distribution and expression of PrP observed in our experiments when PrP is co-expressed with TH.

The observation that PrP does not affect TH activity in vitro could be due to the fact that PrP binds the regulatory, but not catalytic domain of TH. Several proteins bind to TH, one of the most studied being 14-3-3. Also in this case, binding between 14-3-3 and TH occurs through the N-terminal regulatory domain of TH (Halskau et al. 2009), with an affinity comparable to that

observed for PrP towards TH (Kleppe et al. 2001). The 14-3-3 protein does not influence TH catalytic activity directly, but rather the latter's accessibility to kinases and phosphatases. For example, PrP could mask the TH N-terminal domain in such a way as to prevent phosphorylation and activation. α-Synuclein, which is involved in Parkinson disease, can also modulate TH activity by inhibiting its phosphorylation and consequently dopamine synthesis (Peng et al. 2005). PrP itself undergoes phosphorylation and is capable of modulating the phosphorylation of several kinases (Negro et al. 2000; Meggio et al. 2000). One cannot exclude that PrP may modulate TH activity in a similar manner.

All these data seems to suggest important physiological and pathological roles for TH-PrP interaction and is possible to hypothize some scenarios involving this binding. For example one might speculate that in Parkinson disease, characterized by a loss of dopaminergic neurons, PrP acts to sequester TH released from compromised neurons and hence supports the remaining surviving cells. On the other hand it is also possible that in physiological condition TH could be a direct modulator of PrP expression and distribution inside the cell, while in pathological conditions the over-expression or down-regulation of one of the protein leads to an alteration of the binding resulting in pathological processes such as the accumulation of misfolded PrP inside the cell. This hypothesis is in line with recent ideas suggesting that protein-protein interaction can ameliorate protein-misfolded diseases allowing the normal biological function of proteins and preventing their aggregation and accumulation (Pastore and Temussi 2012).

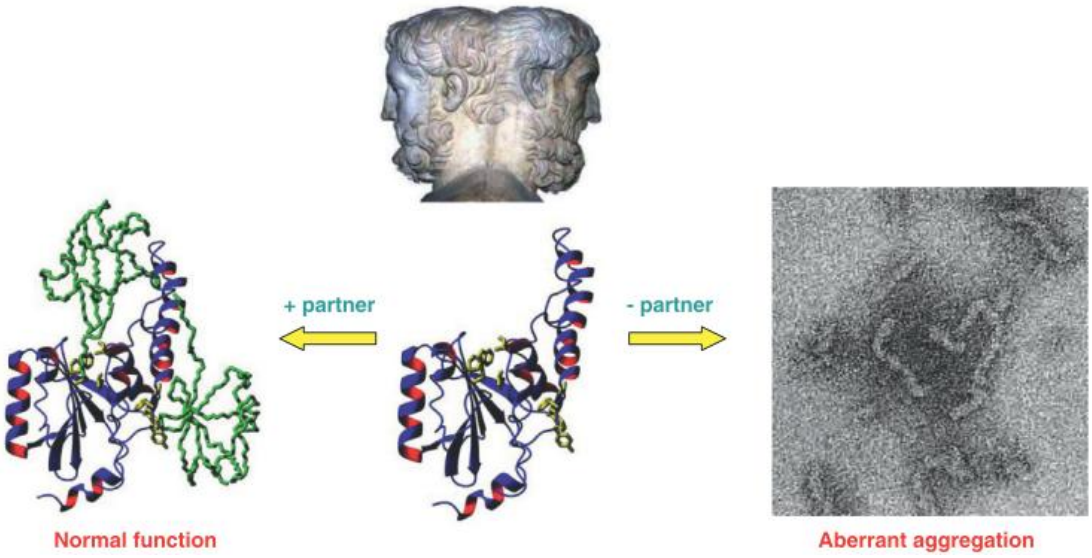

Fig: 51. Schematic representation of the protein fate. The interaction with a partner allows the normal function of the protein, while the absence of the binding partner leads to aberrant aggregation of the protein (Pastore and Temussi 2012).

Our data show that TH could be a direct modulator of PrP expression and, conceivably, decreased TH expression could increase PrP levels. To further strengthen this idea we're going to express short interference RNA for tyrosine hydroxylase in cells expressing high amount of the enzyme and very low amount of prion protein. If our statements are true, the inhibition of TH expression mediated by siRNA should lead to an increase of PrP expression and localization on the plasma membrane. Moreover, future studies should be directed to determine if these relationships occur also in diseases human brain.

Prion protein-Heat shock protein B8 interaction

Western blotting, dot blot and surface plasmon resonance analyses indicate a strong interaction between PrP and the small heat shock protein HSPB8. As in the case of tyrosine hydroxylase, the heat shock protein recognizes PrP of various species, but is unable to bind the human doppel protein. PrP recognizes the heat shock protein through its C-terminal domain PrP(90-230), while the N-terminal domain is not involved in binding. Western blotting analyses reveal that the interaction occurs not only with the wild type form of the protein, but also with the two pathological mutants, even if with less strength. Western blotting analysis with the three forms of the heat shock protein immobilized on the PVDF membrane and PrP used as analyte are not possible because of the incapability of the proteins to refold on the membrane. Dot-blot experiments, that don't need any denaturation steps, confirm the interaction between the heat shock protein forms and the prion protein, underling that it is stronger for the wild type forms than for the mutant forms. The SPR analysis show KD values falling in the range 367nM- 546nM when PrP is immobilized on the sensor chip. The quantitative data of the surface plasmon resonance confirm the results obtained with western blotting and dot-blot indicating that the stronger interaction occurs between the wild type heat shock protein and the prion protein, while the weakest binding is that between PrP and the K141E mutant form of the HSPB8. As expected, the mutations associated with the development of distal motor neuropathy type II and Charcot-Marie-Tooth disease type 2 show less binding affinity for the prion protein with respect to the wild type protein.

In order to verify if this lower affinity leads to some functional changing we tested the *in vitro* protection of PrP degradation mediate by proteinase K. Our results indicate that HSPB8 is always able to protect the prion protein from proteolysis but that the mutant forms are less performing, in particular for what concern HSPB8K141N. It is possible that the single amino acid substitution of the mutant forms of the heat shock protein not only affects the strength of the interaction with PrP but it also uncovers a cleavage site for the proteinase K on the PrP sequence leading to a faster degradation of the protein.

Data from circular dichroism has also shown that the incubation with the small heat shock protein B8 wild type is able to improve the prion protein denaturation under heat stress conditions.

The interaction between the prion protein and the heat shock protein is confirmed by the immune-localization data in intact cells, where they show a co-localization pattern. When the HSPB8 wild type or mutant forms are co-expressed with PrP, the latter undergoes to a change from a plasma membrane GPI-anchored expression to a prevalent intracellular expression that overlap the expression of the heat shock protein. This changing is particularly clear in the case of the wild type heat shock protein, while is less clear with the pathological forms of the protein, especially for what concern the lysine to asparagine substitution. It is intriguing that the various forms of the heat shock protein show different behaviors also where they are expressed alone in intact cell. HSPB8, in fact, tends to form small aggregates inside the cell. The number and size of these aggregates becomes bigger for the mutant forms of the protein. Once, again, the K141N show the worst phenotype. One might speculate that the wild type form of the protein exist in a semi-soluble state inside the cell and that the mutation affecting the lysine at position 141 makes the mutants less soluble leading to their aggregation inside the cell.

Western blotting data show that when the two proteins are co-expressed in intact cells, the protein expression of both PrP and HSPB8 decreased. This down-regulation is quite comparable for the wild type heat shock protein and for the lysine to glutamic acid substitution at position 141, while for the K141N mutation we can observe a different phenotype in which the level of heat shock protein are extensively down-regulated, while the PrP protein expression levels are affected only minimally. These results are in good agreement with the *in vitro* results and indicate that the interaction between prion protein and heat shock protein is able to modulate the expression and localization of both the proteins. It is intriguing that the K141N mutant, even if SPR data indicate that it doesn't have the lower affinity for the prion protein, shows the worst phenotype in all the experiments conducted. It is possible to postulate that heat shock protein acts on PrP in the same way it was found to act with polyglutamine proteins leading to their degradation by stimulating macroautophagy. Our findings suggest that this process is dependent not only on the strength of the interaction but also on the nature of the amino acid substitution that can alter the physical-chemical property of the heat shock protein or its interaction with other proteins inside the cell. One may speculate that heat shock protein has a dual function in the cell with respect to the prion protein: on one way it acts as a molecular chaperone, helping the proper folding of the prion protein, on the other way it facilitates the turnover of the protein and the degradation of misfolded PrP maintaining the levels of the prion protein at a physiological state and preserving its biological function. It

seems reasonable that the mutations associated with the development of neuropathies, in particular in the case of the lysine to asparagines substitution, change not only the strength of the binding with the prion protein but also the physical-chemical properties of the heat shock protein that tends to aggregate inside the cell. It is possible that this aggregation state may prevent the chaperone activity of the heat shock protein and its capacity to stimulate the degradation of misfolded protein leading to the accumulation of intracellular prion protein that might cause neurological disorders.

An opposite effect is obtained when cells are treated with TATPrPGFP11 and TATHSPB8WT. In this case, western blot analyses reveal that the heat shock protein co-expression is able to protect the prion protein from the degradation, leading to higher yields of the protein inside the cells. This data reflect the protection of the prion protein from the *in vitro* degradation by the proteinase K mediated by the heat shock protein. The inconsistency with the results obtain with the co-transfection of the proteins in intact cells can be due to the different fate of the protein inside the cells. When PrP is tranfected, in fact, it is subjected to a series of translocation and post translational modification (including its translocation to the Golgi apparatus and its glycosilation) leading to a plasma membrane localization, while when the prion protein enter the cell via Tat it is immediately available for the degradation ad the small heat shock protein can bind the prion protein preventing its turnover. In light of these results, it is reasonable that the heat shock protein may function as a molecular chaperone on the prion protein, being able in different conditions or concentrations of both preventing or helping its clearance inside the cells.

As in the case of tyrosine hydroxylase future studies should be directed to determine if these relationships between PrP and heat shock protein occur also in diseases human brain. If this were confirmed, the wild type heat shock protein would be a promising target for a therapeutic approach aimed to prevent the aggregation and accumulation of aberrant PrP molecules, which is at the basis of all the transmissible spongiform encephalopathies.

BIBLIOGRAPHY

Aguzzi A, Calella AM. 2009 Prions: protein aggregation and infectious diseases. *Physiol Rev.* 89:1105-52.

Anagnostou G, Akbar MT, Paul P, Angelinetta C, Steiner TJ, de Belleroche J. 2010 Vesicle associated membrane protein B (VAPB) is decreased in ALS spinal cord. *Neurobiol Aging.* 31:969-85.

Antonyuk SV, Trevitt CR, Strange RW, Jackson GS, Sangar D, Batchelor M, Cooper S, Fraser C, Jones S, Georgiou T, Khalili-Shirazi A, Clarke AR, Hasnain SS, Collinge J. 2009 Crystal structure of human prion protein bound to a therapeutic antibody. *Proc Natl Acad Sci*. 106:2554–2558.

Arrigo AP, Gibert B. 2013 Protein interactomes of three stress inducible small heat shock proteins: HspB1, HspB5 and HspB8. *Int J Hyperthermia.* 29:409-22.

Aurelian L, Laing JM, Lee KS. 2012 H11/HspB8 and Its Herpes Simplex Virus Type 2 Homologue ICP10PK Share Functions That Regulate Cell Life/Death Decisions and Human Disease. *Autoimmune Dis.* 2012:395329.

Aurelian L, Smith CC, Winchurch R, Kulka M, Gyotoku T, Zaccaro L, Chrest FJ, Burnett JW. 2001 A novel gene expressed in human keratinocytes with long-term in vitro growth potential is required for cell growth. *J Invest Dermatol.* 116, 286-95.

Badri KR, Modem S, Gerard HC, Khan I, Bagchi M, Hudson AP, Reddy TR. 2006 Regulation of Sam68 activity by small heat shock protein 22. *J Cell Biochem*. 99:1353-62.

Bartelt-Kirbach B, Golenhofen N. 2013 Reaction of small heat-shock proteins to different kinds of cellular stress in cultured rat hippocampal neurons. *Cell Stress Chaperones.*

Behl C. 2011 BAG3 and friends: co-chaperones in selective autophagy during aging and disease. *Autophagy*. 7:795-8.

Belay ED. 1999 Transmissible spongiform encephalopathies in humans. *Annu Rev Microbiol.* 53:283-314.

Benndorf R, Sun X, Gilmont RR, Biederman KJ, Molloy MP, Goodmurphy CW, Cheng H, Andrews PC, Welsh MJ. 2001 HSP22, a new member of the small heat shock protein superfamily, interacts with mimic of phosphorylated HSP27 ((3D)HSP27). *J Biol Chem.* 276, 26753-61.

Botto L, Masserini M, Cassetti A, Palestini P. 2004 Immunoseparation of Prion protein-enriched domains from other detergent-resistant membrane fractions, isolated from neuronal cells. *FEBS Lett.* 557:143-147.

Bounhar Y, Zhang Y, Goodyer CG, LeBlanc A. 2001 Prion protein protects human neurons against Bax-mediated apoptosis. *J Biol Chem.* 276:39145-9.

Brini M, Miuzzo M, Pierobon N, Negro A, Sorgato MC. 2005 The prion protein and its paralogue Doppel affect calcium signaling in Chinese hamster ovary cells. *Mol Biol Cell.* 16:2799-2808.

Brown P, Goldfarb LG, Brown WT, Goldgaber D, Rubenstein R, Kascsak RJ, Guiroy DC, Piccardo P, Boellaard JW, Gajdusek DC. 1991 Clinical and molecular genetic study of a large German kindred with Gerstmann-Sträussler-Scheinker syndrome. *Neurology.* 41:375-9.

Brown DR, Schmidt B, Kretzschmar HA. 1998 Effects of copper on survival of prion protein knockout neurons and glia. *J Neurochem.* 70:1686-1693.

Brown DR, Wong BS, Hafiz F, Clive C, Haswell SJ, Jones IM. 1999 Normal prion protein has an activity like that of superoxide dismutase. *Biochem J.* 1:1-5.

Bruinsma IB, Bruggink KA, Kinast K, Versleijen AA, Segers-Nolten IM, Subramaniam V, Kuiperij HB, Boelens W, de Waal RM, Verbeek MM. 2011a Inhibition of α-synuclein aggregation by small heat shock proteins. *Proteins.* 79:2956-67.

Bruinsma IB, de Jager M, Carrano A, Versleijen AA, Veerhuis R, Boelens W, Rozemuller AJ, de Waal RM, Verbeek MM. 2011b Small heat shock proteins induce a cerebral inflammatory reaction. *J Neurosci.* 31:11992-2000.

Büeler H, Aguzzi A, Sailer A, Greiner RA, Autenried P, Aguet M, Weissmann C. 1993 Mice devoid of PrP are resistant to scrapie. *Cell.* 73:1339-47.

Cantin GT, Yi W, Lu B, Park SK, Xu T, Lee JD, Yates JR 3rd. 2008 Combining protein-based IMAC, peptide-based IMAC, and MudPIT for efficient phosphoproteomic analysis. *J Proteome Res.* 7:1346-51.

Capponi S, Geroldi A, Fossa P, Grandis M, Ciotti P, Gulli R, Schenone A, Mandich P, Bellone E. 2011 HSPB1 and HSPB8 in inherited neuropathies: study of an Italian cohort of dHMN and CMT2 patients. *J Peripher Nerv Syst.* 16:287-94.

Carra S. 2009 The stress-inducible HspB8-Bag3 complex induces the eIF2alpha kinase pathway: implications for protein quality control and viral factory degradation? *Autophagy.* 5, 428-9.

Carra S, Boncoraglio A, Kanon B, Brunsting JF, Minoia M, Rana A, Vos MJ, Seidel K, Sibon OC, Kampinga HH. 2010 Identification of the Drosophila ortholog of HSPB8: implication of HSPB8 loss of function in protein folding diseases. *J Biol Chem.* 285:37811-22.

Carra S, Brunsting JF, Lambert H, Landry J, Kampinga HH. 2009 HspB8 participates in protein quality control by a non-chaperone-like mechanism that requires eIF2{alpha} phosphorylation. *J Biol Chem.* 284:5523-32.

Carra S, Crippa V, Rusmini P, Boncoraglio A, Minoia M, Giorgetti E, Kampinga HH, Poletti A. 2012 Alteration of protein folding and degradation in motor neuron diseases: Implications and protective functions of small heat shock proteins. *Prog Neurobiol.* 97:83-100.

Carra S, Seguin SJ, Lambert H, Landry J. 2008a HspB8 chaperone activity toward poly(Q)-containing proteins depends on its association with Bag3, a stimulator of macroautophagy. *J Biol Chem.* 283:1437-44.

Carra S, Seguin SJ, Landry J. 2008b HspB8 and Bag3: a new chaperone complex targeting misfolded proteins to macroautophagy. *Autophagy.* 4:237-9.

Carra S, Sivilotti M, Chávez Zobel AT, Lambert H, Landry J. 2005 HspB8, a small heat shock protein mutated in human neuromuscular disorders, has in vivo chaperone activity in cultured cells. *Hum Mol Genet.* 14:1659-69.

Cereghetti GM, Negro A, Vinck E, Massimino ML, Sorgato MC, Van Doorslaer S. 2004 Copper(II) binding to the human Doppel protein may mark its functional diversity from the prion protein. *J Biol Chem.* 279:36497-503.

Charpentier AH, Bednarek AK, Daniel RL, Hawkins KA, Laflin KJ, Gaddis S, MacLeod MC, Aldaz CM. 2000 Effects of estrogen on global gene expression: identification of novel targets of estrogen action. *Cancer Res.* 60:5977-83.

Chávez Zobel AT, Loranger A, Marceau N, Thériault JR, Lambert H, Landry J. 2003 Distinct chaperone mechanisms can delay the formation of aggresomes by the myopathy-causing R120G alphaB-crystallin mutant. *Hum Mol Genet.* 12:1609-20.

Chen L, Lizano P, Zhao X, Sui X, Dhar SK, Shen YT, Vatner DE, Vatner SF, Depre C. 2011 Preemptive conditioning of the swine heart by H11 kinase/Hsp22 provides cardiac protection through inducible nitric oxide synthase. *Am J Physiol Heart Circ Physiol.* 300:H1303-10.

Chen R, Wei J, Fowler SC, Wu JY. 2003 Demonstration of functional coupling between dopamine synthesis and its packaging into synaptic vesicles. *J Biomed Sci.* 10:774-81.

Chiarini LB, Freitas AR, Zanata SM, Brentani RR, Martins VR, Linden R. 2002 Cellular prion protein transduces neuroprotective signals. *EMBO J.* 21:3317-3326.

Chowdary TK, Raman B, Ramakrishna T, Rao CM. 2004 Mammalian Hsp22 is a heat-inducible small heat-shock protein with chaperone-like activity. *Biochem J.* 381:379-87.

Chowdary TK, Raman B, Ramakrishna T, Rao ChM. 2007 Interaction of mammalian Hsp22 with lipid membranes. *Biochem J.* 401:437-45.

Clarke R. 2011 Cannibalism, cell survival, and endocrine resistance in breast cancer. *Breast Cancer Res.* 13:311.

Cohen SN, Chang AC, Hsu L. 1972 Nonchromosomal antibiotic resistance in bacteria: genetic transformation of Escherichia coli by R-factor DNA. *Proc Natl Acad Sci U S A.* 69:2110-4.

Colby DW, Prusiner SB. 2011 Prions. *Cold Spring Harb Perspect Biol.*

Collinge J. 2005 Molecular neurology of prion disease. *J Neurol Neurosurg Psychiatry.* 76:906-19.

Craig SP, Buckle VJ, Lamouroux A, Mallet J, Craig I. 1986 Localization of the human tyrosine hydroxylase gene to 11p15: gene duplication and evolution of metabolic pathways. *Cytogenet Cell Genet.* 42:29-32.

Craig EA, McCarthy BJ. 1980 Four Drosophila heat shock genes at 67B: characterization of recombinant plasmids. *Nucleic Acids Res.* 8:4441-57.

Crippa V, Sau D, Rusmini P, Boncoraglio A, Onesto E, Bolzoni E, Galbiati M, Fontana E, Marino M, Carra S, Bendotti C, De Biasi S, Poletti A. 2010a The small heat shock protein B8 (HspB8)

promotes autophagic removal of misfolded proteins involved in amyotrophic lateral sclerosis (ALS). *Hum Mol Genet.* 19:3440-56.

Crippa V, Carra S, Rusmini P, Sau D, Bolzoni E, Bendotti C, De Biasi S, Poletti A. 2010b A role of small heat shock protein B8 (HspB8) in the autophagic removal of misfolded proteins responsible for neurodegenerative diseases. *Autophagy.* 6:958-60.

Cui XY, Wang N, Yang BX, Gao WF, Lin YM, Yao XR, Ma XT. 2012 HSPB8 is methylated in hematopoietic malignancies and overexpression of HSPB8 exhibits antileukemia effect. *Exp Hematol.* 40:14-21.

Danan IJ, Rashed ER, Depre C. 2007 Therapeutic potential of H11 kinase for the ischemic heart. *Cardiovasc Drug Rev.* 25:14-29.

Datskevich PN, Mymrikov EV, Gusev NB. 2012a Utilization of fluorescent chimeras for investigation of heterooligomeric complexes formed by human small heat shock proteins. *Biochimie.* 94:1794-804.

Datskevich PN, Nefedova VV, Sudnitsyna MV, Gusev NB. 2012b Mutations of small heat shock proteins and human congenital diseases. *Biochemistry (Mosc).* 77:1500-14.

Daubner SC, Le T, Wang S. 2011 Tyrosine hydroxylase and regulation of dopamine synthesis. *Arch Biochem Biophys.* 508:1-12.

Dephoure N, Zhou C, Villén J, Beausoleil SA, Bakalarski CE, Elledge SJ, Gygi SP. 2008 A quantitative atlas of mitotic phosphorylation. *Proc Natl Acad Sci U S A.* 105:10762-7.

Depre C, Hase M, Gaussin V, Zajac A, Wang L, Hittinger L, Ghaleb B, Yu X, Kudej RK, Wagner T, Sadoshima J, Vatner SF. 2002 H11 kinase is a novel mediator of myocardial hypertrophy in vivo. *Circ Res.* 91:1007-14.

Depre C, Tomlinson JE, Kudej RK, Gaussin V, Thompson E, Kim SJ, Vatner DE, Topper JN, Vatner SF. 2001 Gene program for cardiac cell survival induced by transient ischemia in conscious pigs. *Proc Natl Acad Sci U S A.* 98:9336-41.

Depre C, Wang L, Sui X, Qiu H, Hong C, Hedhli N, Ginion A, Shah A, Pelat M, Bertrand L, Wagner T, Gaussin V, Vatner SF. 2006 H11 kinase prevents myocardial infarction by preemptive preconditioning of the heart. *Circ Res.* 98:280-8.

Dierick I, Baets J, Irobi J, Jacobs A, De Vriendt E, Deconinck T, Merlini L, Van den Bergh P, Rasic VM, Robberecht W, Fischer D, Morales RJ, Mitrovic Z, Seeman P, Mazanec R, Kochanski A, Jordanova A, Auer-Grumbach M, Helderman-van den Enden AT, Wokke JH, Nelis E, De Jonghe P, Timmerman V. 2008 Relative contribution of mutations in genes for autosomal dominant distal hereditary motor neuropathies: a genotype-phenotype correlation study. *Brain.* 131:1217-27.

Dierick I, Irobi J, De Jonghe P, Timmerman V. 2005 Small heat shock proteins in inherited peripheral neuropathies. *Ann Med.* 37:413-22.

Dlouhy SR, Hsiao K, Farlow MR, Foroud T, Conneally PM, Johnson P, Prusiner SB, Hodes ME, Ghetti B. 1992 Linkage of the Indiana kindred of Gerstmann-Sträussler-Scheinker disease to the prion protein gene. *Nat Genet.* 1:64-7.

Duffy P, Wolf J, Collins G, DeVoe AG, Streeten B, Cowen D. 1974 Possible person-to-person transmission of Creutzfeldt-Jakob disease. *N Engl J Med.* 290:692-693.

Dunkley PR, Bobrovskaya L, Graham ME, von Nagy-Felsobuki EI, Dickson PW. 2004 Tyrosine hydroxylase phosphorylation: regulation and consequences. *J Neurochem.* 91:1025-43.

Fioriti L, Dossena S, Stewart LR, Stewart RS, Harris DA, Forloni G, Chiesa R. 2005 Cytosolic prion protein (PrP) is not toxic in N2a cells and primary neurons expressing pathogenic PrP mutations. *J Biol Chem.* 280:11320-11328.

Fitzpatrick PF. 1999 Tetrahydropterin-dependent amino acid hydroxylases. *Annu Rev Biochem.* 68:355-81.

Fontaine JM, Sun X, Benndorf R, Welsh MJ. 2005 Interactions of HSP22 (HSPB8) with HSP20, alphaB-crystallin, and HSPB3. *Biochem Biophys Res Commun.* 337:1006-11.

Fontaine JM, Sun X, Hoppe AD, Simon S, Vicart P, Welsh MJ, Benndorf R. 2006 Abnormal small heat shock protein interactions involving neuropathy-associated HSP22 (HSPB8) mutants. *FASEB J.* 20:2168-70.

Ford MJ, Burton LJ, Li H, Graham CH, Frobert Y, Grassi J, Hall SM, Morris RJ. 2002 A marked disparity between the expression of prion protein and its message by neurones of the CNS. *Neuroscience.* 111:533-51.

Fuchs M, Poirier DJ, Seguin SJ, Lambert H, Carra S, Charette SJ, Landry J. 2009 Identification of the key structural motifs involved in HspB8/HspB6-Bag3 interaction. *Biochem J.* 425:245-55.

Gahn LG, Roskoski R Jr. 1995 Thermal stability and CD analysis of rat tyrosine hydroxylase. *Biochemistry.* 34:252-6.

Gentil BJ, Cooper L. 2012 Molecular basis of axonal dysfunction and traffic impairments in CMT. *Brain Res Bull.* 88:444-53.

Glasse R. 1967 Cannibalism in the Kuru region of New Guinea. *Trans N Y Acad Sci.* 29:748-54.

Gober MD, Depre C, Aurelian L. 2004 Correspondence regarding M.V. Kim et al. "Some properties of human small heat shock protein Hsp22 (H11 or HspB8)". *Biochem Biophys Res Commun.* 321:267-8.

Gober MD, Smith CC, Ueda K, Toretsky JA, Aurelian L. 2003 Forced expression of the H11 heat shock protein can be regulated by DNA methylation and trigger apoptosis in human cells. *J Biol Chem.* 278:37600-9.

Goldfarb LG, Haltia M, Brown P, Nieto A, Kovanen J, McCombie WR, Trapp S, Gajdusek DC. 1991 New mutation in scrapie amyloid precursor gene (at codon 178) in Finnish Creutzfeldt-Jakob kindred. *Lancet.* 337:425.

Gonzalez-Malerva L, Park J, Zou L, Hu Y, Moradpour Z, Pearlberg J, Sawyer J, Stevens H, Harlow E, LaBaer J. 2011 High-throughput ectopic expression screen for tamoxifen resistance identifies an atypical kinase that blocks autophagy. *Proc Natl Acad Sci U S A.* 108:2058-63.

Goodwill KE, Sabatier C, Marks C, Raag R, Fitzpatrick PF, Stevens RC. 1997 Crystal structure of tyrosine hydroxylase at 2.3 A and its implications for inherited neurodegenerative diseases. *Nat Struct Biol.* 4:578-85.

Grima B, Lamouroux A, Boni C, Julien JF, Javoy-Agid F, Mallet J. 1987 A single human gene encoding multiple tyrosine hydroxylases with different predicted functional characteristics. *Nature.* 326:707-11.

Haavik J, Toska K. 1998 Tyrosine hydroxylase and Parkinson's disease. *Mol Neurobiol.* 16:285-309.

Halskau Ø Jr, Ying M, Baumann A, Kleppe R, Rodriguez-Larrea D, Almås B, Haavik J, Martinez A. 2009 Three-way interaction between 14-3-3 proteins, the N-terminal region of tyrosine hydroxylase, and negatively charged membranes. *J Biol Chem.* 284:32758-69.

Hartl FU, Bracher A, Hayer-Hartl M. 2011 Molecular chaperones in protein folding and proteostasis. *Nature.* 475:324-32.

Hartl FU, Hayer-Hartl M. 2009 Converging concepts of protein folding in vitro and in vivo. *Nat Struct Mol Biol.* 16:574-8.

Hase M, Depre C, Vatner SF, Sadoshima J. 2005 H11 has dose-dependent and dual hypertrophic and proapoptotic functions in cardiac myocytes. *Biochem J.* 388:475-83.

Haycock JW. 1990 Phosphorylation of tyrosine hydroxylase in situ at serine 8, 19, 31, and 40. *J Biol Chem.* 265:11682-91.

Haycock JW. 2002 Species differences in the expression of multiple tyrosine hydroxylase protein isoforms. *J Neurochem.* 81:947-53.

Haycock JW, Wakade AR. 1992 Activation and multiple-site phosphorylation of tyrosine hydroxylase in perfused rat adrenal glands. *J Neurochem.* 58:57-64.

Hedhli N, Wang L, Wang Q, Rashed E, Tian Y, Sui X, Madura K, Depre C. 2008 Proteasome activation during cardiac hypertrophy by the chaperone H11 Kinase/Hsp22. *Cardiovasc Res.* 77:497-505.

Hegde RS, Mastrianni JA, Scott MR, DeFea KA, Tremblay P, Torchia M, DeArmond SJ, Prusiner SB, Lingappa VR. 1998 A transmembrane form of the prion protein in neurodegenerative disease. *Science.* 279:827-34.

Herms J, Tings T, Gall S, Madlung A, Giese A, Siebert H, Schürmann P, Windl O, Brose N, Kretzschmar H. 1999 Evidence of presynaptic location and function of the prion protein. *J Neurosci.* 19:8866-75.

Hishiya A, Salman MN, Carra S, Kampinga HH, Takayama S. 2011 BAG3 directly interacts with mutated alphaB-crystallin to suppress its aggregation and toxicity. *PLoS One.* 6:e16828.

Horiuchi M, Yamazaki N, Ikeda T, Ishiguro N, Shinagawa M. 1995 A cellular form of prion protein (PrPC) exists in many non-neuronal tissues of sheep. *J. Gen. Virol*. 76:2583–2587.

Hsiao K, Baker HF, Crow TJ, Poulter M, Owen F, Terwilliger JD, Westaway D, Ott J, Prusiner SB. 1989 Linkage of a prion protein missense variant to Gerstmann-Sträussler syndrome. *Nature.* 338:342-5.

Hsiao KK, Cass C, Schellenberg GD, Bird T, Devine-Gage E, Wisniewski H, Prusiner SB. 1991 A prion protein variant in a family with the telencephalic form of Gerstmann-Sträussler-Scheinker syndrome. *Neurology.* 41:681-4.

Hu Z, Chen L, Zhang J, Li T, Tang J, Xu N, Wang X. 2007 Structure, function, property, and role in neurologic diseases and other diseases of the sHsp22. *J Neurosci Res.* 85:2071-9.

Ichimura T, Isobe T, Okuyama T, Yamauchi T, Fujisawa H. 1987 Brain 14-3-3 protein is an activator protein that activates tryptophan 5-monooxygenase and tyrosine 3-monooxygenase in the presence of Ca2+,calmodulin-dependent protein kinase II. *FEBS Lett.* 219:79-82.

Ichinose H, Ohye T, Fujita K, Yoshida M, Ueda S, Nagatsu T. 1993 Increased heterogeneity of tyrosine hydroxylase in humans. *Biochem Biophys Res Commun.* 195:158-65.

Ingolia TD, Craig EA. 1981 Primary sequence of the 5' flanking regions of the Drosophila heat shock genes in chromosome subdivision 67B. *Nucleic Acids Res.* 9:1627-42.

Irobi J, Almeida-Souza L, Asselbergh B, De Winter V, Goethals S, Dierick I, Krishnan J, Timmermans JP, Robberecht W, De Jonghe P, Van Den Bosch L, Janssens S, Timmerman V. 2010 Mutant HSPB8 causes motor neuron-specific neurite degeneration. *Hum Mol Genet.* 19:3254-65.

Irobi J, De Jonghe P, Timmerman V. 2004a Molecular genetics of distal hereditary motor neuropathies. *Hum Mol Genet.* 2:R195-202.

Irobi J, Holmgren A, De Winter V, Asselbergh B, Gettemans J, Adriaensen D, Ceuterick-de Groote C, Van Coster R, De Jonghe P, Timmerman V. 2012 Mutant HSPB8 causes protein aggregates and a reduced mitochondrial membrane potential in dermal fibroblasts from distal hereditary motor neuropathy patients. *Neuromuscul Disord.* 22:699-711.

Irobi J, Van Impe K, Seeman P, Jordanova A, Dierick I, Verpoorten N, Michalik A, De Vriendt E, Jacobs A, Van Gerwen V, Vennekens K, Mazanec R, Tournev I, Hilton-Jones D, Talbot K, Kremensky I, Van Den Bosch L, Robberecht W, Van Vandekerckhove J, Van Broeckhoven C, Gettemans J, De Jonghe P, Timmerman V. 2004b Hot-spot residue in small heat-shock protein 22 causes distal motor neuropathy. *Nat Genet.* 36:597-601.

Jackson GS, Murray I, Hosszu LL, Gibbs N, Waltho JP, Clarke AR, Collinge J. 2001 Location and properties of metal-binding sites on the human prion protein. *Proc Natl Acad Sci.* 98:8531-5.

James PA, Talbot K. 2006 The molecular genetics of non-ALS motor neuron diseases. *Biochim Biophys Acta.* 1762:986-1000.

Kappé G, Verschuure P, Philipsen RL, Staalduinen AA, Van de Boogaart P, Boelens WC, De Jong WW. 2001 Characterization of two novel human small heat shock proteins: protein kinase-related HspB8 and testis-specific HspB9. *Biochim Biophys Acta.* 1520:1-6.

Kasakov AS, Bukach OV, Seit-Nebi AS, Marston SB, Gusev NB. 2007 Effect of mutations in the beta5-beta7 loop on the structure and properties of human small heat shock protein HSP22 (HspB8, H11). *FEBS J*. 274:5628-42.

Kazakov AS, Markov DI, Gusev NB, Levitsky DI. 2009 Thermally induced structural changes of intrinsically disordered small heat shock protein Hsp22. *Biophys Chem*. 145:79-85.

Ke L, Meijering RA, Hoogstra-Berends F, Mackovicova K, Vos MJ, Van Gelder IC, Henning RH, Kampinga HH, Brundel BJ. 2011 HSPB1, HSPB6, HSPB7 and HSPB8 protect against RhoA GTPase-induced remodeling in tachypaced atrial myocytes. *PLoS One.* 6:e20395.

Kim MV, Seit-Nebi AS, Gusev NB. 2004a The problem of protein kinase activity of small heat shock protein Hsp22 (H11 or HspB8). *Biochem Biophys Res Commun.* 325:649-52.

Kim MV, Seit-Nebi AS, Marston SB, Gusev NB. 2004b Some properties of human small heat shock protein Hsp22 (H11 or HspB8). *Biochem Biophys Res Commun.* 315:796-801.

Kim MV, Kasakov AS, Seit-Nebi AS, Marston SB, Gusev NB. 2006 Structure and properties of K141E mutant of small heat shock protein HSP22 (HspB8, H11) that is expressed in human neuromuscular disorders. *Arch Biochem Biophys.* 454:32-41.

Kirbach BB, Golenhofen N. 2011 Differential expression and induction of small heat shock proteins in rat brain and cultured hippocampal neurons. *J Neurosci Res.* 89:162-75.

Kitamoto T, Amano N, Terao Y, Nakazato Y, Isshiki T, Mizutani T, Tateishi J. 1993b A new inherited prion disease (PrP-P105L mutation) showing spastic paraparesis. *Ann Neurol.* 34:808-13.

Kitamoto T, Iizuka R, Tateishi J. 1993 An amber mutation of prion protein in Gerstmann-Sträussler syndrome with mutant PrP plaques. *Biochem Biophys Res Commun.* 192:525-31.

Klemenz R, Gehring WJ. 1986 Sequence requirement for expression of the Drosophila melanogaster heat shock protein hsp22 gene during heat shock and normal development. *Mol Cell Biol.* 6:2011-9.

Kleppe R, Toska K, Haavik J. 2001 Interaction of phosphorylated tyrosine hydroxylase with 14-3-3 proteins: evidence for a phosphoserine 40-dependent association. *J Neurochem.* 77:1097-107.

Kobayashi K, Kaneda N, Ichinose H, Kishi F, Nakazawa A, Kurosawa Y, Fujita K, Nagatsu T. 1988 Structure of the human tyrosine hydroxylase gene: alternative splicing from a single gene accounts for generation of four mRNA types. *J Biochem.* 103:907-12.

Kobayashi K, Morita S, Sawada H, Mizuguchi T, Yamada K, Nagatsu I, Hata T, Watanabe Y, Fujita K, Nagatsu T. 1995 Targeted disruption of the tyrosine hydroxylase locus results in severe catecholamine depletion and perinatal lethality in mice. *J Biol Chem.* 270:27235-43.

Kobayashi K, Nagatsu T. 2005 Molecular genetics of tyrosine 3-monooxygenase and inherited diseases. *Biochem Biophys Res Commun.* 338:267-70.

Kobayashi K, Noda Y, Matsushita N, Nishii K, Sawada H, Nagatsu T, Nakahara D, Fukabori R, Yasoshima Y, Yamamoto T, Miura M, Kano M, Mamiya T, Miyamoto Y, Nabeshima T. 2000

Modest neuropsychological deficits caused by reduced noradrenaline metabolism in mice heterozygous for a mutated tyrosine hydroxylase gene. *J Neurosci.* 20:2418-26.

Knappskog PM, Flatmark T, Mallet J, Lüdecke B, Bartholomé K. 1995 Recessively inherited L-DOPA-responsive dystonia caused by a point mutation (Q381K) in the tyrosine hydroxylase gene. *Hum Mol Genet.* 4:1209-12.

Kristiansen M, Deriziotis P, Dimcheff DE, Jackson GS, Ovaa H, Naumann H, Clarke AR, van Leeuwen FW, Menéndez-Benito V, Dantuma NP, Portis JL, Collinge J, Tabrizi SJ. 2007 Disease-associated prion protein oligomers inhibit the 26S proteasome. *Mol Cell.* 26:175-88.

Kuhn DM, Arthur R Jr, Yoon H, Sankaran K. 1990 Tyrosine hydroxylase in secretory granules from bovine adrenal medulla. Evidence for an integral membrane form. *J Biol Chem.* 265:5780-6.

Kumer SC, Vrana KE. 1996 Intricate regulation of tyrosine hydroxylase activity and gene expression. *J Neurochem.* 67:443-62.

Kwok AS, Phadwal K, Turner BJ, Oliver PL, Raw A, Simon AK, Talbot K, Agashe VR. 2011 HspB8 mutation causing hereditary distal motor neuropathy impairs lysosomal delivery of autophagosomes. *J Neurochem.* 119:1155-61.

Laure L, Long R, Lizano P, Zini R, Berdeaux A, Depre C, Morin D. 2012 Cardiac H11 kinase/Hsp22 stimulates oxidative phosphorylation and modulates mitochondrial reactive oxygen species production: Involvement of a nitric oxide-dependent mechanism. *Free Radic Biol Med.* 52:2168-76.

Lehmann IT, Bobrovskaya L, Gordon SL, Dunkley PR, Dickson PW. 2006 Differential regulation of the human tyrosine hydroxylase isoforms via hierarchical phosphorylation. *J Biol Chem.* 281:17644-51.

Li B, Smith CC, Laing JM, Gober MD, Liu L, Aurelian L. 2007 Overload of the heat-shock protein H11/HspB8 triggers melanoma cell apoptosis through activation of transforming growth factor-beta-activated kinase 1. *Oncogene.* 26:3521-31.

Linden R, Martins VR, Prado MA, Cammarota M, Izquierdo I, Brentani RR. 2008 Physiology of the prion protein. *Physiol Rev.* 88:673-728.

Lüdecke B, Dworniczak B, Bartholomé K. 1995 A point mutation in the tyrosine hydroxylase gene associated with Segawa's syndrome. *Hum Genet.* 95:123-5.

Lüdecke B, Knappskog PM, Clayton PT, Surtees RA, Clelland JD, Heales SJ, Brand MP, Bartholomé K, Flatmark T. 1996 Recessively inherited L-DOPA-responsive parkinsonism in infancy caused by a point mutation (L205P) in the tyrosine hydroxylase gene. *Hum Mol Genet.* 5:1023-8.

Ma J, Wollmann R, Lindquist S. 2002 Neurotoxicity and neurodegeneration when PrP accumulates in the cytosol. *Science.* 298:1781-5.

Mandel M, Higa A. 1970 Calcium-dependent bacteriophage DNA infection. *J Mol Biol.* 53:159-62.

Martínez del Hoyo G, López-Bravo M, Metharom P, Ardavín C, Aucouturier P. 2006 Prion protein expression by mouse dendritic cells is restricted to the nonplasmacytoid subsets and correlates with the maturation state. *J Immunol*. 177:6137-42.

Martins VR, Graner E, Garcia-Abreu J, de Souza SJ, Mercadante AF, Veiga SS, Zanata SM, Neto VM, Brentani RR. 1997 Complementary hydropathy identifies a cellular prion protein receptor. *Nat Med.* 3:1376-1382.

Marunouchi T, Abe Y, Murata M, Inomata S, Sanbe A, Takagi N, Tanonaka K. 2013Changes in small heat shock proteins HSPB1, HSPB5 and HSPB8 in mitochondria of the failing heart following myocardial infarction in rats. *Biol Pharm Bull.* 36:529-39.

McKnight S, Tjian R. 1986 Transcriptional selectivity of viral genes in mammalian cells. *Cell.* 46:795-805.

Medori R, Tritschler HJ, LeBlanc A, Villare F, Manetto V, Chen HY, Xue R, Leal S, Montagna P, Cortelli P, et al. 1992 Fatal familial insomnia, a prion disease with a mutation at codon 178 of the prion protein gene. *N Engl J Med*. 326:444-9.

Meggio F, Negro A, Sarno S, Ruzzene M, Bertoli A, Sorgato MC, Pinna LA. 2000 Bovine prion protein as a modulator of protein kinase CK2. *Biochem J.* 352:191-6.

Meyer RK, McKinley MP, Bowman KA, Braunfeld MB, Barry RA, Prusiner SB. 1986 Separation and properties of cellular and scrapie prion proteins. *Proc Nail Acad Sci*. 83:2310-2314.

Mironov A Jr, Latawiec D, Wille H, Bouzamondo-Bernstein E, Legname G, Williamson RA, Burton D, DeArmond SJ, Prusiner SB, Peters PJ. 2003 Cytosolic prion protein in neurons. *J Neurosci.* 23:7183-93.

Modem S, Chinnakannu K, Bai U, Reddy GP, Reddy TR. 2011 Hsp22 (HspB8/H11) knockdown induces Sam68 expression and stimulates proliferation of glioblastoma cells. *J Cell Physiol.* 226:2747-51.

Moore RC, Lee IY, Silverman GL, Harrison PM, Strome R, Heinrich C, Karunaratne A, Pasternak SH, Chishti MA, Liang Y, Mastrangelo P, Wang K, Smit AF, Katamine S, Carlson GA, Cohen FE, Prusiner SB, Melton DW, Tremblay P, Hood LE, Westaway D. 1999 Ataxia in prion protein (PrP)-deficient mice is associated with upregulation of the novel PrP-like protein doppel. *J Mol Biol.* 292:797-817.

Morimoto RI. 1998 Regulation of the heat shock transcriptional response: cross talk between a family of heat shock factors, molecular chaperones, and negative regulators. *Genes Dev.* 12:3788-96.

Morrow G, Battistini S, Zhang P, Tanguay RM. 2004a Decreased lifespan in the absence of expression of the mitochondrial small heat shock protein Hsp22 in Drosophila. *J Biol Chem.* 279:43382-5.

Morrow G, Heikkila JJ, Tanguay RM. 2006 Differences in the chaperone-like activities of the four main small heat shock proteins of Drosophila melanogaster. *Cell Stress Chaperones.* 11:51-60.

Morrow G, Inaguma Y, Kato K, Tanguay RM. 2000 The small heat shock protein Hsp22 of Drosophila melanogaster is a mitochondrial protein displaying oligomeric organization. *J Biol Chem*. 275:31204-10.

Morrow G, Samson M, Michaud S, Tanguay RM. 2004b Overexpression of the small mitochondrial Hsp22 extends Drosophila life span and increases resistance to oxidative stress. *FASEB J*. 18:598-9.

Mouillet-Richard S, Ermonval M, Chebassier C, Laplanche JL, Lehmann S, Launay JM, Kellermann O. 2000 Signal transduction through prion protein. *Science.* 289:1925-8.

Muchowski PJ, Wacker JL. 2005 Modulation of neurodegeneration by molecular chaperones. *Nat Rev Neurosci.* 6:11-22.

Muhammad I and Saqib M. 2011 An overview of human prion diseases. *Virol J.* 8:559.

Mymrikov EV, Seit-Nebi AS, Gusev NB. 2011 Large potentials of small heat shock proteins. *Physiol Rev.* 91:1123-59.

Mymrikov EV, Seit-Nebi AS, Gusev NB. 2012 Heterooligomeric complexes of human small heat shock proteins. *Cell Stress Chaperones.* 17:157-69.

Nagatsu T. 1995 Tyrosine hydroxylase: human isoforms, structure and regulation in physiology and pathology. *Essays Biochem.* 30:15-35.

Nagatsu T, Levitt M, Udenfriend S. 1964 Tyrosine hydroxylase. The initial step in norepinephrine biosynthesis. *J Biol Chem.* 239:2910-7.

Nakashima A, Hayashi N, Kaneko YS, Mori K, Sabban EL, Nagatsu T, Ota A. 2009 Role of N-terminus of tyrosine hydroxylase in the biosynthesis of catecholamines. *J Neural Transm.* 116:1355-62.

Nandi PK. 1997 Interaction of prion peptide HuPrP106-126 with nucleic acid. *Arch Virol.* 142:2537-45.

Nakhro K, Park JM, Kim YJ, Yoon BR, Yoo JH, Koo H, Choi BO, Chung KW. 2013 A novel Lys141Thr mutation in small heat shock protein 22 (HSPB8) gene in Charcot-Marie-Tooth disease type 2L. *Neuromuscul Disord*. 23:656-63.

Negro A, De Filippis V, Skaper SD, James P, Sorgato MC. 1997 The complete mature bovine prion protein highly expressed in Escherichia coli: biochemical and structural studies. *FEBS Lett.* 412:359-64.

Negro A, Meggio F, Bertoli A, Battistutta R, Sorgato MC, Pinna LA. 2000 Susceptibility of the prion protein to enzymic phosphorylation. *Biochem Biophys Res Commun.* 271:337-41.

Nieznanski K. 2010 Interactions of prion protein with intracellular proteins: so many partners and no consequences? *Cell Mol Neurobiol.* 30:653-66.

Nivon M, Abou-Samra M, Richet E, Guyot B, Arrigo AP, Kretz-Remy C. 2012 NF-κB regulates protein quality control after heat stress through modulation of the BAG3-HspB8 complex. *J Cell Sci.* 125:1141-51.

Norstrom EM, Ciaccio MF, Rassbach B, Wollmann R, Mastrianni JA. 2007 Cytosolic prion protein toxicity is independent of cellular prion protein expression and prion propagation. *J Virol.* 81:2831-7.

Orsi A, Fioriti L, Chiesa R, Sitia R. 2006 Condition of ER stress favour the accumulation of cytosolic PrP. *J Biol Chem.* 281:30431-30438.

Ostrerova N, Petrucelli L, Farrer M, Mehta N, Choi P, Hardy J, Wolozin B. 1999 alpha-Synuclein shares physical and functional homology with 14-3-3 proteins. *J Neurosci.* 19:5782-91.

Palmer MS, Dryden AJ, Hughes JT, Collinge J. 1991 Homozygous prion protein genotype predisposes to sporadic Creutzfeldt-Jakob disease. *Nature.* 352:340-2.

Pan KM, Baldwin M, Nguyen J, Gasset M, Serban A, Groth D, Mehlhorn I, Huang Z, Fletterick RJ, Cohen FE, et al. 1993 Conversion of alpha-helices into beta-sheets features in the formation of the scrapie prion proteins. *Proc Natl Acad Sci.* 90:10962-6.

Parizek P, Roeckl C, Weber J, Flechsig E, Aguzzi A, Raeber AJ. 2001 Similar turnover and shedding of the cellular prion protein in primary lymphoid and neuronal cells. *J Biol Chem.* 276:44627-32.

Pastore A, Temussi PA. 2012 The two faces of Janus: functional interactions and protein aggregation. *Curr Opin Struct Biol.* 22:30-7.

Peng X, Tehranian R, Dietrich P, Stefanis L, Perez RG. 2005 Alpha-synuclein activation of protein phosphatase 2A reduces tyrosine hydroxylase phosphorylation in dopaminergic cells. *J Cell Sci.* 118:3523-30.

Perez RG, Waymire JC, Lin E, Liu JJ, Guo F, Zigmond MJ. 2002 A role for alpha-synuclein in the regulation of dopamine biosynthesis. *J Neurosci.* 22:3090-9.

Perkins D, Pereira EF, Aurelian L. 2003 The herpes simplex virus type 2 R1 protein kinase (ICP10 PK) functions as a dominant regulator of apoptosis in hippocampal neurons involving activation of the ERK survival pathway and upregulation of the antiapoptotic protein Bag-1. *J Virol.* 77:1292-305.

Perkins D, Pereira EF, Gober M, Yarowsky PJ, Aurelian L. 2002 The herpes simplex virus type 2 R1 protein kinase (ICP10 PK) blocks apoptosis in hippocampal neurons, involving activation of the MEK/MAPK survival pathway. *J Virol.* 76:1435-49.

Peroni D, Negro A, Bähr M, Dietz GP. 2007 Intracellular delivery of Neuroglobin using HIV-1 TAT protein transduction domain fails to protect against oxygen and glucose deprivation. *Neurosci Lett.* 421:110-4.

Pickel VM, Joh TH, Field PM, Becker CG, Reis DJ. 1975 Cellular localization of tyrosine hydroxylase by immunohistochemistry. *J Histochem Cytochem.* 23:1-12.

Poulter M, Baker HF, Frith CD, Leach M, Lofthouse R, Ridley RM, Shah T, Owen F, Collinge J, Brown J, et al. 1992 Inherited prion disease with 144 base pair gene insertion. 1. Genealogical and molecular studies. *Brain.* 115:675-85.

Prusiner SB. 1982 Novel proteinaceous infectious particles cause scrapie. *Science.* 216:136-44.

Prusiner SB. 1991 Molecular biology of prion diseases. *Science.* 252:1515-22.

Prusiner SB. 1998 Prions. *Proc Natl Acad Sci.* 95:13363-13383.

Prusiner SB, Groth DF, Bolton DC, Kent SB and Hood LE. 1984 Purification and structural studies of a major scrapie prion protein. *Cell.* 38:127-134.

Qiu H, Lizano P, Laure L, Sui X, Rashed E, Park JY, Hong C, Gao S, Holle E, Morin D, Dhar SK, Wagner T, Berdeaux A, Tian B, Vatner SF, Depre C. 2011 H11 kinase/heat shock protein 22 deletion impairs both nuclear and mitochondrial functions of STAT3 and accelerates the transition into heart failure on cardiac overload. *Circulation.* 124:406-15.

Quraishe S, Asuni A, Boelens WC, O'Connor V, Wyttenbach A. 2008 Expression of the small heat shock protein family in the mouse CNS: differential anatomical and biochemical compartmentalization. *Neuroscience.* 153:483-91.

Ramírez-Rodríguez G, Babu H, Klempin F, Krylyshkina O, Baekelandt V, Gijsbers R, Debyser Z, Overall RW, Nicola Z, Fabel K, Kempermann G. 2013 The α crystallin domain of small heat shock protein b8 (Hspb8) acts as survival and differentiation factor in adult hippocampal neurogenesis. *J Neurosci.* 33:5785-96.

Ramsey AJ, Fitzpatrick PF. 1998 Effects of phosphorylation of serine 40 of tyrosine hydroxylase on binding of catecholamines: evidence for a novel regulatory mechanism. *Biochemistry.* 37:8980-6.

Ramsey AJ, Fitzpatrick PF. 2000 Effects of phosphorylation on binding of catecholamines to tyrosine hydroxylase: specificity and thermodynamics. *Biochemistry.* 39:773-8.

Ramsey AJ, Hillas PJ, Fitzpatrick PF. 1996 Characterization of the active site iron in tyrosine hydroxylase. Redox states of the iron. *J Biol Chem.* 271:24395-400.

Rikova K, Guo A, Zeng Q, Possemato A, Yu J, Haack H, Nardone J, Lee K, Reeves C, Li Y, Hu Y, Tan Z, Stokes M, Sullivan L, Mitchell J, Wetzel R, Macneill J, Ren JM, Yuan J, Bakalarski CE, Villen J, Kornhauser JM, Smith B, Li D, Zhou X, Gygi SP, Gu TL, Polakiewicz RD, Rush J, Comb MJ. 2007 Global survey of phosphotyrosine signaling identifies oncogenic kinases in lung cancer. *Cell.* 131:1190-203.

Roelofs MF, Boelens WC, Joosten LA, Abdollahi-Roodsaz S, Geurts J, Wunderink LU, Schreurs BW, van den Berg WB, Radstake TR. 2006 Identification of small heat shock protein B8 (HSP22) as a novel TLR4 ligand and potential involvement in the pathogenesis of rheumatoid arthritis. *J Immunol.* 176:7021-7.

Rohkamm B, Reilly MM, Lochmüller H, Schlotter-Weigel B, Barisic N, Schöls L, Nicholson G, Pareyson D, Laurà M, Janecke AR, Miltenberger-Miltenyi G, John E, Fischer C, Grill F, Wakeling W, Davis M, Pieber TR, Auer-Grumbach M. 2007 Further evidence for genetic heterogeneity of distal HMN type V, CMT2 with predominant hand involvement and Silver syndrome. *J Neurol Sci.* 263:100-6.

Rossor AM, Kalmar B, Greensmith L, Reilly MM. 2012 The distal hereditary motor neuropathies. *J Neurol Neurosurg Psychiatry*. 83:6-14.

Roucou X, Guo Q, Zhang Y, Goodyer CG, LeBlanc AC. 2003 Cytosolic prion protein is not toxic and protects against Bax-mediated cell death in human primary neurons. *J Biol Chem*. 278:40877-81.

Rusmini P, Crippa V, Giorgetti E, Boncoraglio A, Cristofani R, Carra S, Poletti A. 2013 Clearance of the mutant androgen receptor in motoneuronal models of spinal and bulbar muscular atrophy. *Neurobiol Aging.* 34:2585-603.

Sanbe A, Daicho T, Mizutani R, Endo T, Miyauchi N, Yamauchi J, Tanonaka K, Glabe C, Tanoue A. 2009 Protective effect of geranylgeranylacetone via enhancement of HSPB8 induction in desmin-related cardiomyopathy. *PLoS One.* 4:e5351.

Sanbe A, Marunouchi T, Abe T, Tezuka Y, Okada M, Aoki S, Tsumura H, Yamauchi J, Tanonaka K, Nishigori H, Tanoue A. 2013 Phenotype of cardiomyopathy in cardiac-specific heat shock protein B8 K141N transgenic mouse. *J Biol Chem.* 288:8910-21.

Sanbe A, Yamauchi J, Miyamoto Y, Fujiwara Y, Murabe M, Tanoue A. 2007 Interruption of CryAB-amyloid oligomer formation by HSP22. *J Biol Chem.* 282:555-63.

Seidel K, Vinet J, Dunnen WF, Brunt ER, Meister M, Boncoraglio A, Zijlstra MP, Boddeke HW, Rüb U, Kampinga HH, Carra S. 2012 The HSPB8-BAG3 chaperone complex is upregulated in astrocytes in the human brain affected by protein aggregation diseases. *Neuropathol Appl Neurobiol.* 38:39-53.

Shemetov AA, Gusev NB. 2011 Biochemical characterization of small heat shock protein HspB8 (Hsp22)-Bag3 interaction. *Arch Biochem Biophys.* 513:1-9.

Shemetov AA, Seit-Nebi AS, Bukach OV, Gusev NB. 2008a Phosphorylation by cyclic AMP-dependent protein kinase inhibits chaperone-like activity of human HSP22 in vitro. *Biochemistry (Mosc).* 73:200-8.

Shemetov AA, Seit-Nebi AS, Gusev NB. 2008b Structure, properties, and functions of the human small heat-shock protein HSP22 (HspB8, H11, E2IG1): a critical review. *J Neurosci Res.* 86:64-9.

Shemetov AA, Seit-Nebi AS, Gusev NB. 2011 Phosphorylation of human small heat shock protein HspB8 (Hsp22) by ERK1 protein kinase. *Mol Cell Biochem.* 355:47-55.

Shibuya S, Higuchi J, Shin RW, Tateishi J, Kitamoto T. 1998 Codon 219 Lys allele of PRNP is not found in sporadic Creutzfeldt-Jakob disease. *Ann Neurol.* 43:826-8.

Smith CC, Lee KS, Li B, Laing JM, Hersl J, Shvartsbeyn M, Aurelian L. 2012 Restored expression of the atypical heat shock protein H11/HspB8 inhibits the growth of genetically diverse melanoma tumors through activation of novel TAK1-dependent death pathways. *Cell Death Dis.* 3:e371.

Smith CC, Li B, Liu J, Lee KS, Aurelian L. 2011 The Levels of H11/HspB8 DNA methylation in human melanoma tissues and xenografts are a critical molecular marker for 5-Aza-2'-deoxycytidine therapy. *Cancer Invest.* 29:383-95.

Smith CC, Nelson J, Aurelian L, Gober M, Goswami BB. 2000a Ras-GAP binding and phosphorylation by herpes simplex virus type 2 RR1 PK (ICP10) and activation of the

Ras/MEK/MAPK mitogenic pathway are required for timely onset of virus growth. *J Virol.* 74:10417-29.

Smith CC, Yu YX, Kulka M, Aurelian L. 2000b A novel human gene similar to the protein kinase (PK) coding domain of the large subunit of herpes simplex virus type 2 ribonucleotide reductase (ICP10) codes for a serine-threonine PK and is expressed in melanoma cells. *J Biol Chem.* 275:25690-9.

Stahl N, Baldwin MA, Teplow DB, Hood L, Gibson BW, Burlingame AL, Prusiner SB. 1993 Structural analysis of the scrapie prion protein using mass spectrometry andamino acid sequencing. *Biochemistry.* 32:1991-2002.

Stahl N, Prusiner SB. 1991 Prions and prion proteins. *FASEB J.* 5:2799-807.

Sui X, Li D, Qiu H, Gaussin V, Depre C. 2009 Activation of the bone morphogenetic protein receptor by H11kinase/Hsp22 promotes cardiac cell growth and survival. *Circ Res.* 104:887-95.

Sun X, Fontaine JM, Bartl I, Behnam B, Welsh MJ, Benndorf R. 2007 Induction of Hsp22 (HspB8) by estrogen and the metalloestrogen cadmium in estrogen receptor-positive breast cancer cells. *Cell Stress Chaperones.* 12:307-19.

Sun X, Fontaine JM, Hoppe AD, Carra S, DeGuzman C, Martin JL, Simon S, Vicart P, Welsh MJ, Landry J, Benndorf R. 2010 Abnormal interaction of motor neuropathy-associated mutant HspB8 (Hsp22) forms with the RNA helicase Ddx20 (gemin3). *Cell Stress Chaperones.* 15:567-82.

Sun X, Fontaine JM, Rest JS, Shelden EA, Welsh MJ, Benndorf R. 2004 Interaction of human HSP22 (HSPB8) with other small heat shock proteins. *J Biol Chem*. 279:2394-402.

Sutherland C, Alterio J, Campbell DG, Le Bourdellès B, Mallet J, Haavik J, Cohen P. 1993 Phosphorylation and activation of human tyrosine hydroxylase in vitro by mitogen-activated protein (MAP) kinase and MAP-kinase-activated kinases 1 and 2. *Eur J Biochem.* 217:715-22.

Tang BS, Zhao GH, Luo W, Xia K, Cai F, Pan Q, Zhang RX, Zhang FF, Liu XM, Chen B, Zhang C, Shen L, Jiang H, Long ZG, Dai HP. 2005 Small heat-shock protein 22 mutated in autosomal dominant Charcot-Marie-Tooth disease type 2L. *Hum Genet.* 116:222-4.

Tao D, Lu J, Sun H, Zhao YM, Yuan ZG, Li XX, Huang BQ. 2004 Trichostatin A extends the lifespan of Drosophila melanogaster by elevating hsp22 expression. *Acta Biochim Biophys Sin (Shanghai).* 36:618-22.

Teigen K, McKinney JA, Haavik J, Martínez A. 2007 Selectivity and affinity determinants for ligand binding to the aromatic amino acid hydroxylases. *Curr Med Chem.* 14:455-67.

Tian C, Dong X. 2013 The structure of prion: is it enough for interpreting the diverse phenotypes of prion diseases? *Acta Biochim Biophys Sin.* 45:429-34.

Towbin H, Staehelin T, Gordon J. 1992 Electrophoretic transfer of proteins from polyacrylamide gels to nitrocellulose sheets: procedure and some applications. *Biotechnology.* 24:145-9.

Trent S, Yang C, Li C, Lynch M, Schmidt EV. 2007 Heat shock protein B8, a cyclin-dependent kinase-independent cyclin D1 target gene, contributes to its effects on radiation sensitivity. *Cancer Res.* 67:10774-81.

Turk E, Teplow DB, Hood LE, Prusiner SB. 1988 Purification and properties of the cellular and scrapie hamster prion proteins. *Eur J Biochem.* 176:21-30.

Vana K, Zuber C, Nikles D, Weiss S. 2007 Novel aspects of prions, their receptor molecules, and innovative approaches for TSE therapy. *Cell Mol Neurobiol.* 27:107-28.

Van den Heuvel LP, Luiten B, Smeitink JA, de Rijk-van Andel JF, Hyland K, Steenbergen-Spanjers GC, Janssen RJ, Wevers RA. 1998 A common point mutation in the tyrosine hydroxylase gene in autosomal recessive L-DOPA-responsive dystonia in the Dutch population. *Hum Genet.* 102:644-6.

Vassallo N, Herms J, Behrens C, Krebs B, Saeki K, Onodera T, Windl O, Kretzschmar HA. 2005 Activation of phosphatidylinositol 3-kinase by cellular prion protein and its role in cell survival. *Biochem Biophys Res Commun.* 332:75-82.

Verschuure P, Tatard C, Boelens WC, Grongnet JF, David JC. 2003 Expression of small heat shock proteins HspB2, HspB8, Hsp20 and cvHsp in different tissues of the perinatal developing pig. *Eur J Cell Biol.* 82:523-30.

Villén J, Beausoleil SA, Gerber SA, Gygi SP. 2007 Large-scale phosphorylation analysis of mouse liver. *Proc Natl Acad Sci U S A.* 104:1488-93.

Vos MJ, Hageman J, Carra S, Kampinga HH. 2008 Structural and functional diversities between members of the human HSPB, HSPH, HSPA, and DNAJ chaperone families. *Biochemistry.* 47:7001-11.

Vos MJ, Zijlstra MP, Kanon B, van Waarde-Verhagen MA, Brunt ER, Oosterveld-Hut HM, Carra S, Sibon OC, Kampinga HH. 2010 HSPB7 is the most potent polyQ aggregation suppressor within the HSPB family of molecular chaperones. *Hum Mol Genet.* 19:4677-93.

Vrana KE, Walker SJ, Rucker P, Liu X. 1994 A carboxyl terminal leucine zipper is required for tyrosine hydroxylase tetramer formation. *J Neurochem.* 63:2014-20.

Wadhwa R, Ryu J, Gao R, Choi IK, Morrow G, Kaur K, Kim I, Kaul SC, Yun CO, Tanguay RM. 2010 Proproliferative functions of Drosophila small mitochondrial heat shock protein 22 in human cells. *J Biol Chem.* 285:3833-9.

Wang L, Zajac A, Hedhli N, Depre C. 2004 Increased expression of H11 kinase stimulates glycogen synthesis in the heart. *Mol Cell Biochem.* 265:71-8.

Watts JC, Westaway D. 2007 The prion protein family: diversity, rivalry, and dysfunction. *Biochim Biophys Acta.* 1772:654-72.

Wevers RA, de Rijk-van Andel JF, Bräutigam C, Geurtz B, van den Heuvel LP, Steenbergen-Spanjers GC, Smeitink JA, Hoffmann GF, Gabreëls FJ. 1999 A review of biochemical and molecular genetic aspects of tyrosine hydroxylase deficiency including a novel mutation (291delC). *J Inherit Metab Dis.* 22:364-73.

Wilhelmus MM, Boelens WC, Kox M, Maat-Schieman ML, Veerhuis R, de Waal RM, Verbeek MM. 2009 Small heat shock proteins associated with cerebral amyloid angiopathy of hereditary cerebral hemorrhage with amyloidosis (Dutch type) induce interleukin-6 secretion. *Neurobiol Aging.* 30:229-40.

Wilhelmus MM, Boelens WC, Otte-Höller I, Kamps B, Kusters B, Maat-Schieman ML, de Waal RM, Verbeek MM. 2006 Small heat shock protein HspB8: its distribution in Alzheimer's disease brains and its inhibition of amyloid-beta protein aggregation and cerebrovascular amyloid-beta toxicity. *Acta Neuropathol.* 111:139-49.

Yang C, Trent S, Ionescu-Tiba V, Lan L, Shioda T, Sgroi D, Schmidt EV. 2006 Identification of cyclin D1- and estrogen-regulated genes contributing to breast carcinogenesis and progression. *Cancer Res.* 66:11649-58.

Yang Z, Lu Y, Liu J, Wang Y, Zhao X. 2012 The chaperone-like activity of rat HspB8/Hsp22 and dynamic molecular transition related to oligomeric architectures in vitro. *Protein Pept Lett.* 19:353-9.

Yu YX, Heller A, Liehr T, Smith CC, Aurelian L. 2001 Expression analysis and chromosome location of a novel gene (H11) associated with the growth of human melanoma cells. *Int J Oncol.* 18:05-11.

Yun SW, Choi EK, Ju WK, Ahn MS, Carp RI, Wisniewski HM, Kim YS. 1998 Extensive degeneration of catecholaminergic neurons to scrapie agent 87V in the brains of IM mice. *Mol Chem Neuropathol.* 34:121-32.

Zahn R, Liu A, Lührs T, Riek R, von Schroetter C, López García F, Billeter M, Calzolai L, Wider G, Wüthrich K. 2000 NMR solution structure of the human prion protein. *Proc Natl Acad Sci U S A.* 97:145-50.

Zhang CC, Steele AD, Lindquist S, Lodish HF. 2006 Prion protein is expressed on long-term repopulating hematopoietic stem cells and is important for their self-renewal. *Proc Natl Acad Sci U S A.* 103:2184-9.

Zhang X, Studier FW. 1997 Mechanism of inhibition of bacteriophage T7 RNA polymerase by T7 lysozyme. *J Mol Biol.* 269:10-27.

Zhang FF, Tang BS, Zhao GH, Chen B, Zhang C, Luo W, Liu XM, Xia K, Cai F, Hu ZM, Yan XX, Zhang RX, Guo P. 2005 Mutation analysis of small heat-shock protein 22 gene in Chinese patients with Charcot-Marie-Tooth disease. *Zhonghua Yi Xue Yi Chuan Xue Za Zhi.* 22:361-3.

Zhou QY, Quaife CJ, Palmiter RD. 1995 Targeted disruption of the tyrosine hydroxylase gene reveals that catecholamines are required for mouse fetal development. *Nature.* 374:640-3.

Zomosa-Signoret V, Arnaud JD, Fontes P, Alvarez-Martinez MT, Liautard JP. 2008 Physiological role of the cellular prion protein. *Vet Res.* 39:9.

Züchner S, Vance JM. 2006 Molecular genetics of autosomal-dominant axonal Charcot-Marie-Tooth disease. *Neuromolecular Med.* 8:63-74.